REPRODUCIBLE COPY

N64-11742
NASA CR 52916

FIRST QUARTERLY REPORT

OCTOBER 31, 1963

APPENDIX

BRUSHLESS ROTATING ELECTRICAL GENERATORS FOR SPACE AUXILIARY POWER SYSTEMS

CONTRACT NO. NAS 3-2783

prepared for

NATIONAL AERONAUTICS AND SPACE ADMINISTRATION

by

J. N. Ellis and F. A. Collins

TECHNICAL MANAGEMENT
NASA-LEWIS RESEARCH CENTER
AUXILIARY POWER GENERATION OFFICE
ATTENTION: HOWARD A. SHUMAKER

LSi

LEAR SIEGLER, INC.

POWER EQUIPMENT DIVISION

CLEVELAND 1, OHIO

FIRST QUARTERLY REPORT
OCTOBER 31, 1963

APPENDIX

BRUSHLESS ROTATING ELECTRICAL GENERATORS FOR SPACE AUXILIARY POWER SYSTEMS

CONTRACT NO. NAS 3-2783

prepared for

NATIONAL AERONAUTICS AND SPACE ADMINISTRATION

by

J. N. Ellis and F. A. Collins

TECHNICAL MANAGEMENT
NASA-LEWIS RESEARCH CENTER
AUXILIARY POWER GENERATION OFFICE
ATTENTION: HOWARD A. SHUMAKER

LEAR SIEGLER, INC.
POWER EQUIPMENT DIVISION
CLEVELAND 1, OHIO

TABLE OF CONTENTS

TABLE OF CONTENTS (Cont)

MAGNETIC STEEL

MAGNETIC STEELS

Generators investigated for this study range from low temperature 1800 rpm machines to high temperature 72000 rpm machines. For so great a range of rotor speeds, steels are needed that have good strength as well as good magnetic properties.

All presently known magnetic steel alloys have deficiencies. The alloys with the best saturation magnetization are weak. The Cobalt steels become radioactive under neutron bombardment. The tool steels have relatively poor magnetic properties. In short, all of the magnetic steels are compromises.

The following curves and discussion may help toward making the best compromise.

CURIE POINTS

The magnetic properties of any of the steels, of pure iron or of nickel, exhibit a reversible deterioration as the Curie point of the metal is approached. This deterioration is shown by a generalized curve from Bozorth. A similar curve showing the increased flux-carrying ability of a cobalt-iron alloy is given also. Then the Curie points of several of the better-known alloys are listed.

SATURATION OF IRON, NICKEL & COBALT

VERSUS TEMPERATURE

RELATIVE MAXIMUM SATURATION AT ANY TEMPERATURE VERSUS RATIO OF TEMP. IN °K TO THE CURIE TEMP IN °K

σ_s = SATURATION MAGNETIC MOMENT PER GRAM AT T

σ_o = σ_s AT 0°K

T = ABSOLUTE TEMP. °K

θ = CURIE TEMP IN °K

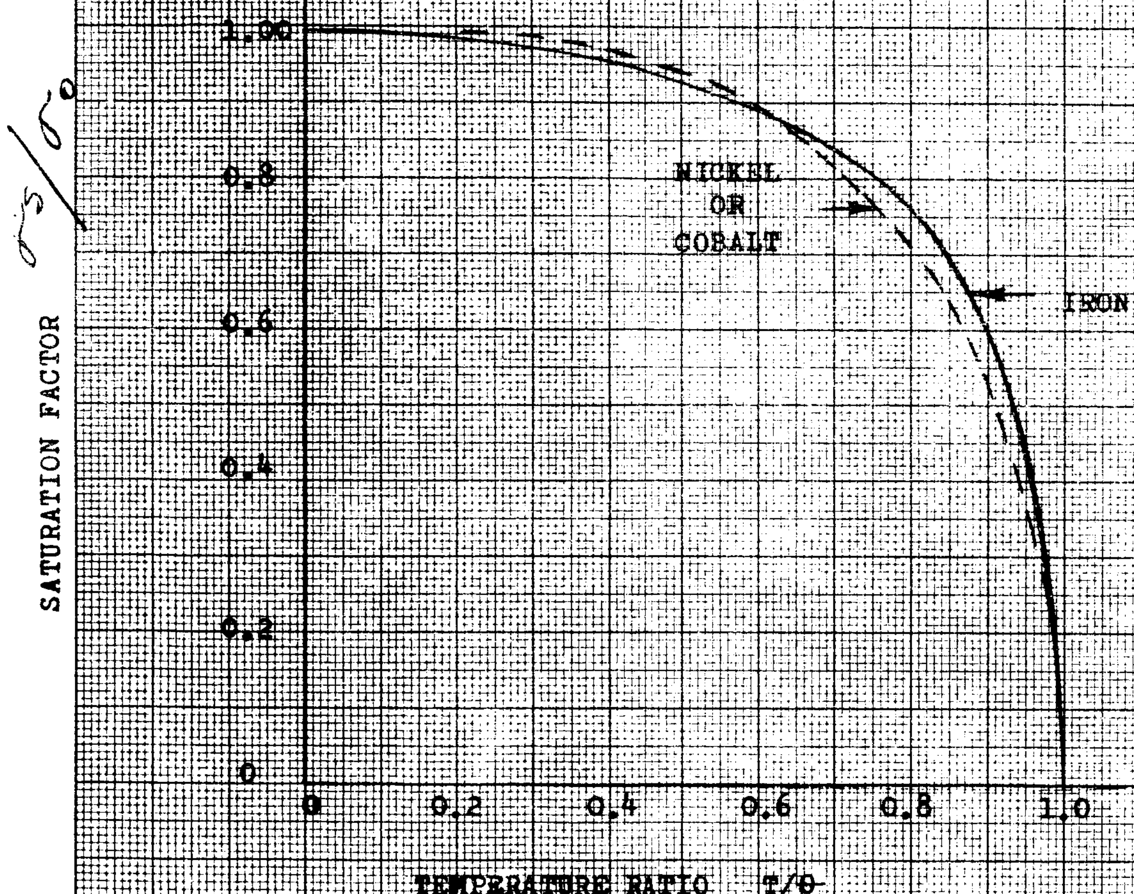

SEE BOZORTH "FERROMAGNETISM" P 431

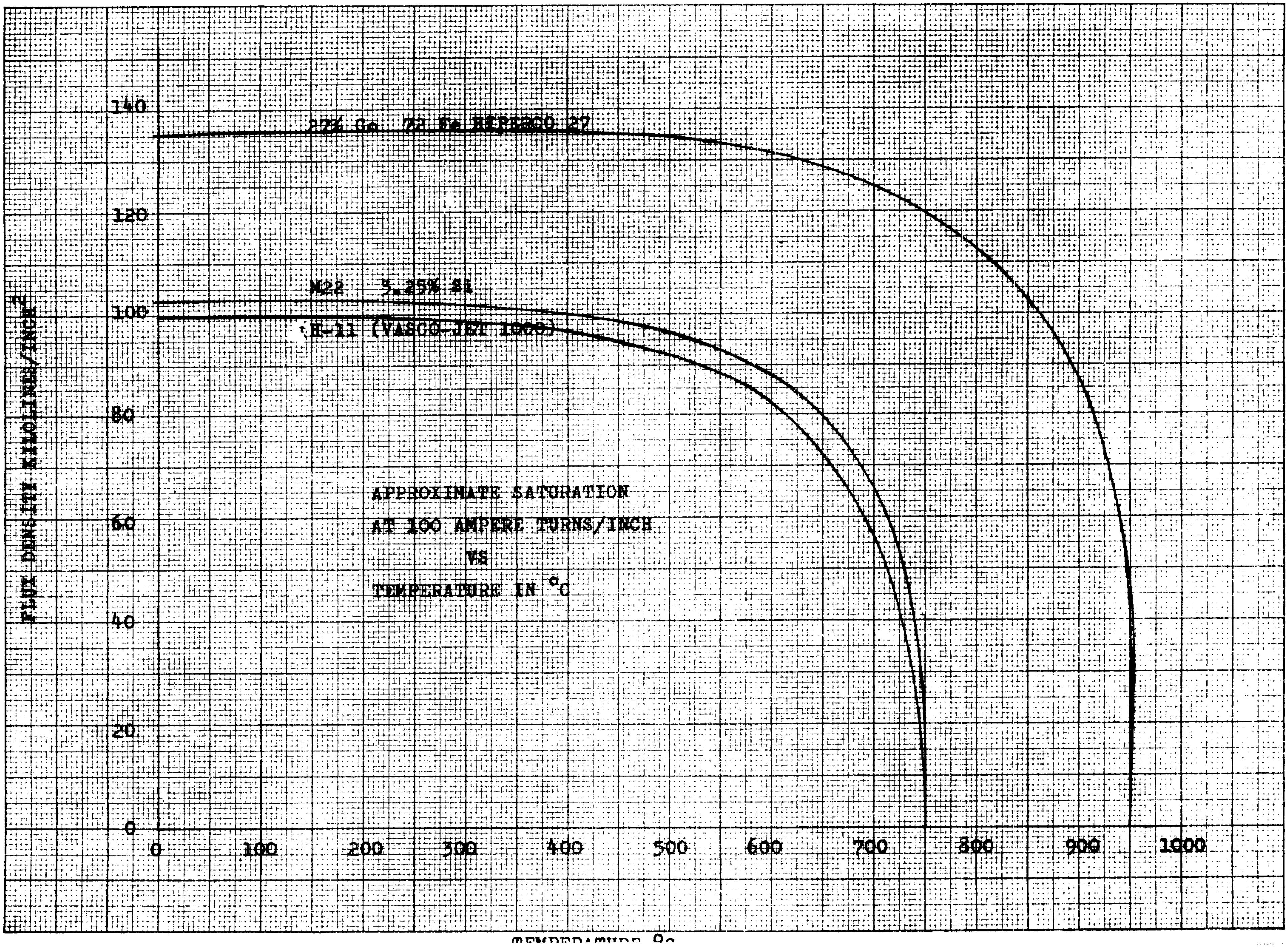
27% Co 72 Fe HIPERCO 27
M22 3.25% Si
H-11 (VASCO-JET 1000)
APPROXIMATE SATURATION
AT 100 AMPERE TURNS/INCH
VS
TEMPERATURE IN °C
FLUX DENSITY KILOLINES/INCH²
140
120
100
80
60
40
20
0
0
100
200
300
400
500
600
700
800
900
1000

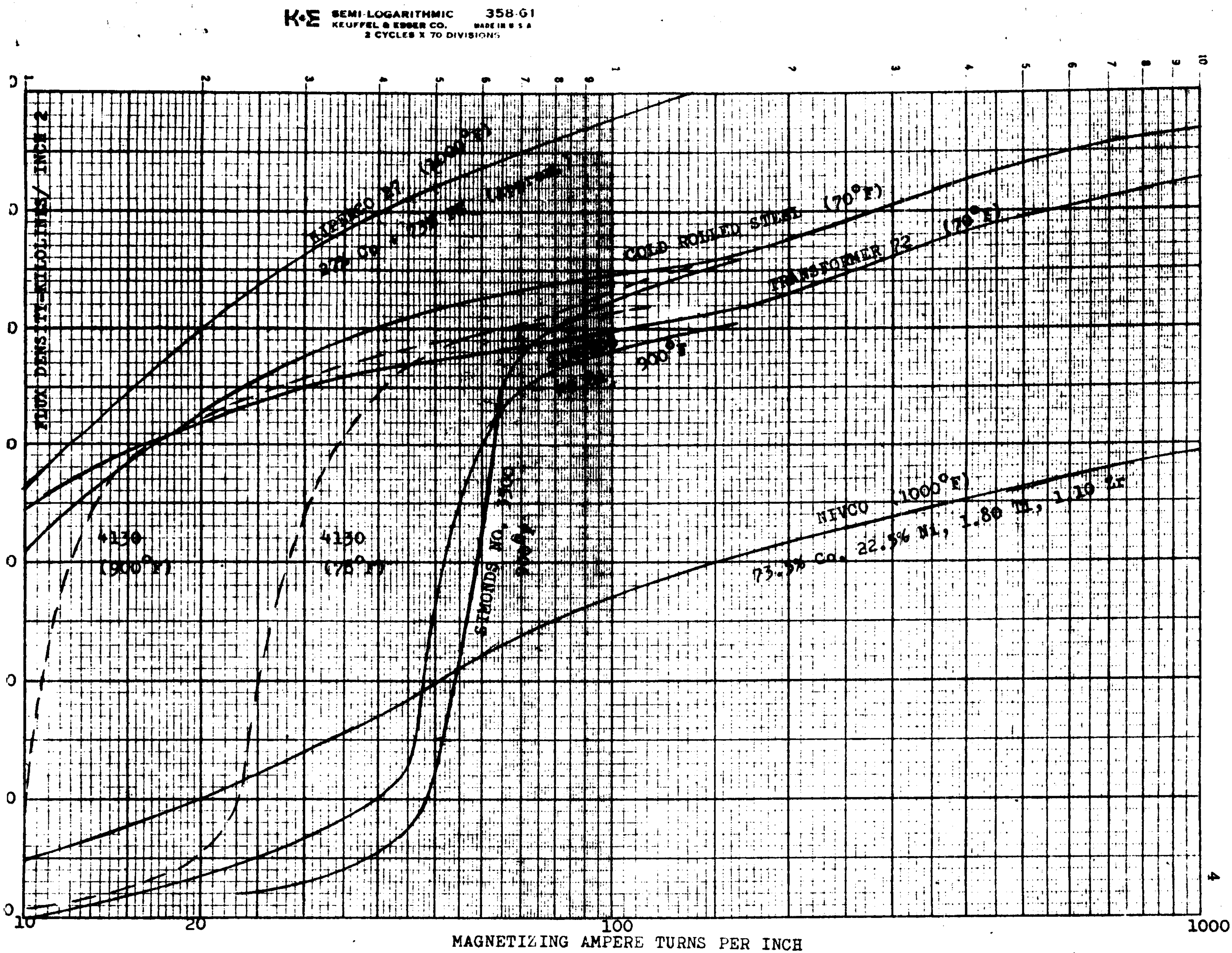
K+E SEMI-LOGARITHMIC 358-61
KEUFFEL & ESSER CO. MADE IN U.S.A.
2 CYCLES X 70 DIVISIONS
FLUX DENSITY-KILOLINES/ INCH 2
MAGNETIZING AMPERE TURNS PER INCH
10
20
100
1000
COLD ROLLED STEEL (70°F)
TRANSFORMER 72 (70°F)
900°F
4130 (900°F)
4130 (75°F)
SIMONDS NO. 1400
NIVCO (1000°F)
73.5% Co, 22.5% Ni, 1.80 Ti, 1.10 Zr

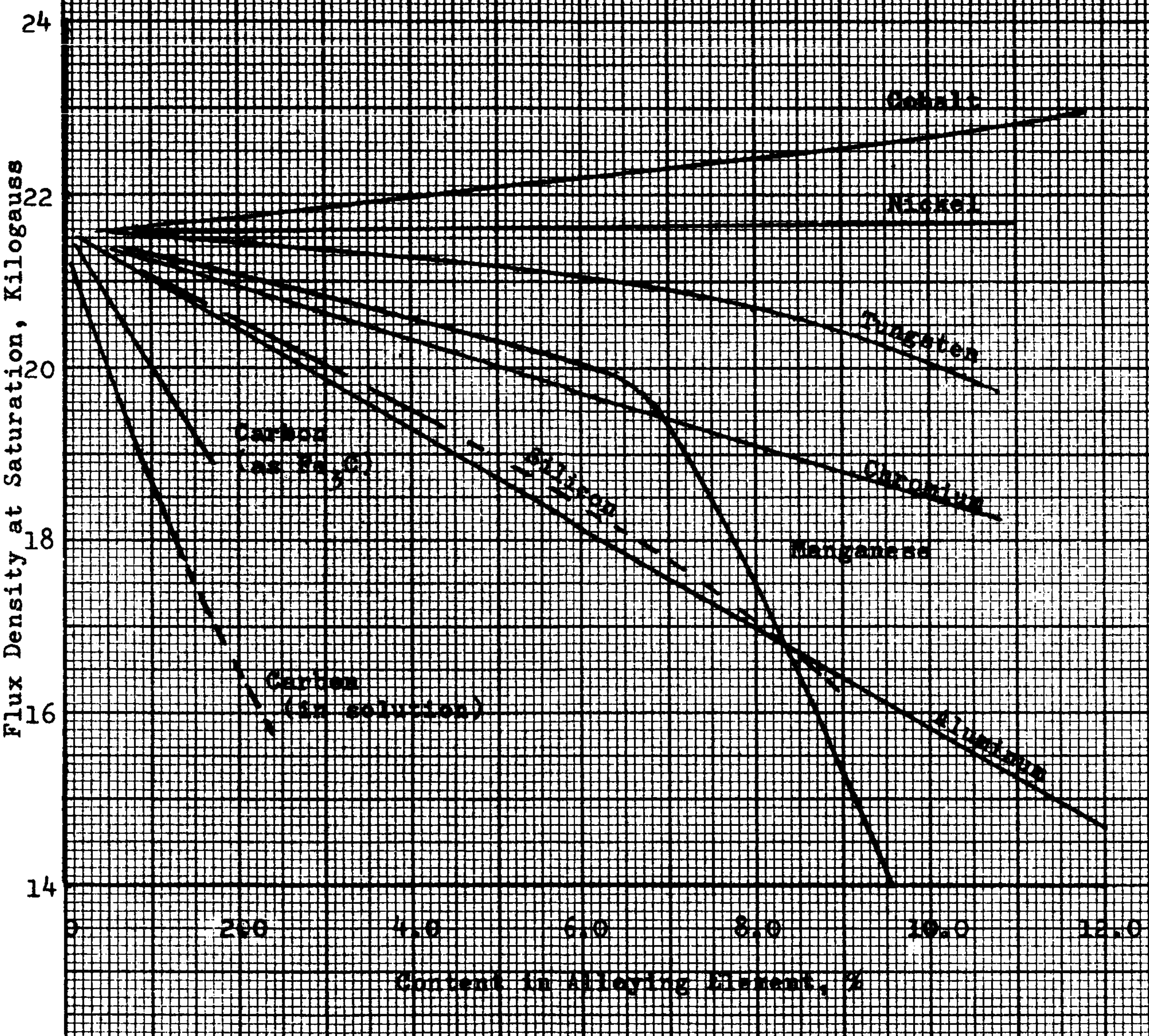

Effect of the principal elements in alloy steel on the flux density at saturation.

From "Magnetically Soft Materials" by Mensen ASM Trans., Vol. 27, 1939.

CURIE POINTS OF THE MAGNETIC MATERIALS

USED IN GENERATORS, MOTORS AND INDUCTORS

Material	Curie Point °C
Iron	770
Cobalt	1130
Nickel	358
50 Co 3 Mn 47 Fe (Permendur)	980
49 Co 2 V 49 Fe (2 V Permendur)	980
35 Co 5 Cr 6 Mn .7 Ni 63 Fe	960
27 Co 5 Cr 6 Mn .7 Ni 71 Fe	940
Silicon-Iron 2 Si	756
Silicon-Iron 8 Si	720
Silicon-Iron 11 Si	690
65 Permalloy 65 Ni - Iron	620
79 Ni Permalloy	580
7-70 Perminvar 70 Ni 7 Co - Fe	650
Perminvar 45 Ni 25 Co - Fe	720
Perminvar 45 Ni 25 Co 7.5 Mo - Fe	535
79 Ni 4 Mo - Fe (P-Alloy)	460
79 Ni 5 Mo - Fe (Supermalloy)	400
47 Ni 3 Mo - Fe (Nonimax)	510
43 Ni 3.25 Si - Fe (Sinimax)	510
76 Ni 1.5 Cr 4 Cu - Fe (Mu-Metal)	450

CURIE POINTS OF THE MAGNETIC MATERIALS USED IN GENERATORS, MOTORS AND INDUCTORS

(Continued)

Material	Curie Point °C
36 Ni - Fe (Invar)	275
42 Ni - Fe	400
50 Ni - Fe (Deltamax)	510
15 AL 3.3 Mo - Fe (Thermenol)	400
Alnico 5 - 24 Co 14 Ni 8 AL 3 Cu	880
Alnico 6 - 24 Co 15 Ni 8 AL 3 Cu 1.25 Ti	880
Chrome Steel .9 C .3 Mn 3.5 Cr	745
3% Cobalt Steel 1.0 C 3 Co 4 Cr .4 Mo	804
17% Cobalt Steel .8 C 17 Co 25 Cr 8 W	840
36% Cobalt Steel .7 C 36 Co 4 Cr 5 W	890

PURE IRON AND SILICON STEEL

Pure iron or almost pure iron is commonly used for yokes of d-c machines and for unidirectional flux circuits that require a high saturation induction. Pure iron has a higher saturation induction than any material except cobalt-iron alloy. Because pure iron has low resistivity, its eddy losses are high when it is used in a-c circuits.

To reduce the eddy losses of iron for use in alternating flux circuits, silicon is commonly added. This increases the resistance, reduces the width of the hysteresis loop and reduces degradation of magnetic properties with age (aging).

A curve of resistivity versus % silicon in iron is provided to show the effect of adding silicon. Since silicon reduces the saturation induction in iron and makes it brittle at the same time, about 4% silicon is the maximum alloy for production use. Six percent (6%) silicon added to iron reduces the magnetostriction to almost zero so that alloy content is of interest for low noise machines and transformers.

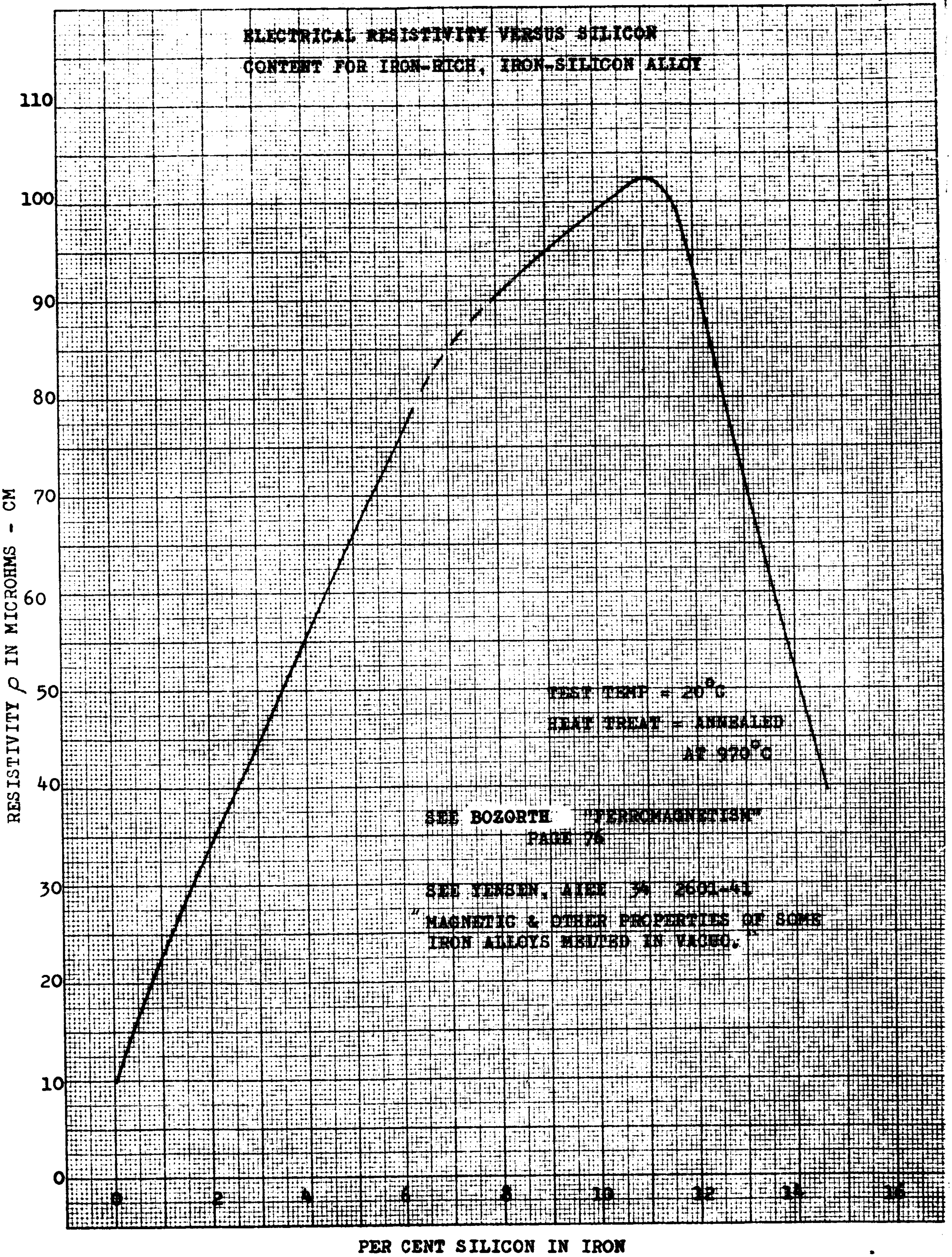

10 X 10 TO THE CM. 359-14
KEUFFEL & ESSER CO. MADE IN U.S.A.

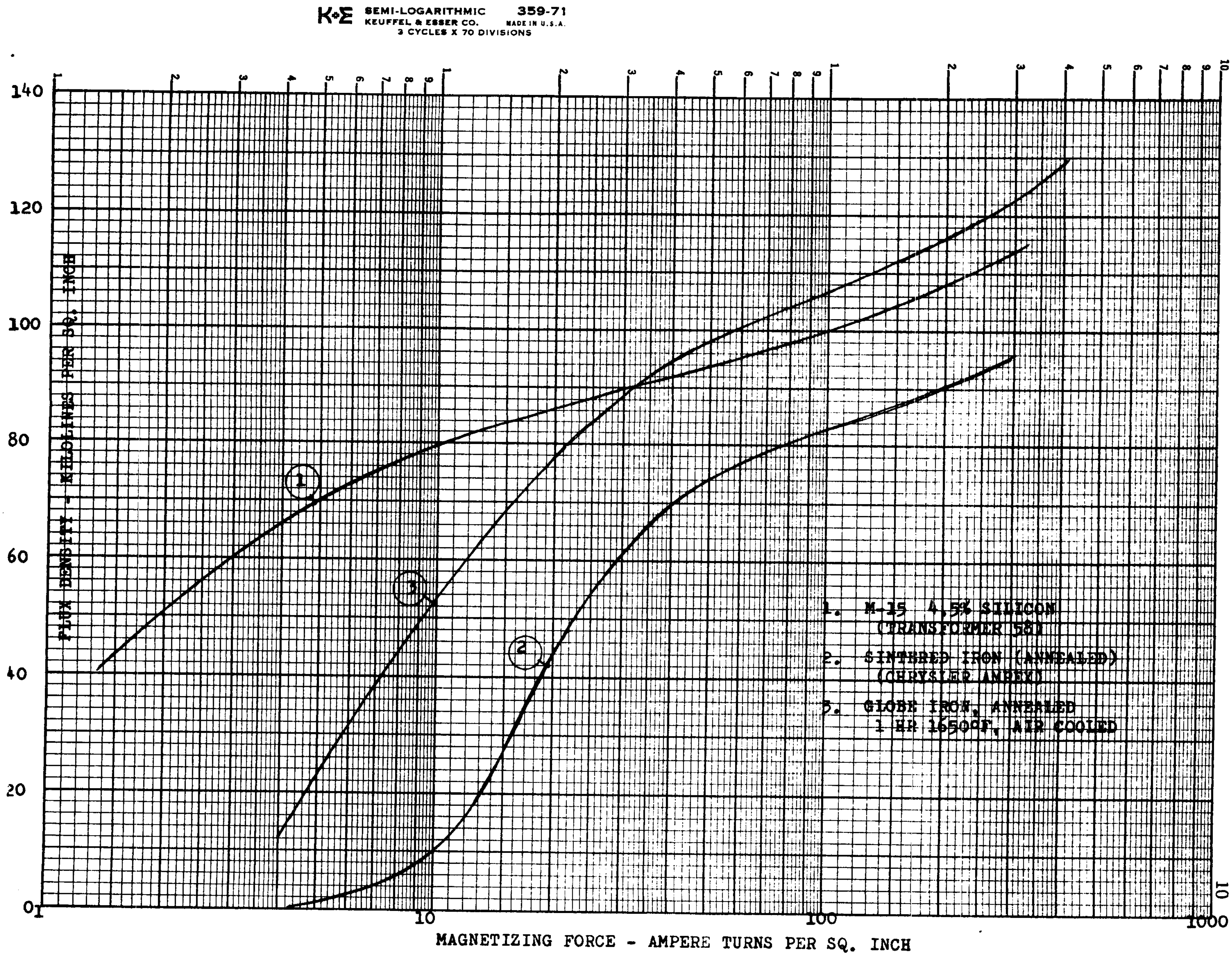

K+E SEMI-LOGARITHMIC 359-71
KEUFFEL & ESSER CO. MADE IN U.S.A.
3 CYCLES X 70 DIVISIONS
FLUX DENSITY - KILOLINES PER SQ. INCH
MAGNETIZING FORCE - AMPERE TURNS PER SQ. INCH
1. M-15 4.5% SILICON (TRANSFORMER 58)
2. SINTERED IRON (ANNEALED) (CHRYSLER AMPEX)
3. GLOBE IRON, ANNEALED 1 HR 1650°F, AIR COOLED
1
2
3
0
20
40
60
80
100
120
140
1
10
100
1000

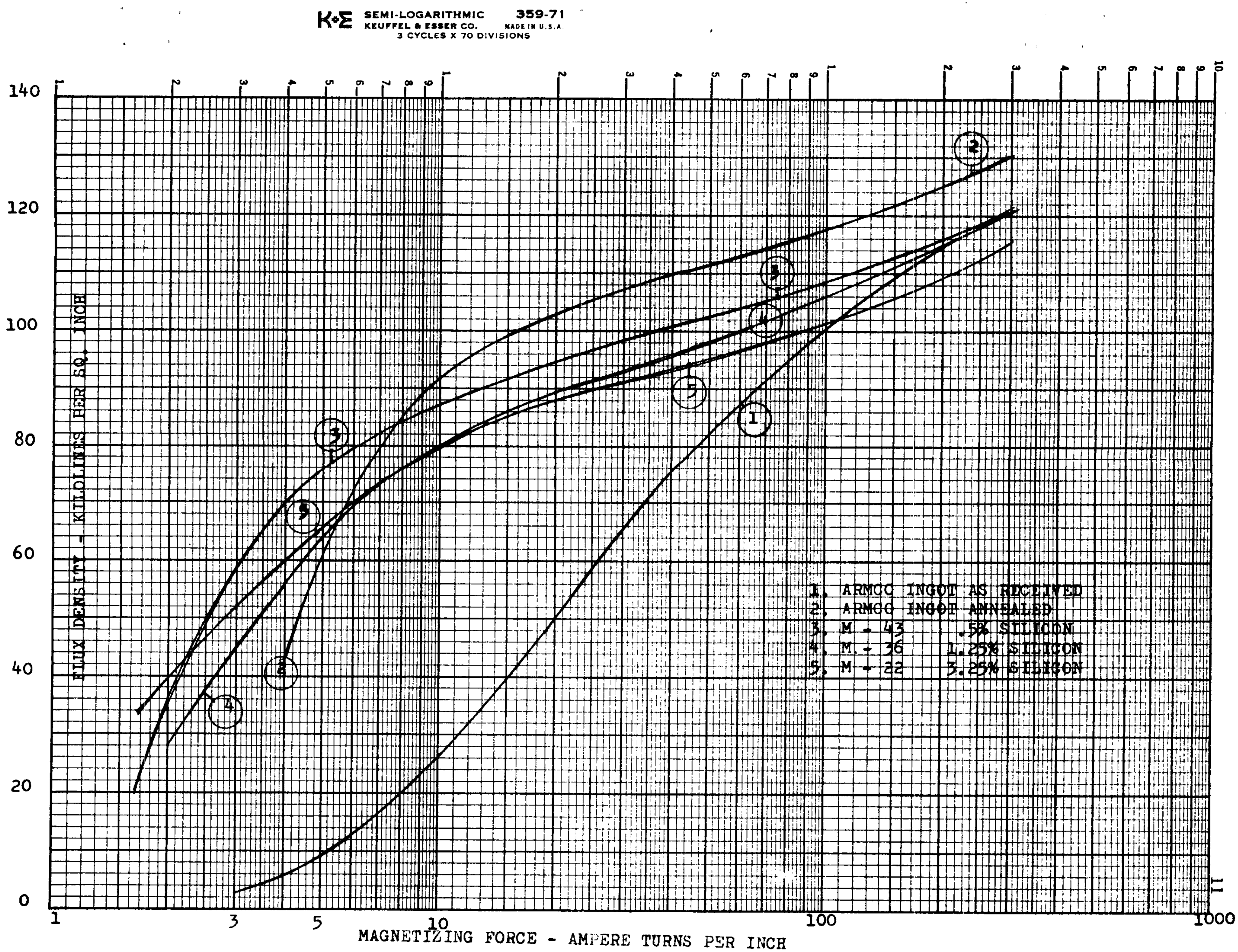

K+E SEMI-LOGARITHMIC 359-71
KEUFFEL & ESSER CO. MADE IN U.S.A.
3 CYCLES X 70 DIVISIONS
11
FLUX DENSITY - KILOLINES PER SQ. INCH
MAGNETIZING FORCE - AMPERE TURNS PER INCH
1. ARMCO INGOT AS RECEIVED
2. ARMCO INGOT ANNEALED
3. M - 43 .5% SILICON
4. M - 36 1.25% SILICON
5. M - 22 3.25% SILICON
140
120
100
80
60
40
20
0
1
3
5
10
100
1000

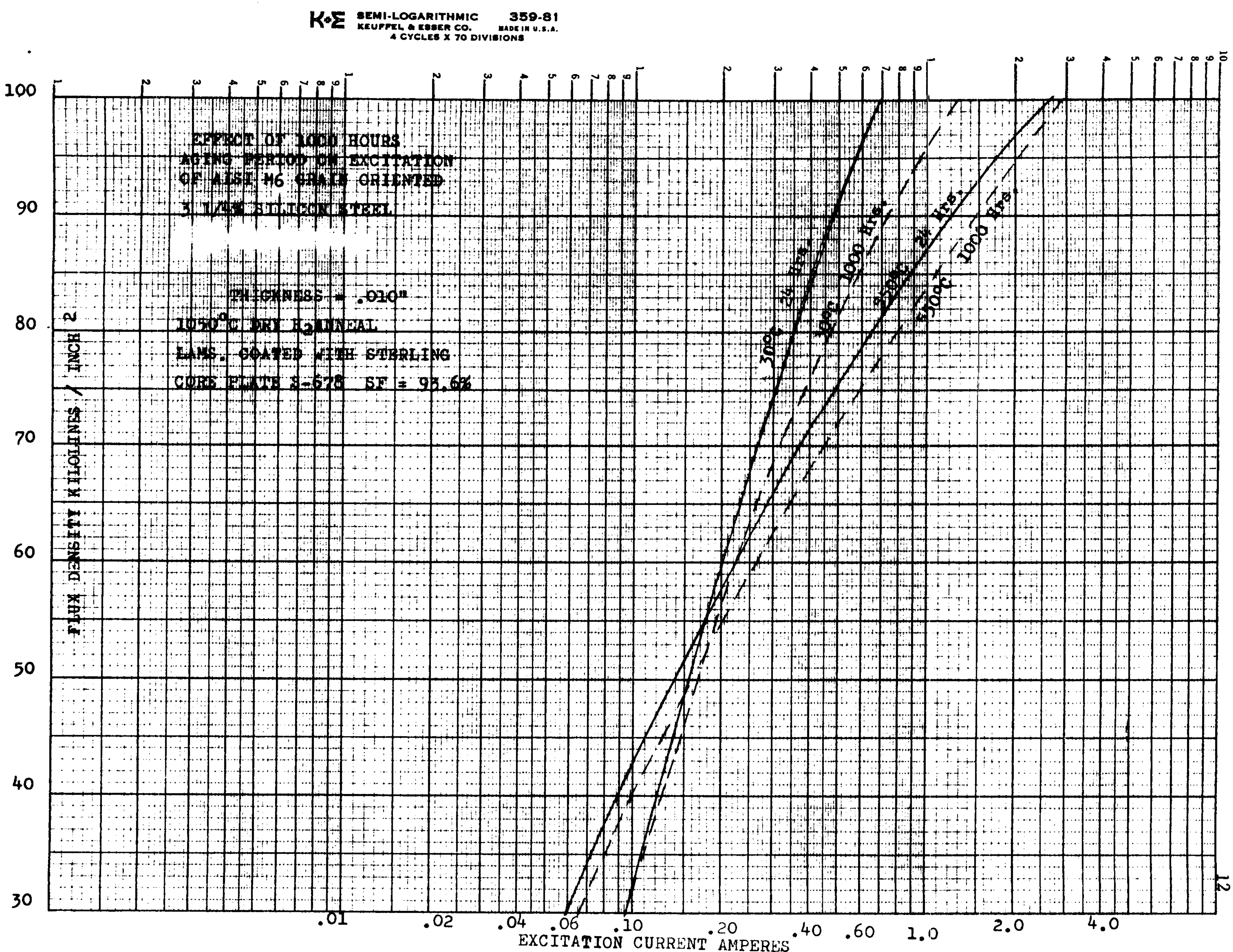
K+E SEMI-LOGARITHMIC 359-81
KEUFFEL & ESSER CO. MADE IN U.S.A.
4 CYCLES X 70 DIVISIONS
EFFECT OF 1000 HOURS
AGING PERIOD ON EXCITATION
OF AISI M6 GRAIN ORIENTED
3 1/4% SILICON STEEL
THICKNESS = .010"
1050°C DRY H2 ANNEAL
LAMS. COATED WITH STERLING
CORE PLATE S-678 SF = 95.6%
300°C 24 Hrs.
300°C 1000 Hrs.
250°C 24 Hrs.
250°C 1000 Hrs.
FLUX DENSITY KILOLINES / INCH 2
100
90
80
70
60
50
40
30
.01
.02
.04
.06
.10
.20
.40
.60
1.0
2.0
4.0
EXCITATION CURRENT AMPERES

NON-MAGNETIC STEELS

The Chrome-Nickel steels of the 300 series are used as non-magnetic spacers and support members in rotor weldments, braces and other structural locations where it is desirable to use a material with a permeability of one (1).

Some of the 300 series steels are non-magnetic in the "soft" condition but when they are work hardened part of the steel changes phase and becomes magnetic. The 18-8 steel (see 301 on chart) becomes useless for non-magnetic needs when cold reduced 25% to 50%.

A table taken from an International Nickel Co. Bulletin is included for guidance.

MAGNETIC PROPERTIES OF Cr Ni STEELS

AISI Type No.	% Cr	% Ni	% Cold Reduction	Magnetic Permeability H = 50 Oersteds	Magnetic Permeability H = 200 Oersteds	Tensile Strength Lb/Sq. In.
Special	19.2	8.4	0	1.0042	1.0048	89,100
			8.3	1.128	1.136	120,400
			16.7	5.70	6.23	138,200
			27.8	13.6	14.1	156,000
			48.0	49.0	33.4	202,000
301	17.6	7.8	0	1.0027	1.0028	95,000
			19.5	1.148	1.257	140,600
			55.0	14.8	19.0	222,400
302	18.4	9.0	0	1.0025	1.0035	95,300
			20.0	1.0076	1.011	130,200
			44.0	1.050	1.120	171,000
			68.0	1.59	2.70	214,000
			84.0	2.15	6.65	236,000
304	19.0	10.7	0	1.0037	1.0040	81,000
			13.8	1.0048	1.0060	101,100
			32.0	1.0371	1.062	145,900
			65.0	1.540	2.12	180,400
			84.5	2.20	4.75	202,800
308	17.9	11.7	0	1.0032	1.0044	88,200
			18.5	1.0040	1.0054	129,100
			34.5	1.017	1.020	154,700
			52.5	1.049	1.063	175,900
			84.0	1.093	1.142	197,800
310	24.3	20.7	0	1.0018	1.0035	107,800
			14.7	1.0016	1.0041	128,100
			26.8	1.0018	1.0043	155,000
			64.2	1.0019	1.0041	192,600
316 2.4% MO.	17.5	13.4	0	1.0030	1.0040	83,600
			20.8	1.0030	1.0043	117,800
			45.0	1.0040	1.0065	159,900
			60.8	1.0065	1.0072	178,000
			81	1.0070	1.0100	194,100

MAGNETIC PROPERTIES OF Cr Ni STEELS (Cont)

AISI Type No.	% Cr	% Ni	% Cold Reduction	Magnetic Permeability H = 50 Oersteds	H = 200 Oersteds	Tensile Strength Lb/Sq. In.
321						
0.68% Ti	18.3	10.3	0	1.0033	1.0035	87,800
			16.5	1.018	1.023	123,200
			41.5	1.40	1.61	162,200
			53.5	2.44	3.34	174,400
			70.5	6.76	9.40	201,300
347						
0.95% Cb.	18.4	10.7	0	1.0037	1.0044	94,800
			13.5	1.0074	1.0085	118,200
			40.0	1.062	1.088	166,100
			60.0	1.245	1.445	179,800
			90.0	1.97	4.12	216,500

Ref: Heat treatment and physical properties of the Austenitic Chromium - Ni Steels - International Nickel Co. Bulletin

COBALT-IRON ALLOYS

The cobalt-iron alloys have the highest curie points of any of the alloys. (Only cobalt has a higher curie temperature.) In some high temperature applications, no other presently known magnetic materials could be used.

The "soft" or high permeability Cobalt-iron alloys are weak in tension and brittle at room temperature so their use in high speed rotor construction becomes difficult.

The Cobalt becomes radioactive when the cobalt-iron is used in a nuclear radiation environment and since the Cobalt radioisotope half-life is 60 years, handling the generator becomes difficult after such exposure.

The large body of permanent magnet alloys remains mostly unexplored for "soft" applications.

RESISTIVITY OF COBALT IRON
ALLOYS VERSUS TEMPERATURE
SEE BOZORTH P 195
SEE P 191 FOR DENSITY &
COEFF. OF EXPANSION

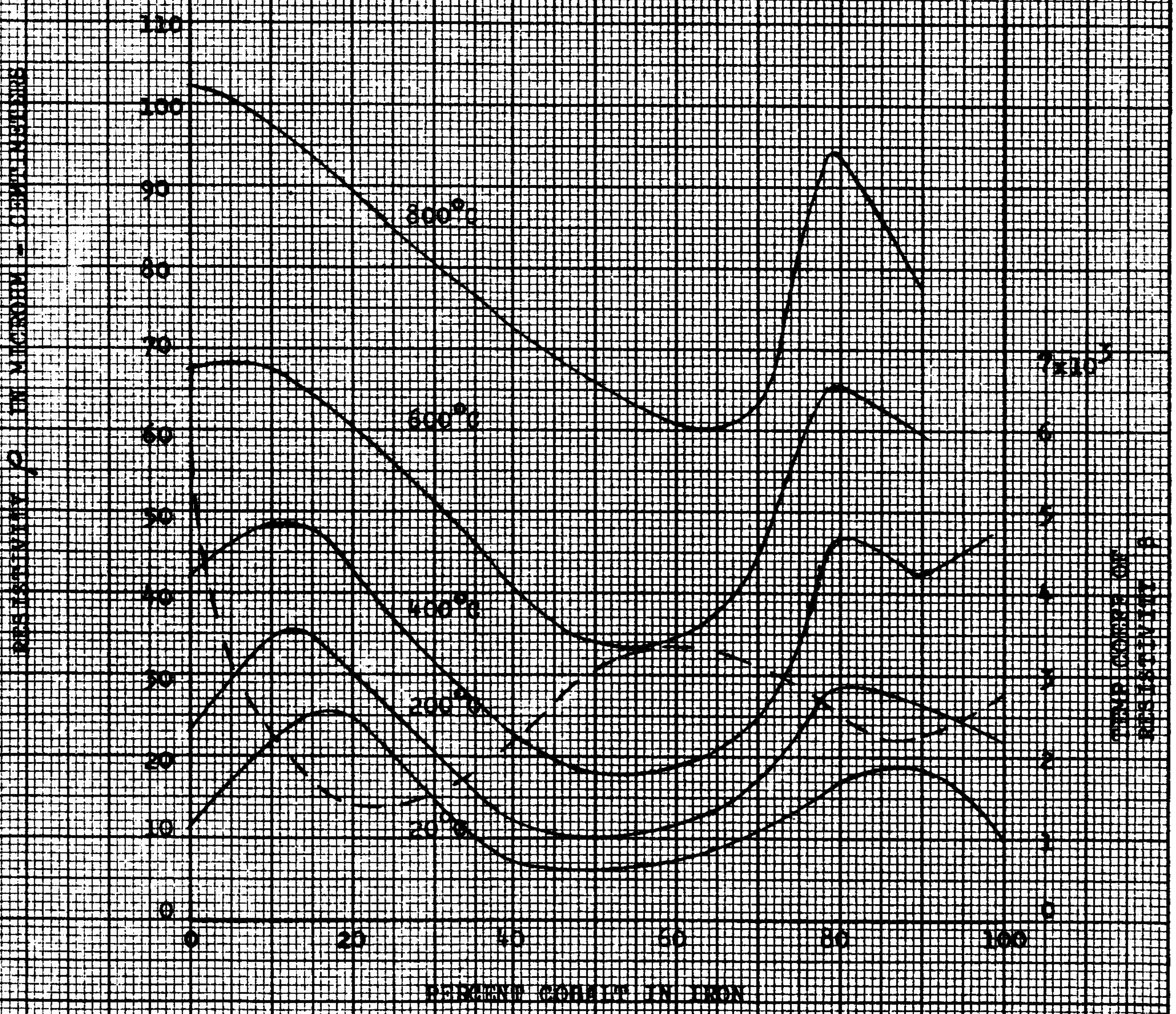

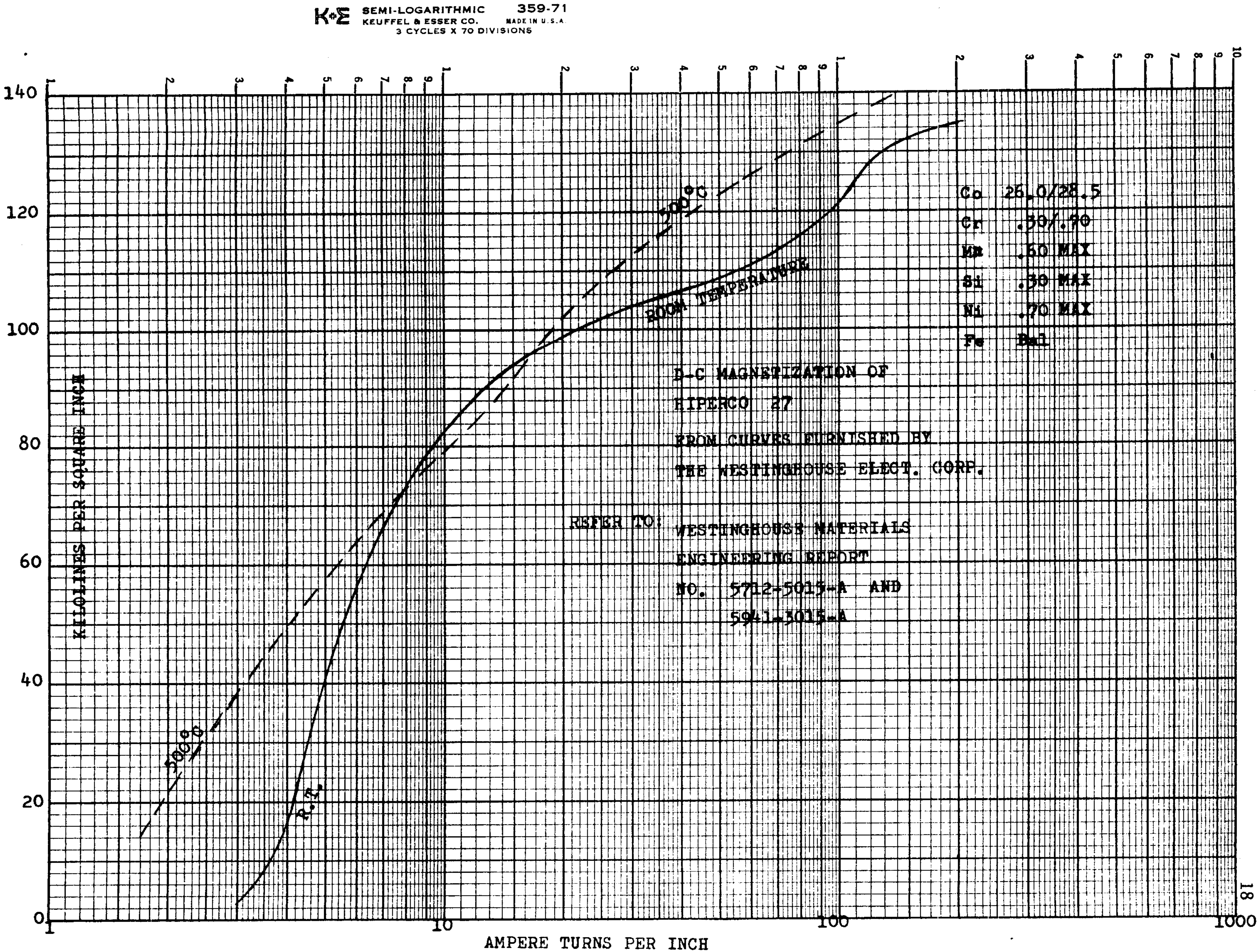
K+E SEMI-LOGARITHMIC 359-71
KEUFFEL & ESSER CO. MADE IN U.S.A.
3 CYCLES X 70 DIVISIONS
KILOLINES PER SQUARE INCH
AMPERE TURNS PER INCH
500°C
ROOM TEMPERATURE
R.T.
Co 26.0/28.5
Cr .30/.70
Mn .60 MAX
Si .30 MAX
Ni .70 MAX
Fe Bal
D-C MAGNETIZATION OF
HIPERCO 27
FROM CURVES FURNISHED BY
THE WESTINGHOUSE ELECT. CORP.
REFER TO: WESTINGHOUSE MATERIALS
ENGINEERING REPORT
NO. 5712-5015-A AND
5941-3015-A

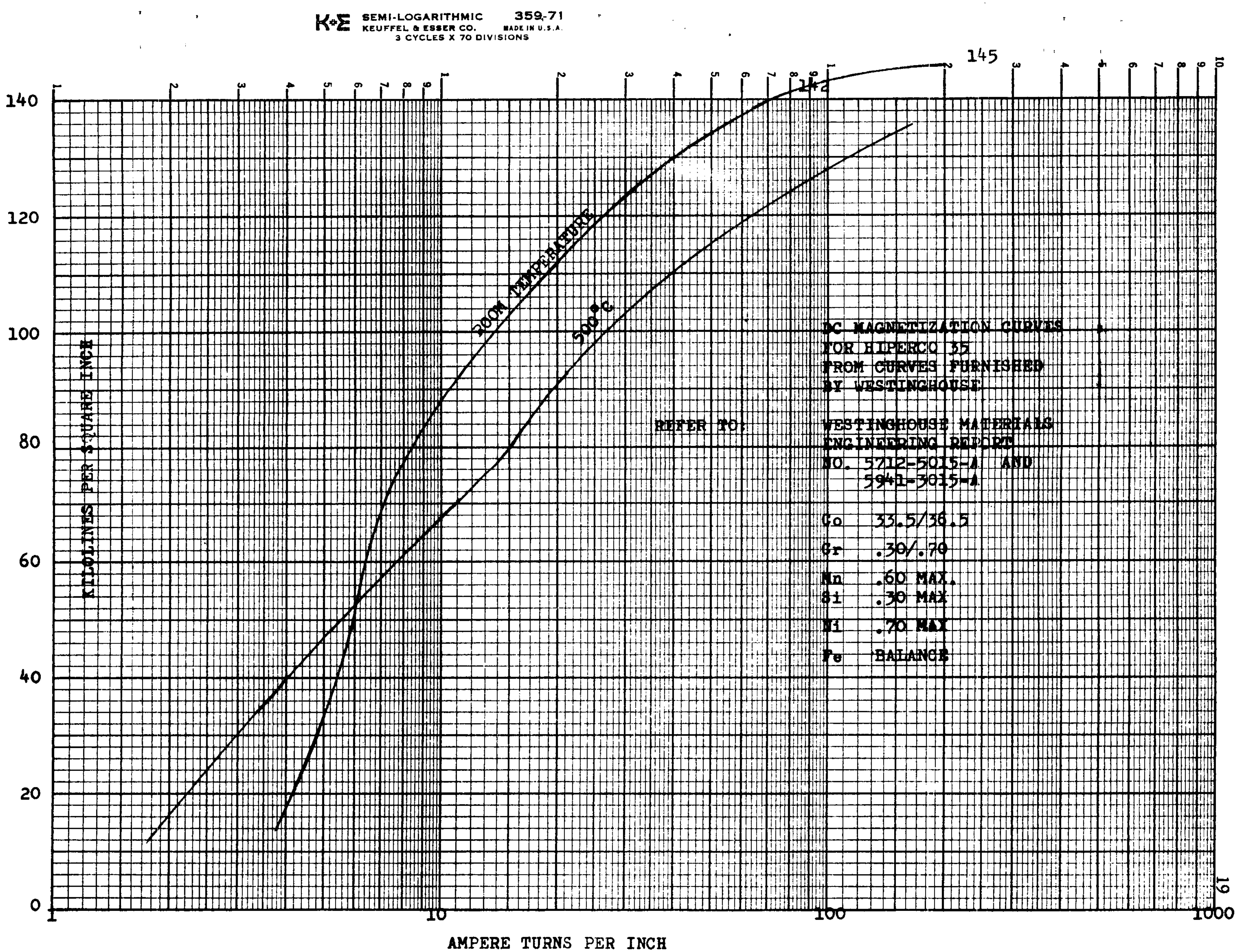

K+E SEMI-LOGARITHMIC 359-71
KEUFFEL & ESSER CO. MADE IN U.S.A.
3 CYCLES X 70 DIVISIONS
145
142
ROOM TEMPERATURE
500°C
DC MAGNETIZATION CURVES
FOR HIPERCO 35
FROM CURVES FURNISHED
BY WESTINGHOUSE
REFER TO:
WESTINGHOUSE MATERIALS
ENGINEERING REPORT
NO. 5712-5015-A AND
5941-3015-A
Co 33.5/36.5
Cr .30/.70
Mn .60 MAX.
Si .30 MAX
Ni .70 MAX
Fe BALANCE
KILOLINES PER SQUARE INCH
AMPERE TURNS PER INCH
0
20
40
60
80
100
120
140
1
10
100
1000
19

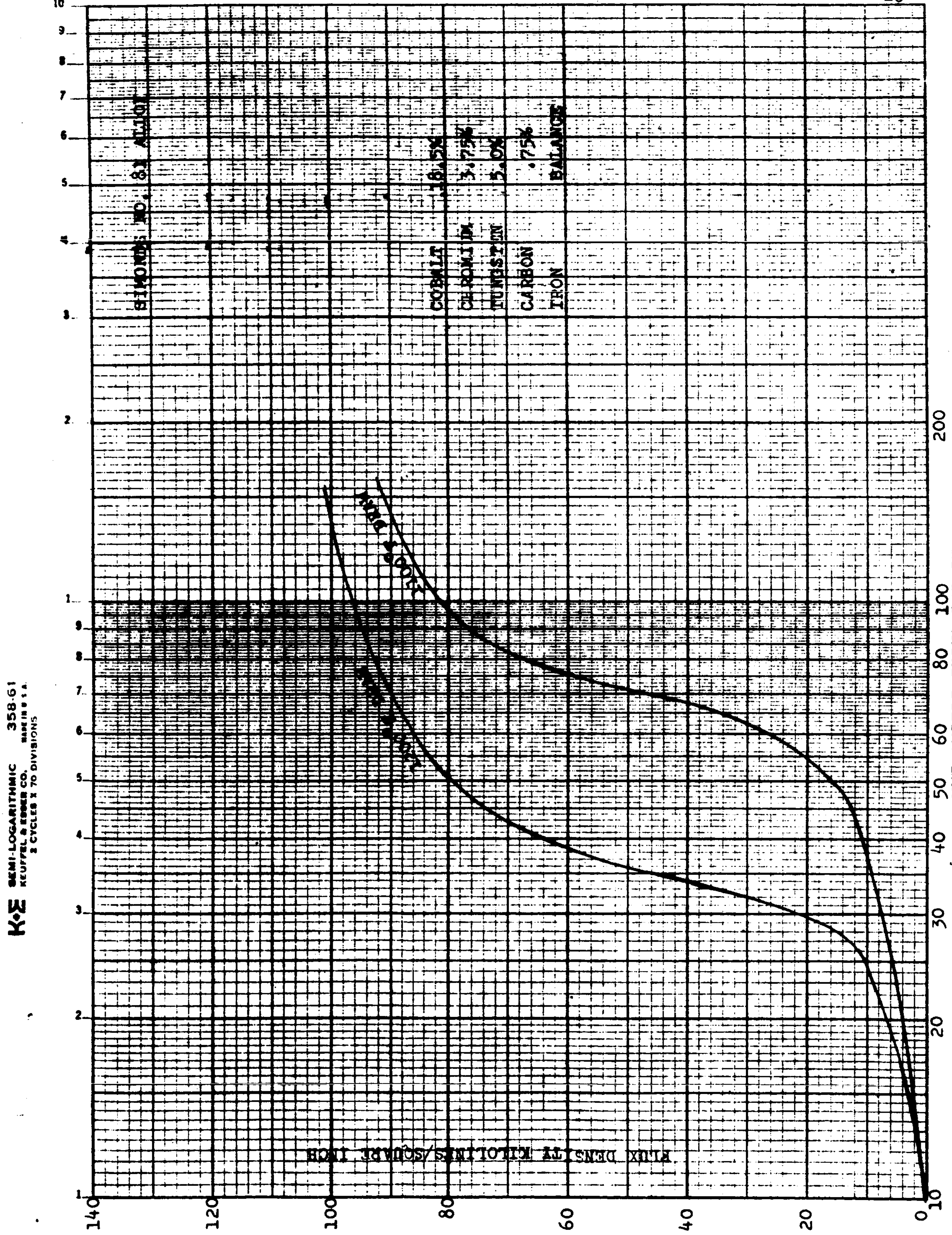
SIMONDS NO. 81 ALLOY
COBALT 18.5%
CHROMIUM 3.75%
TUNGSTEN 5.0%
CARBON .75%
IRON BALANCE
FLUX DENSITY KILOLINES/SQUARE INCH
MMF AMPERE TURNS PER INCH
K+E SEMI-LOGARITHMIC 358-61
KEUFFEL & ESSER CO. MADE IN U.S.A.
2 CYCLES X 70 DIVISIONS

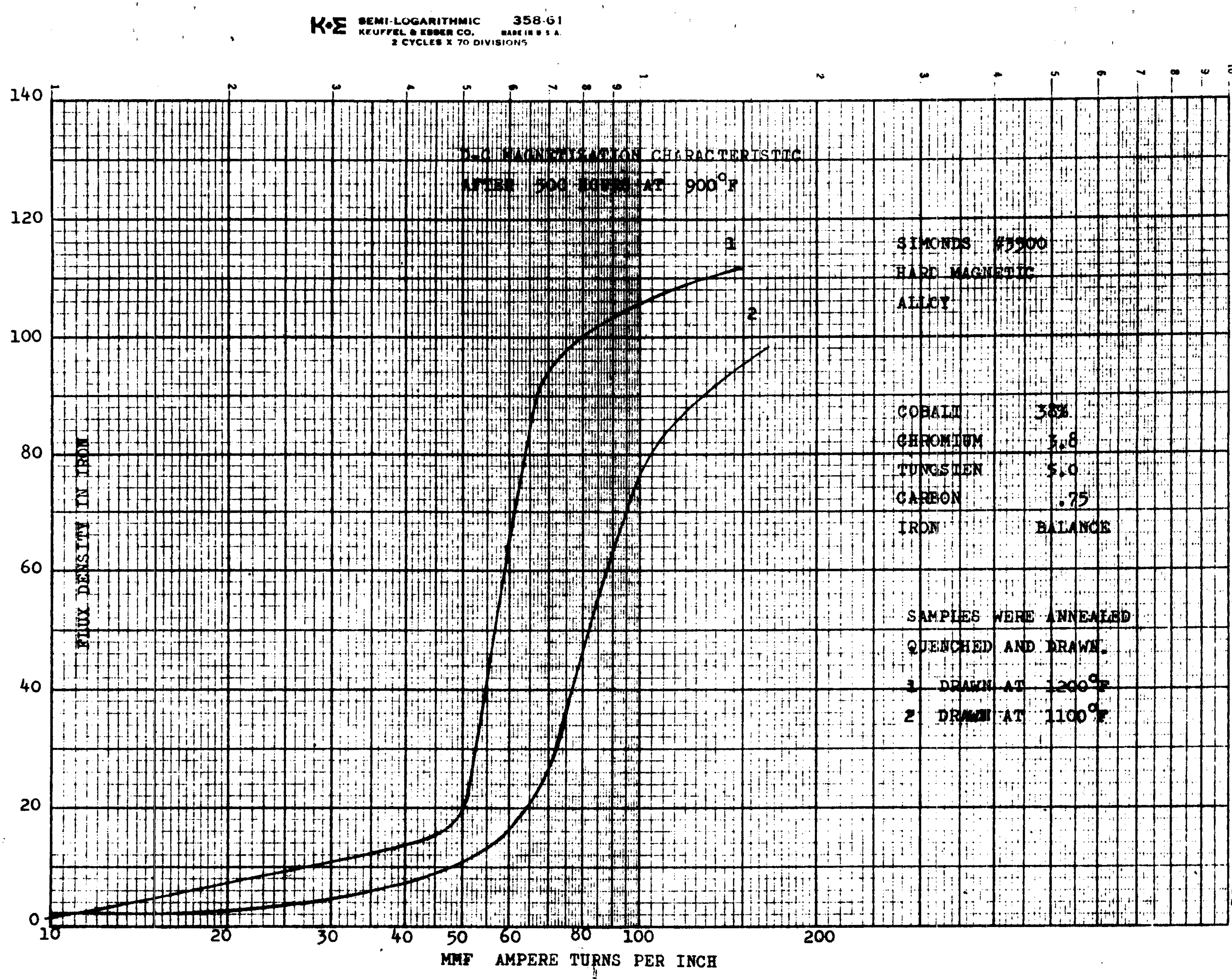
K·E SEMI-LOGARITHMIC 358-61
KEUFFEL & ESSER CO. MADE IN U.S.A.
2 CYCLES X 70 DIVISIONS
D-C MAGNETIZATION CHARACTERISTIC
AFTER 500 HOURS AT 900°F
SIMONDS
HARD MAGNETIC
ALLOY
COBALT 38%
CHROMIUM 3.8
TUNGSTEN 5.0
CARBON .75
IRON BALANCE
SAMPLES WERE ANNEALED
QUENCHED AND DRAWN.
1 DRAWN AT 1200°F
2 DRAWN AT 1100°F
1
2
FLUX DENSITY IN IRON
MMF AMPERE TURNS PER INCH
0
20
40
60
80
100
120
140
10
20
30
40
50
60
80
100
200

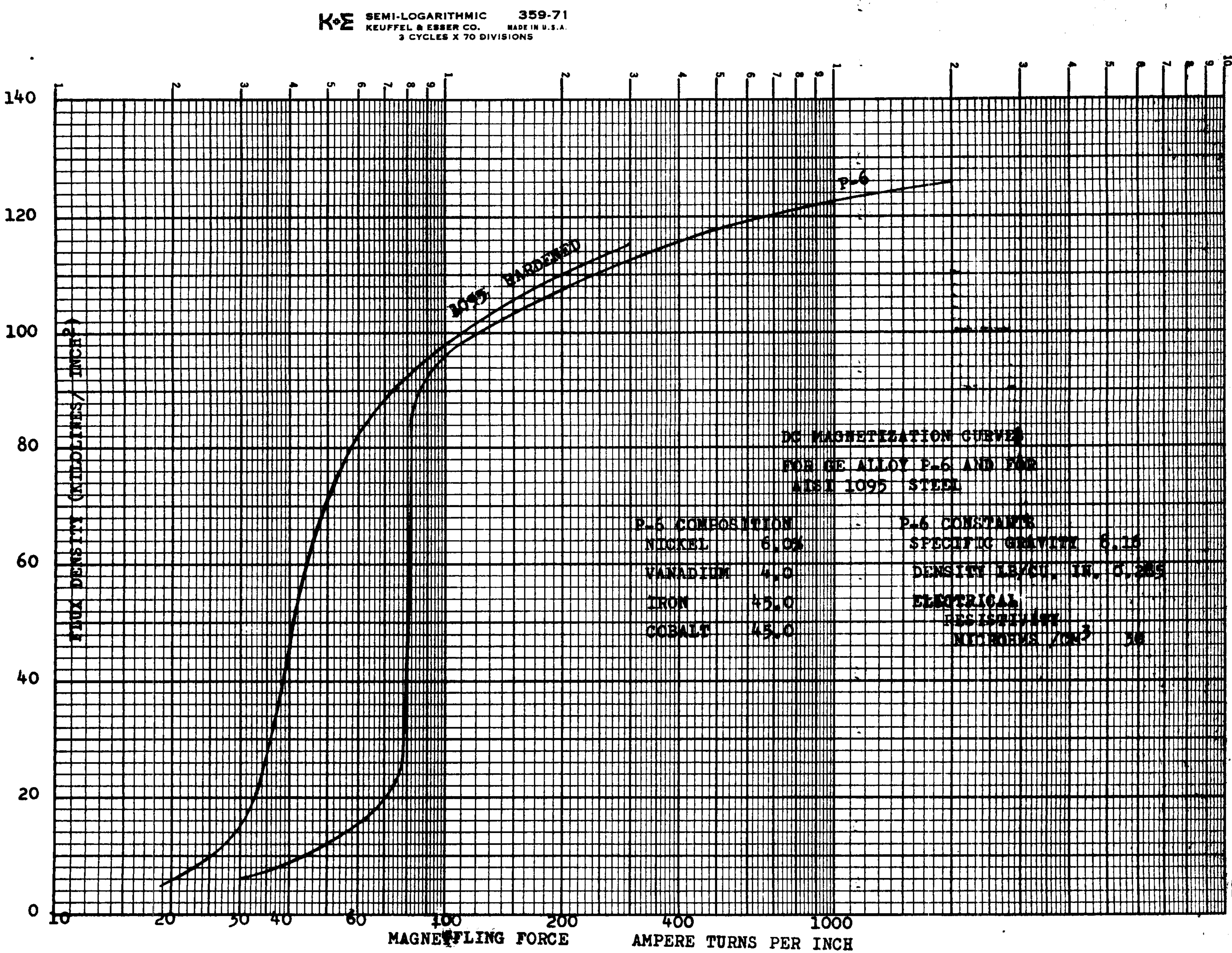
K+E SEMI-LOGARITHMIC 359-71
KEUFFEL & ESSER CO. MADE IN U.S.A.
3 CYCLES X 70 DIVISIONS
DC MAGNETIZATION CURVES
FOR GE ALLOY P-6 AND FOR
AISI 1095 STEEL
P-6 COMPOSITION
NICKEL 6.0%
VANADIUM 4.0
IRON 45.0
COBALT 45.0
P-6 CONSTANTS
SPECIFIC GRAVITY 8.16
DENSITY LB/CU. IN. 0.295
ELECTRICAL
RESISTIVITY
MICROHMS /CM3 36
P-6
1095 HARDENED
FLUX DENSITY (KILOLINES/ INCH2)
MAGNETIZING FORCE AMPERE TURNS PER INCH
0
20
40
60
80
100
120
140
10
20
30
40
60
100
200
400
1000

CREEP STRENGTH

For high temperature applications, the creep strength of the rotor steel must be known. At this time, the creep data available is incomplete and the properties of all known alloys fall far short of those desired.

A table of creep strength for AISI alloys is given and two curves of creep data for carbon steels is given. The creep strength of carbon steel is about the same as most low-alloy steels when 1000°F temperature is exceeded.

CREEP STRENGTH FOR 1% ELONGATION IN 10,000 HOURS

Temperature in °F	Creep Strength in PSI for AISI Steel: 303 / 303 Se	302 / 304	302 B + Columbium	316 / 316 L	317	321	347 / 348	309 / 309 S	310 / 310 S	403 / 410	416 / 416 Se
1000	16500	17000		25000	22500	18000	17000	15900	17000	9200	9200
1100	11500	12000		18200	17000	13000		11600	13000	4200	4200
1200	6500	7000		12700	11000	8000	7000	8000	9000	2000	2000
1300	3500	4000		7900	7100	4500		4500	5000	1000	1000
1500		1200	4500	2800		850		1000	1000		

Temperature in °F	Creep Strength in PSI for AISI Steel: 430 / 430 F	446	431	4340	4140	1040 / 1045	1030 / 1035	1015	
1000	8500	6000		2000-12000	7000-15000	5000	5000	5000	
1100	4300	3000	6800	1000-3000	4000-7000	2000	2000		
1200	2200	1500	3500		1000-2000	1000	1000	600	
1300	1300	700							
1500		300							

Temperature in °F	Creep Strength in PSI: WCI	WC6	WC9	C12	C5	
1000	47000	57000	55000	44000		
1100						
1200	30000	36000	32000	28000	24000	
1300						
1400	13000	15000		14000	12000	
1500					9500	

Ref: "The Ferrous Metals Book," 1961 Edition Machine Design Penton Publishing Co. Thermal and Elect. Properties also.

Aug. 13, 1963

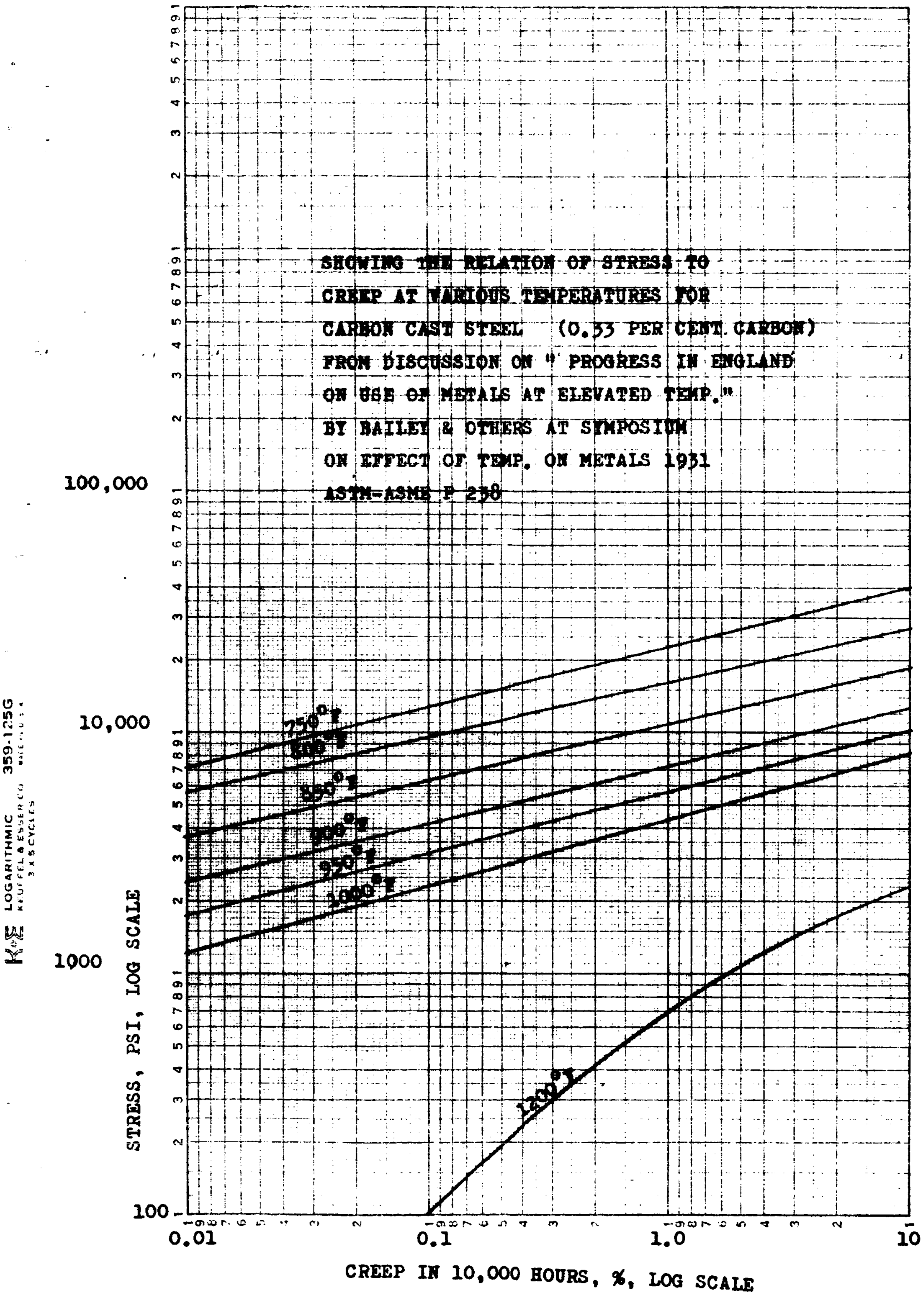
SHOWING THE RELATION OF STRESS TO
CREEP AT VARIOUS TEMPERATURES FOR
CARBON CAST STEEL (0.33 PER CENT CARBON)
FROM DISCUSSION ON " PROGRESS IN ENGLAND
ON USE OF METALS AT ELEVATED TEMP."
BY BAILEY & OTHERS AT SYMPOSIUM
ON EFFECT OF TEMP. ON METALS 1931
ASTM-ASME P 238
750° F
800° F
850° F
900° F
950° F
1000° F
1200° F
100,000
10,000
1000
100
0.01
0.1
1.0
10
STRESS, PSI, LOG SCALE
CREEP IN 10,000 HOURS, %, LOG SCALE
K&E LOGARITHMIC 359-125G
KEUFFEL & ESSER CO.
3 X 5 CYCLES

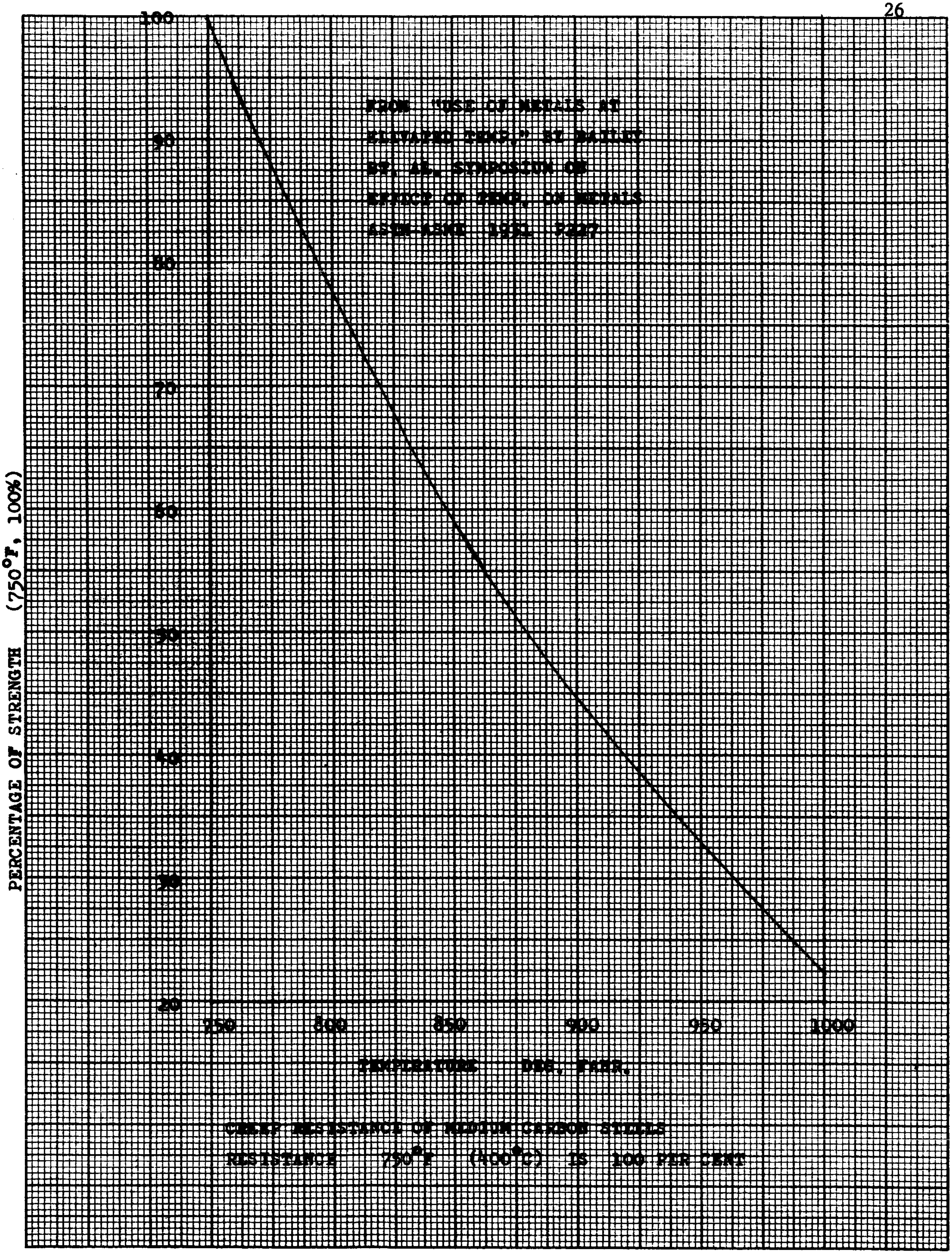
FROM "USE OF METALS AT
ELEVATED TEMP." BY BAILEY
ET. AL. SYMPOSIUM ON
EFFECT OF TEMP. ON METALS
ASTM-ASME 1931 P227
PERCENTAGE OF STRENGTH (750°F, 100%)
100
90
80
70
60
50
40
30
20
750
800
850
900
950
1000
TEMPERATURE DEG. FAHR.
CREEP RESISTANCE OF MEDIUM CARBON STEELS
RESISTANCE 750°F (400°C) IS 100 PER CENT

STRESS IN MAGNETIC STEELS

"The magnetic properties of most ferromagnetic materials change with the application of stress to such an extent that stress may be ranked with field strength and temperature as one of the primary factors affecting magnetic change. In some materials a tension of 10 Kg/mm^2 (14, 200 lb/in^2) will increase the permeability in low fields by a factor of 100; in others, the permeability is decreased by tension and in still others (e.g., iron) the permeability in low fields is increased and that in higher fields decreased.

In all materials, the saturation induction is unaffected by a stress within the elastic limit, and it is affected by stresses large enough to produce plastic flow only when a change of phase or state of atomic ordering occurs in the material." From "Ferromagnetism" by Bozorth, page 595.

ALLOY STRUCTURAL STEELS

Low alloy steels can be used in applications requiring good flux-carrying ability and high strength. Some of them are suitable for use in high-speed rotors at temperatures up to 500° C after which temperature they are little better than ordinary carbon-steel.

Some of the tool steels are usable above 1000° F.

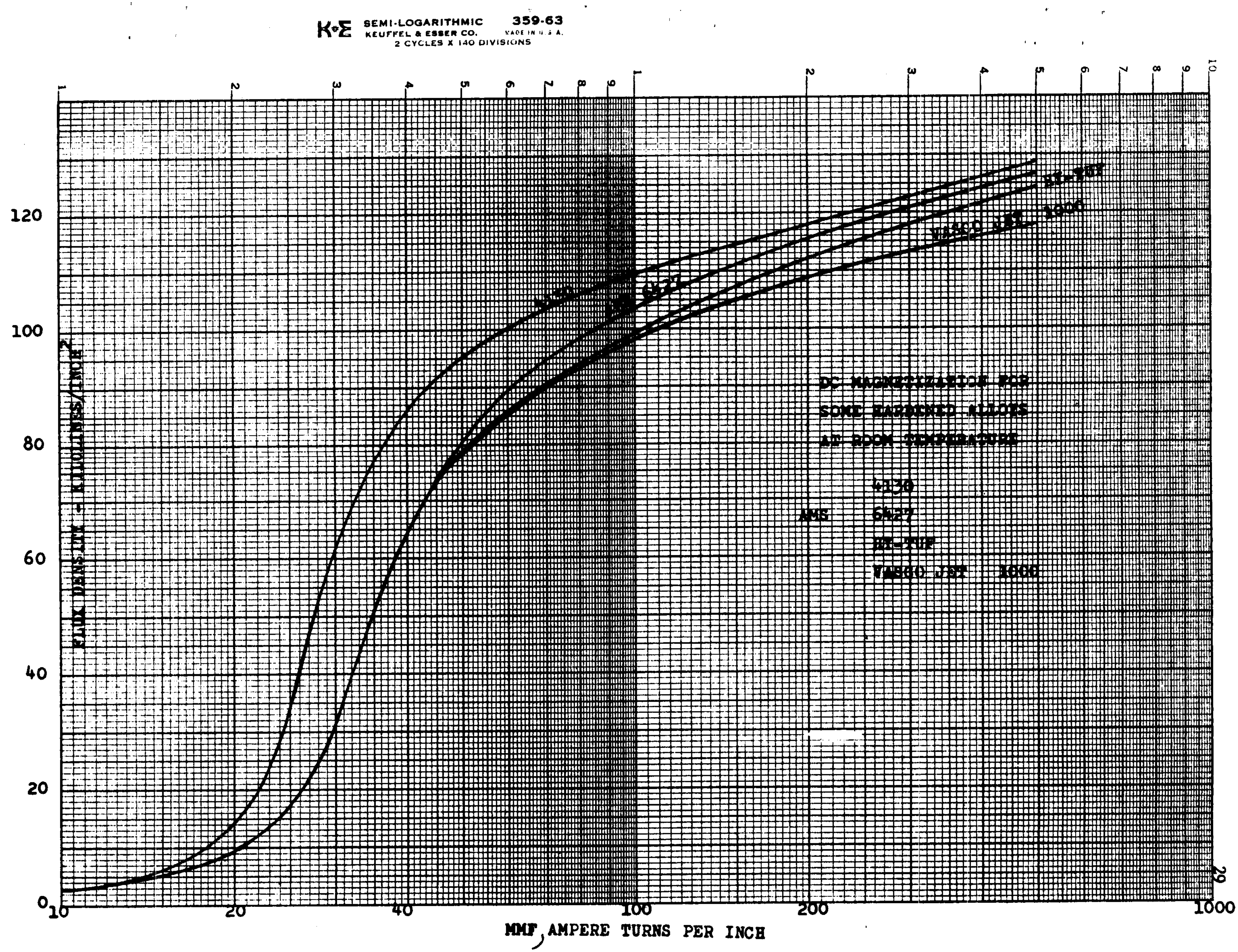
K+E SEMI-LOGARITHMIC 359-63
KEUFFEL & ESSER CO. MADE IN U.S.A.
2 CYCLES X 140 DIVISIONS
DC MAGNETIZATION FOR
SOME HARDENED ALLOYS
AT ROOM TEMPERATURE
4130
AMS 6427
HY-TUF
VASCO JET 1000
4130
6427
HY-TUF
VASCO JET 1000
FLUX DENSITY - KILOLINES/INCH^2
MMF, AMPERE TURNS PER INCH
0
20
40
60
80
100
120
10
20
40
100
200
1000

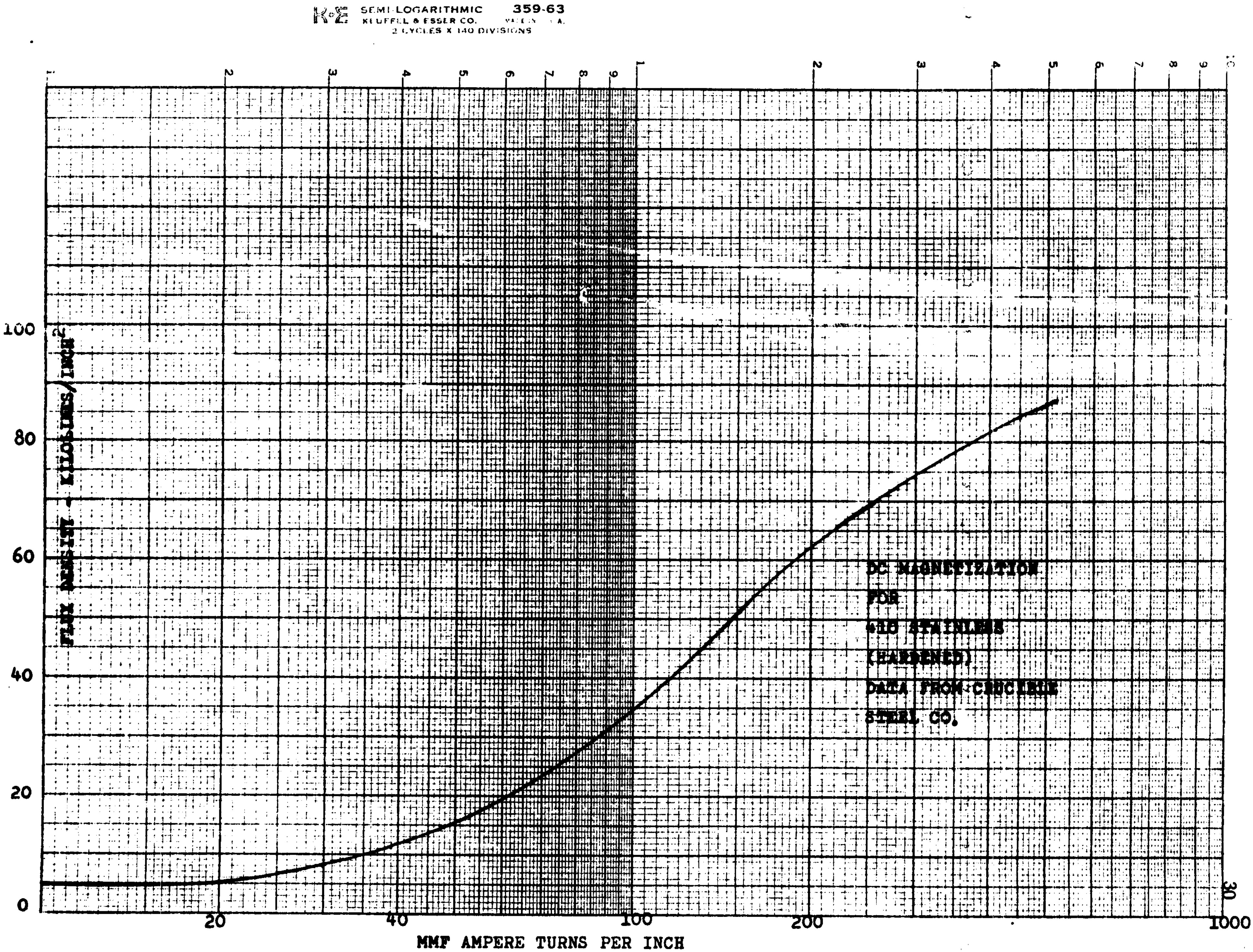

K+E SEMI-LOGARITHMIC 359-63
KEUFFEL & ESSER CO.
2 CYCLES X 140 DIVISIONS
DC MAGNETIZATION
FOR
410 STAINLESS
(HARDENED)
DATA FROM CRUCIBLE
STEEL CO.
FLUX DENSITY - KILOLINES/INCH^2
MMF AMPERE TURNS PER INCH
0
20
40
60
80
100
20
40
100
200
1000
30

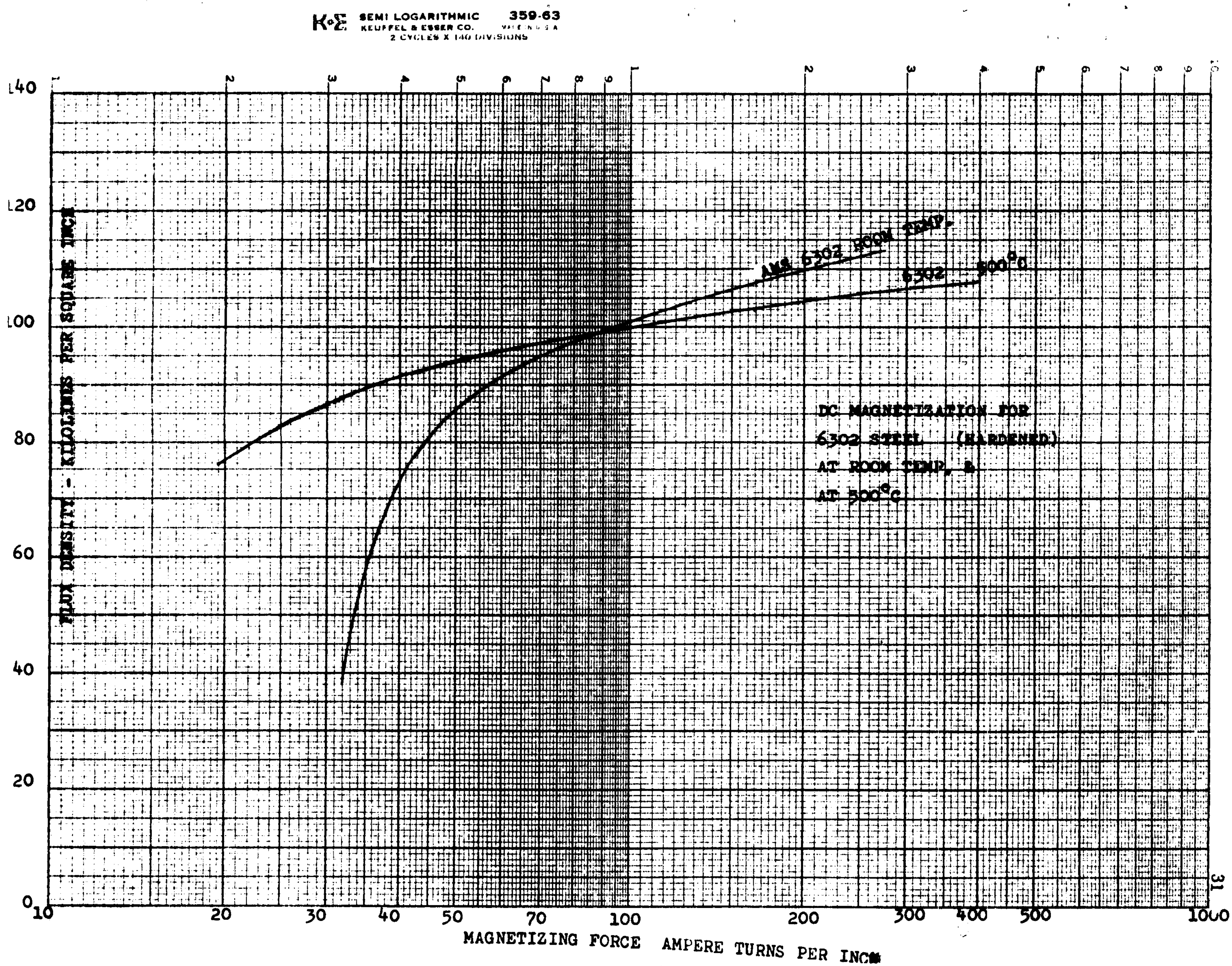

K+E SEMI LOGARITHMIC 359-63
KEUFFEL & ESSER CO.
2 CYCLES X 140 DIVISIONS
AMS 6302 ROOM TEMP.
6302 500°C
DC MAGNETIZATION FOR
6302 STEEL (HARDENED)
AT ROOM TEMP. &
AT 500°C
FLUX DENSITY - KILOLINES PER SQUARE INCH
MAGNETIZING FORCE AMPERE TURNS PER INCH

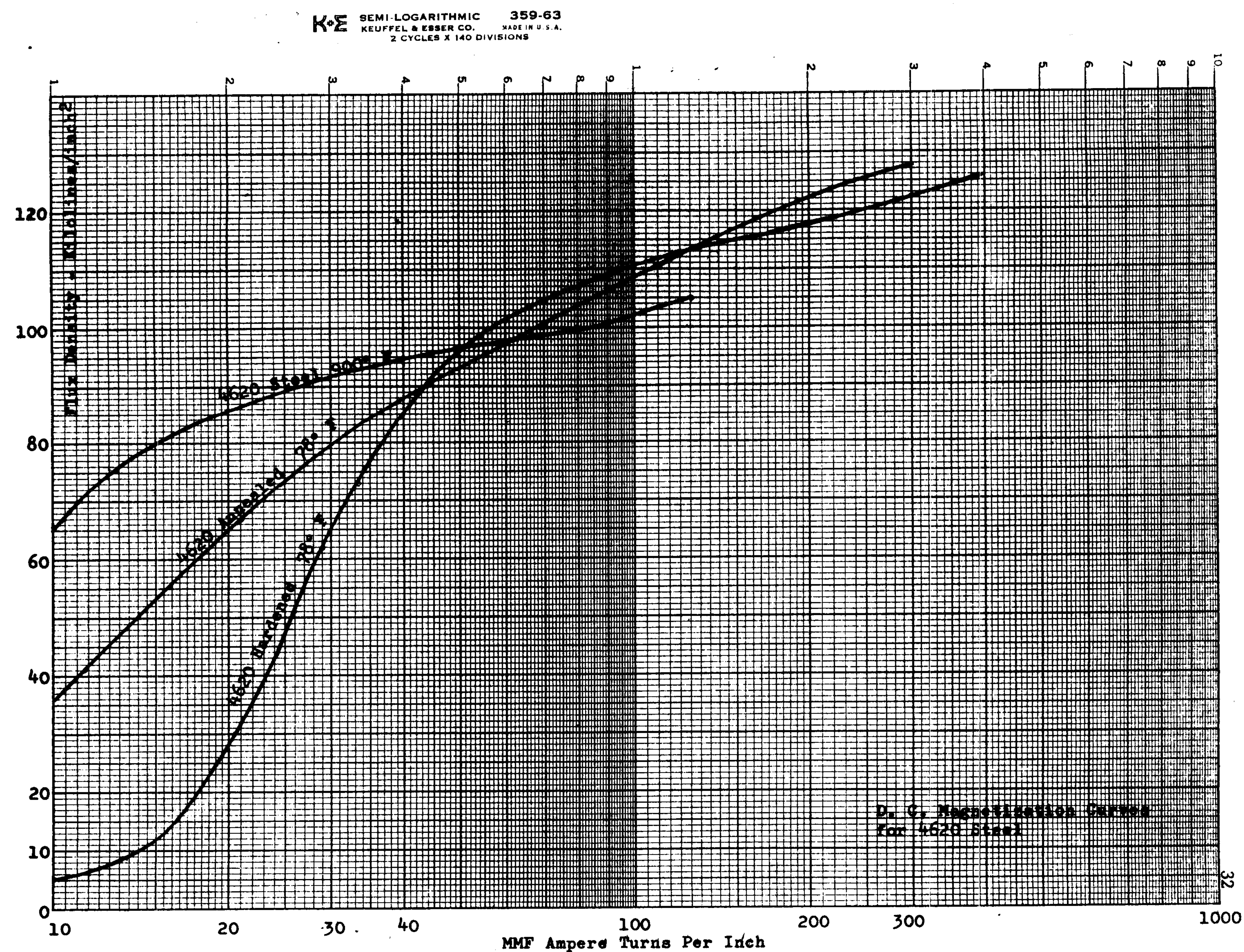

K+E SEMI-LOGARITHMIC 359-63
KEUFFEL & ESSER CO. MADE IN U.S.A.
2 CYCLES X 140 DIVISIONS
D. C. Magnetization Curves
for 4620 Steel
4620 Steel 900° F
4620 Annealed 78° F
4620 Hardened 78° F
Flux Density - Kilolines/inch²
MMF Ampere Turns Per Inch
10
20
30
40
100
200
300
1000
0
10
20
40
60
80
100
120

32

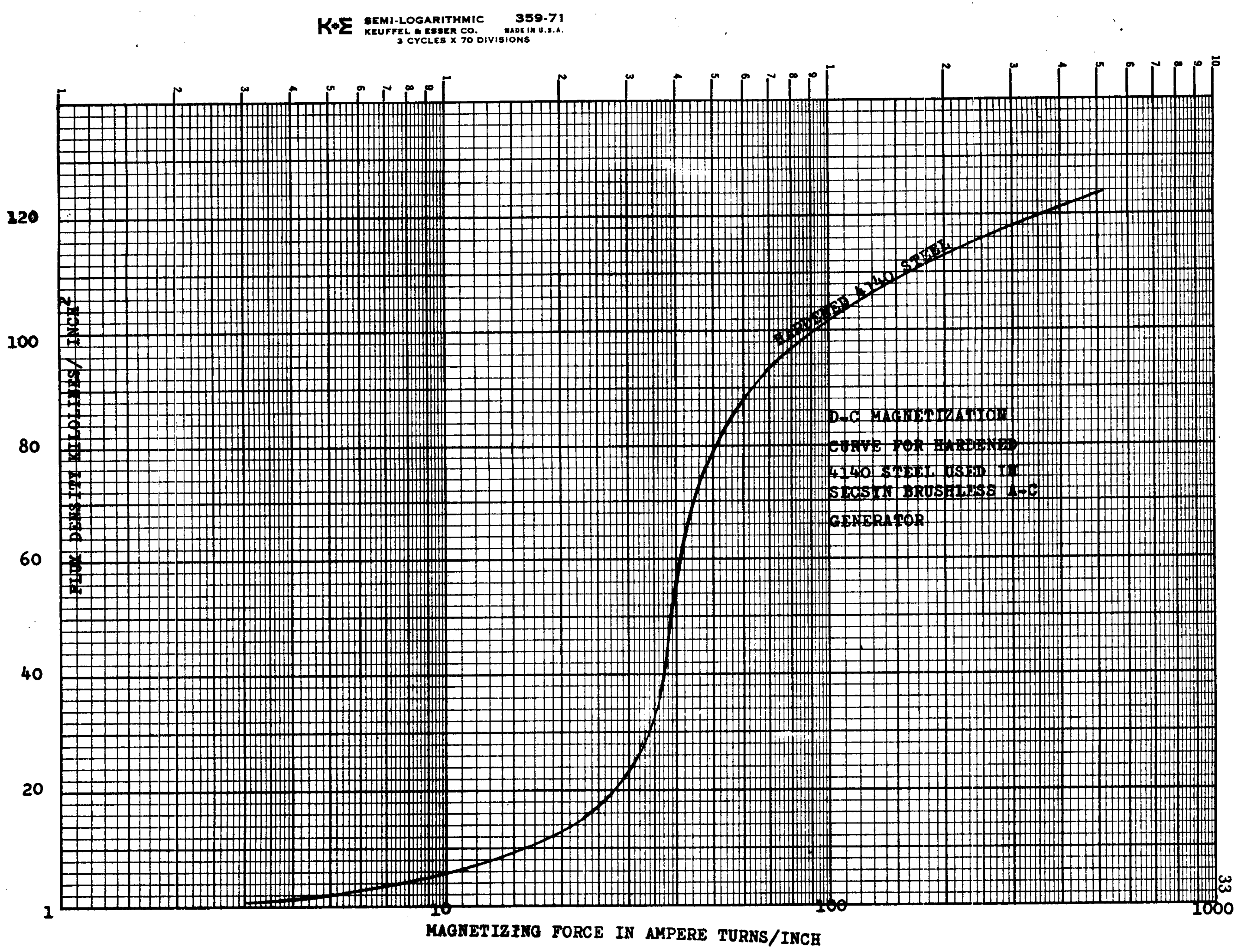
K+E SEMI-LOGARITHMIC 359-71
KEUFFEL & ESSER CO. MADE IN U.S.A.
3 CYCLES X 70 DIVISIONS
HARDENED 4140 STEEL
D-C MAGNETIZATION
CURVE FOR HARDENED
4140 STEEL USED IN
SECSYN BRUSHLESS A-C
GENERATOR
FLUX DENSITY KILOLINES/INCH²
120
100
80
60
40
20
1
10
100
1000
MAGNETIZING FORCE IN AMPERE TURNS/INCH

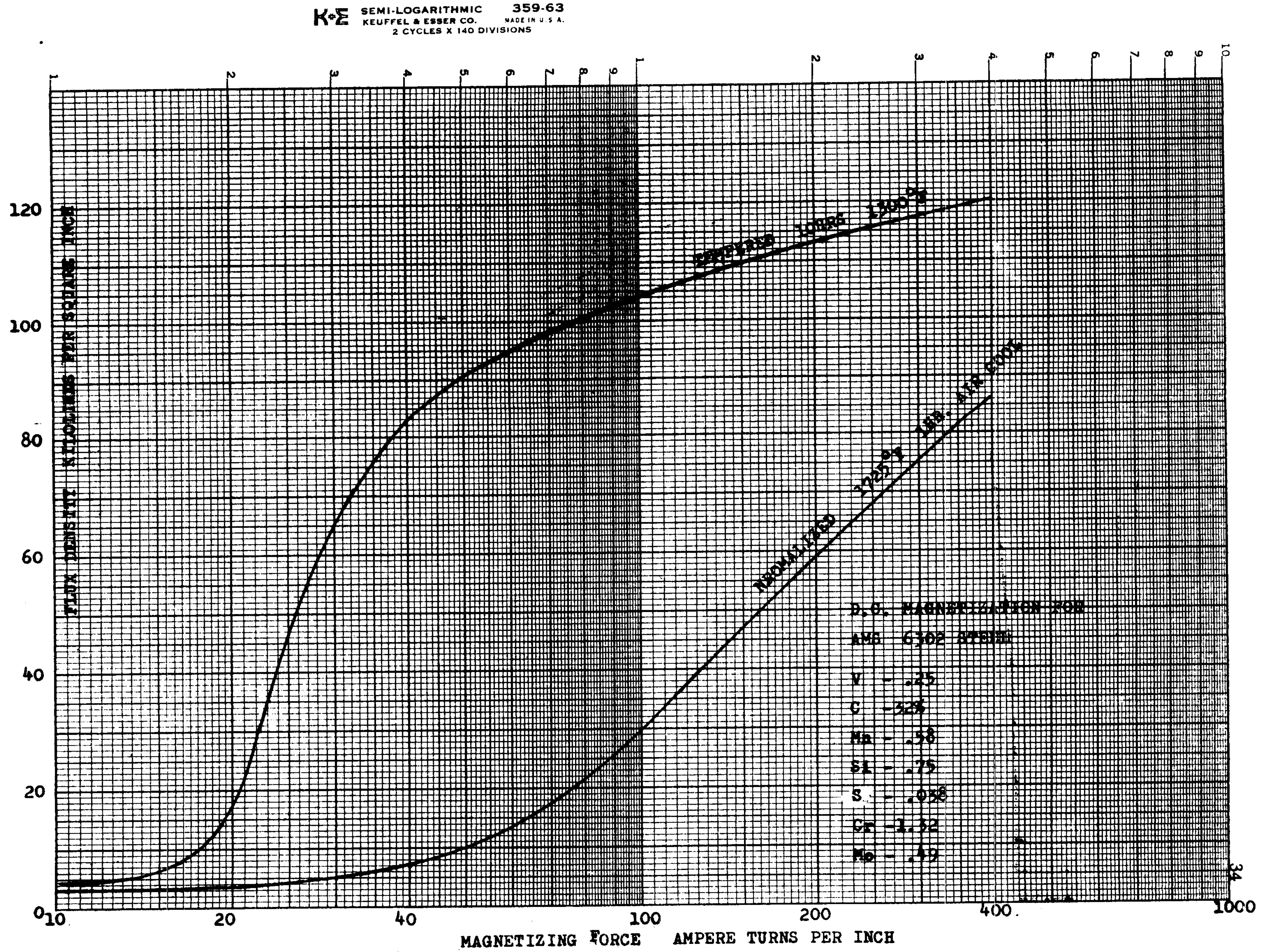
K+E SEMI-LOGARITHMIC 359-63
KEUFFEL & ESSER CO. MADE IN U.S.A.
2 CYCLES X 140 DIVISIONS
FLUX DENSITY KILOLINES PER SQUARE INCH
MAGNETIZING FORCE AMPERE TURNS PER INCH
1300°F
NORMALIZED 1725°F 1 HR. AIR COOL
D.C. MAGNETIZATION FOR
AMS 6302 STEEL
V - .25
C - .32%
Mn - .58
Si - .75
S - .038
Cr - 1.32
Mo - .49
0
20
40
60
80
100
120
10
20
40
100
200
400
1000

PERMANENT-MAGNET STEELS

The Alnicos are used almost exclusively in permanent magnet generators because their energy product is much higher than that of the older magnet alloys. Since permanent magnet materials are sometimes used in rotors of electromagnetic machines (because of strength or residual magnetic properties), the hysteresis loops and BH curves of the various common permanent magnet alloys are given here and a table of the worlds best-known permanent-magnet alloys is included.

One curve shows the effect of alternating magnetic fields on the PM alloys and another the effect of physical impacts.

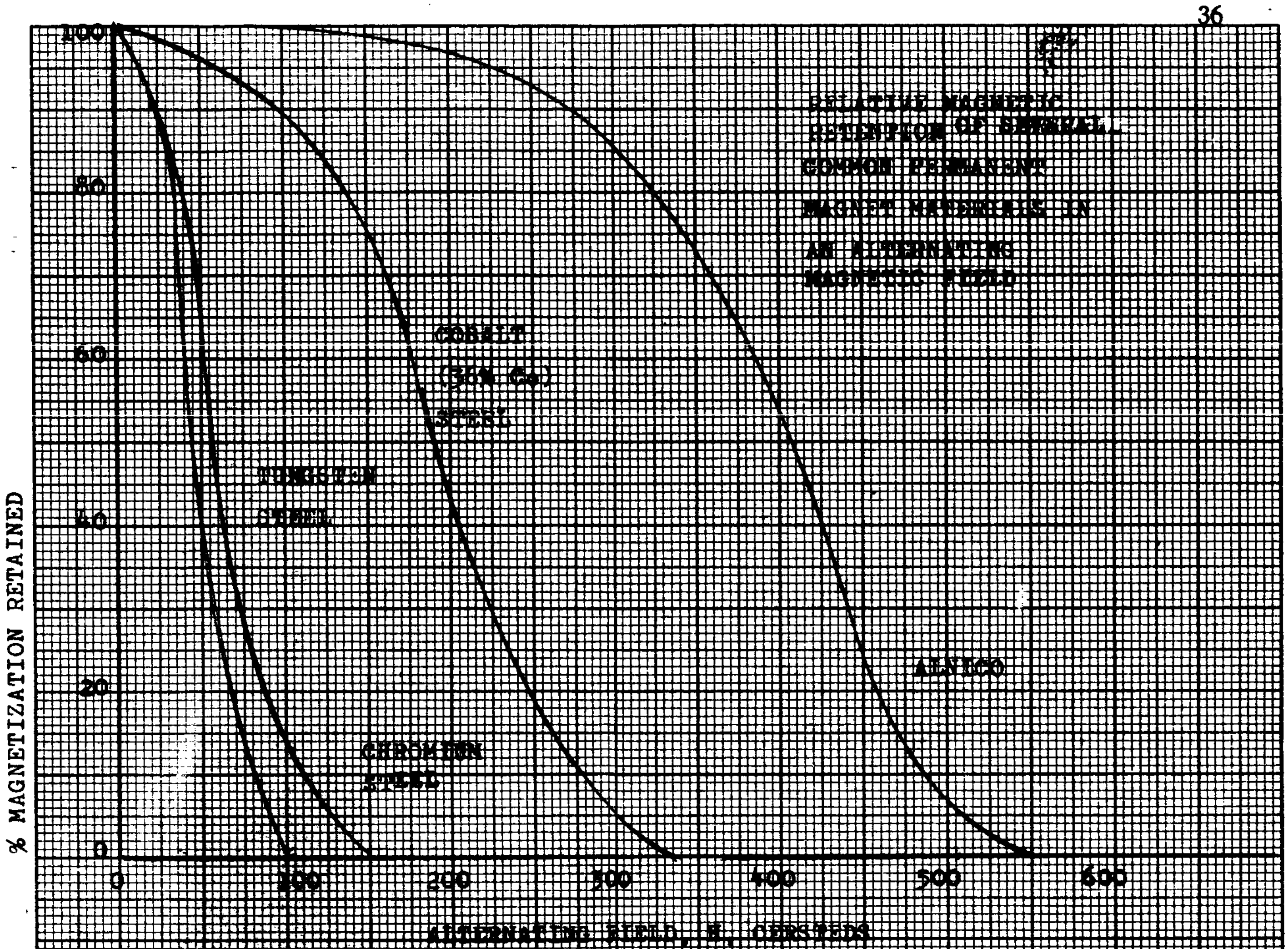
RELATIVE MAGNETIC RETENTION OF SEVERAL COMMON PERMANENT MAGNET MATERIALS IN AN ALTERNATING MAGNETIC FIELD
% MAGNETIZATION RETAINED
100
80
60
40
20
0
COBALT (36% Co) STEEL
TUNGSTEN STEEL
CHROMIUM STEEL
ALNICO
0
100
200
300
400
500
600
ALTERNATING FIELD, H, OERSTEDS

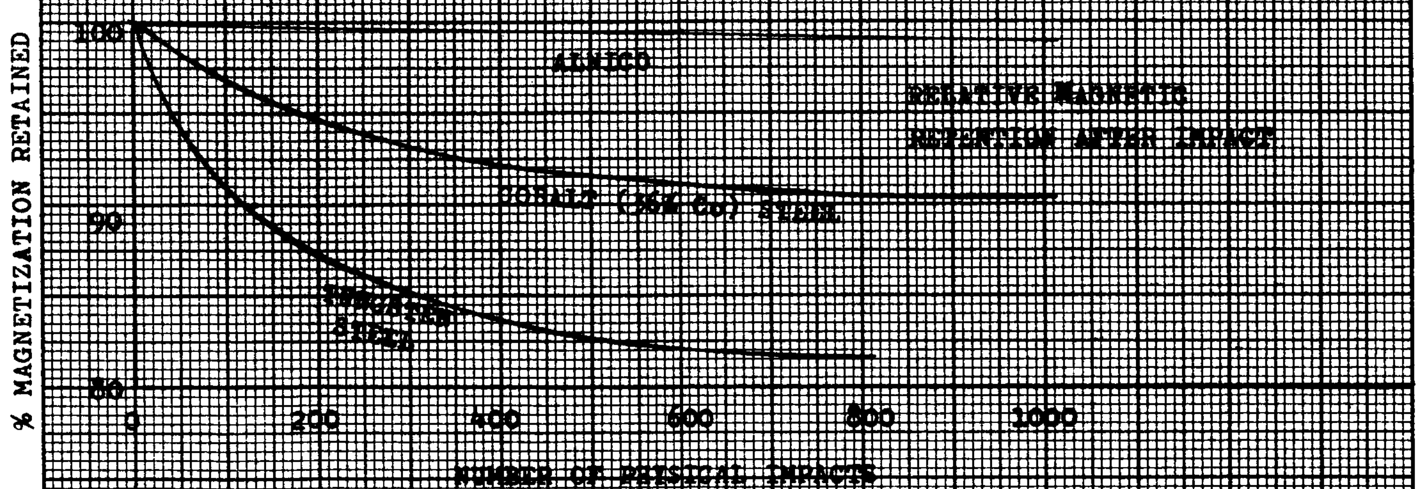
% MAGNETIZATION RETAINED
100
90
80
ALNICO
RELATIVE MAGNETIC RETENTION AFTER IMPACT
COBALT (36% Co) STEEL
TUNGSTEN STEEL
0
200
400
600
800
1000
NUMBER OF PHYSICAL IMPACTS

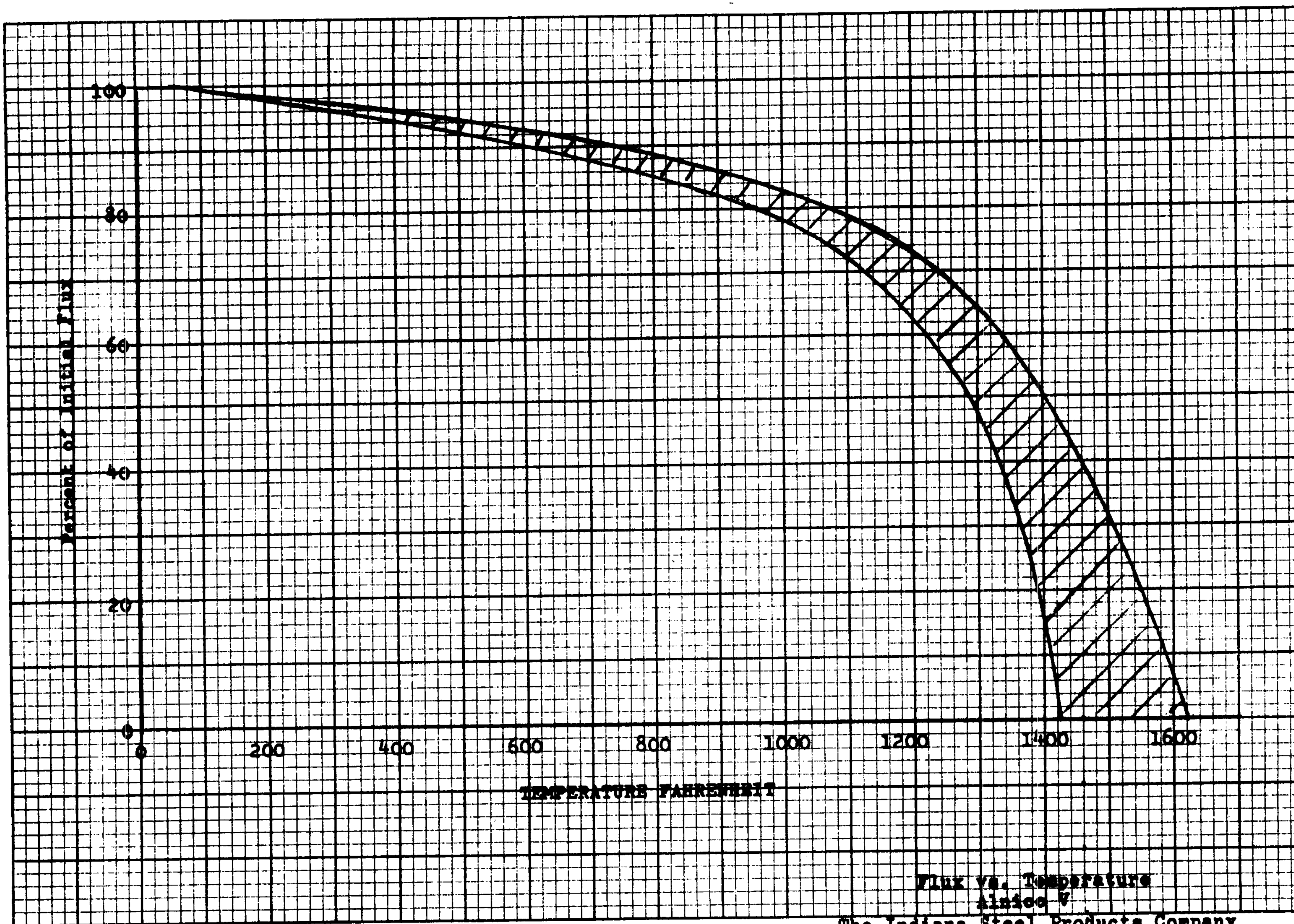

Flux vs. Temperature
Alnico V
The Indiana Steel Products Company
Valparaiso, Indiana

1% CARBON STEEL

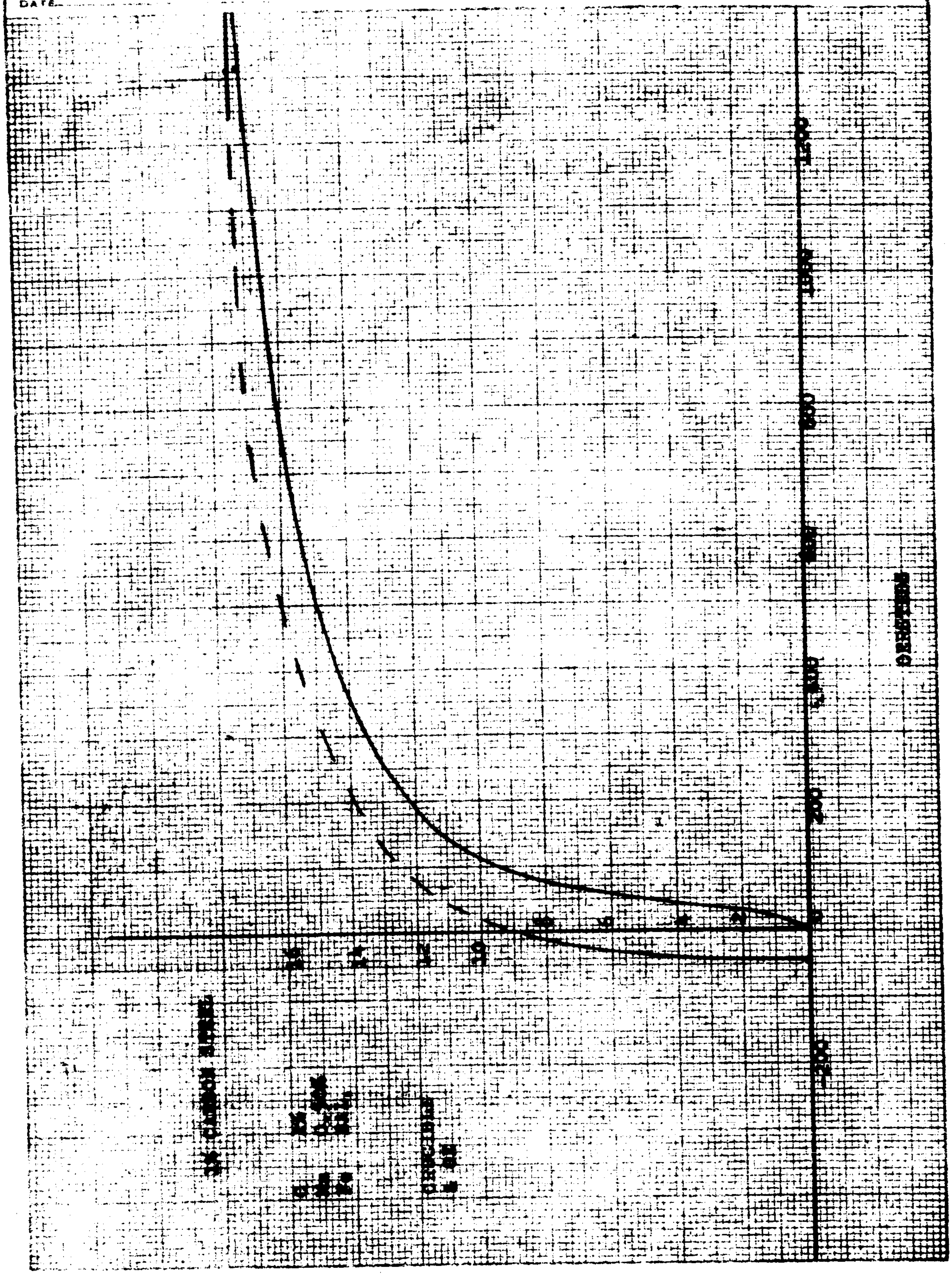

SHOWING

DATE

3.5% CHROME STEEL

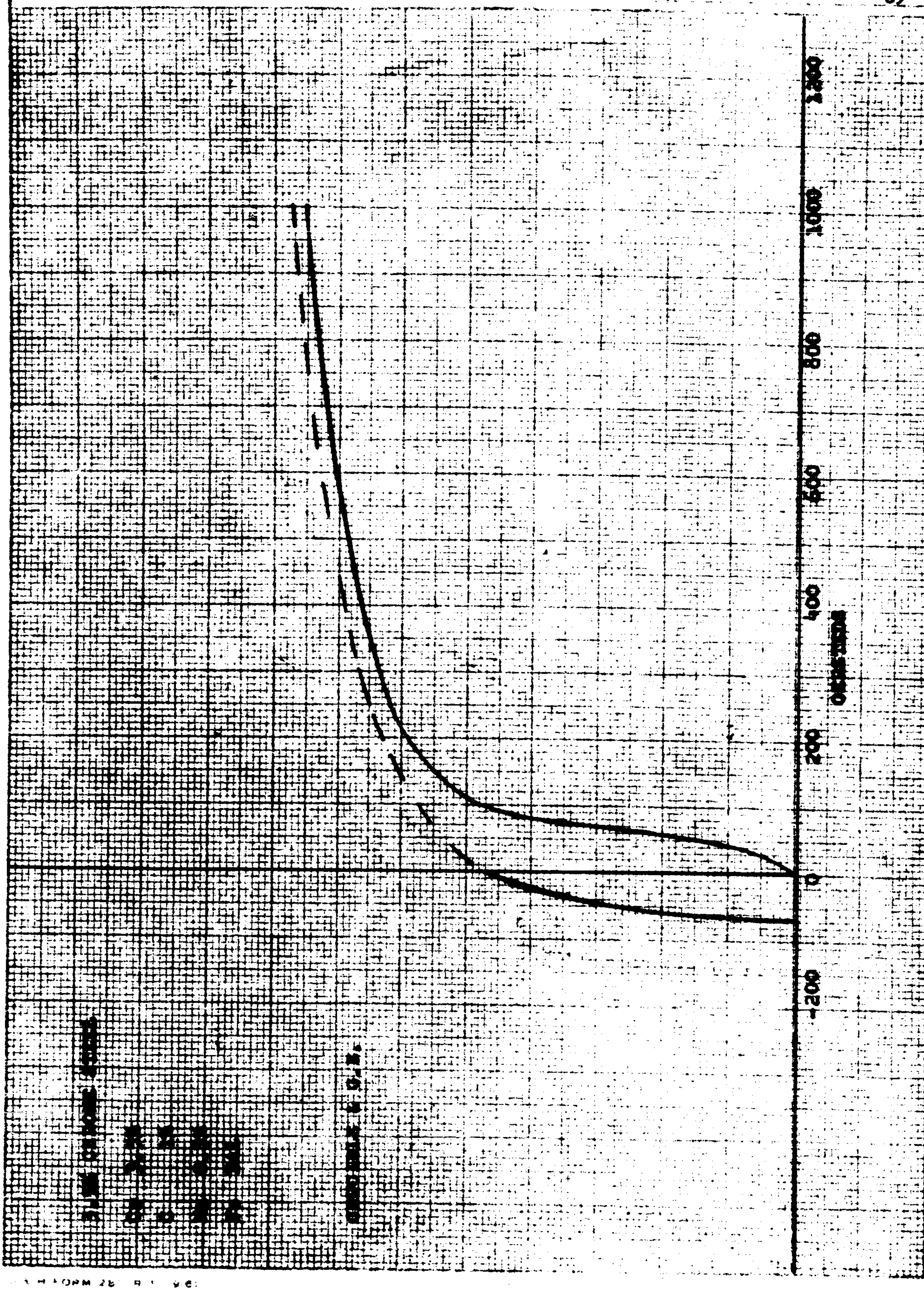

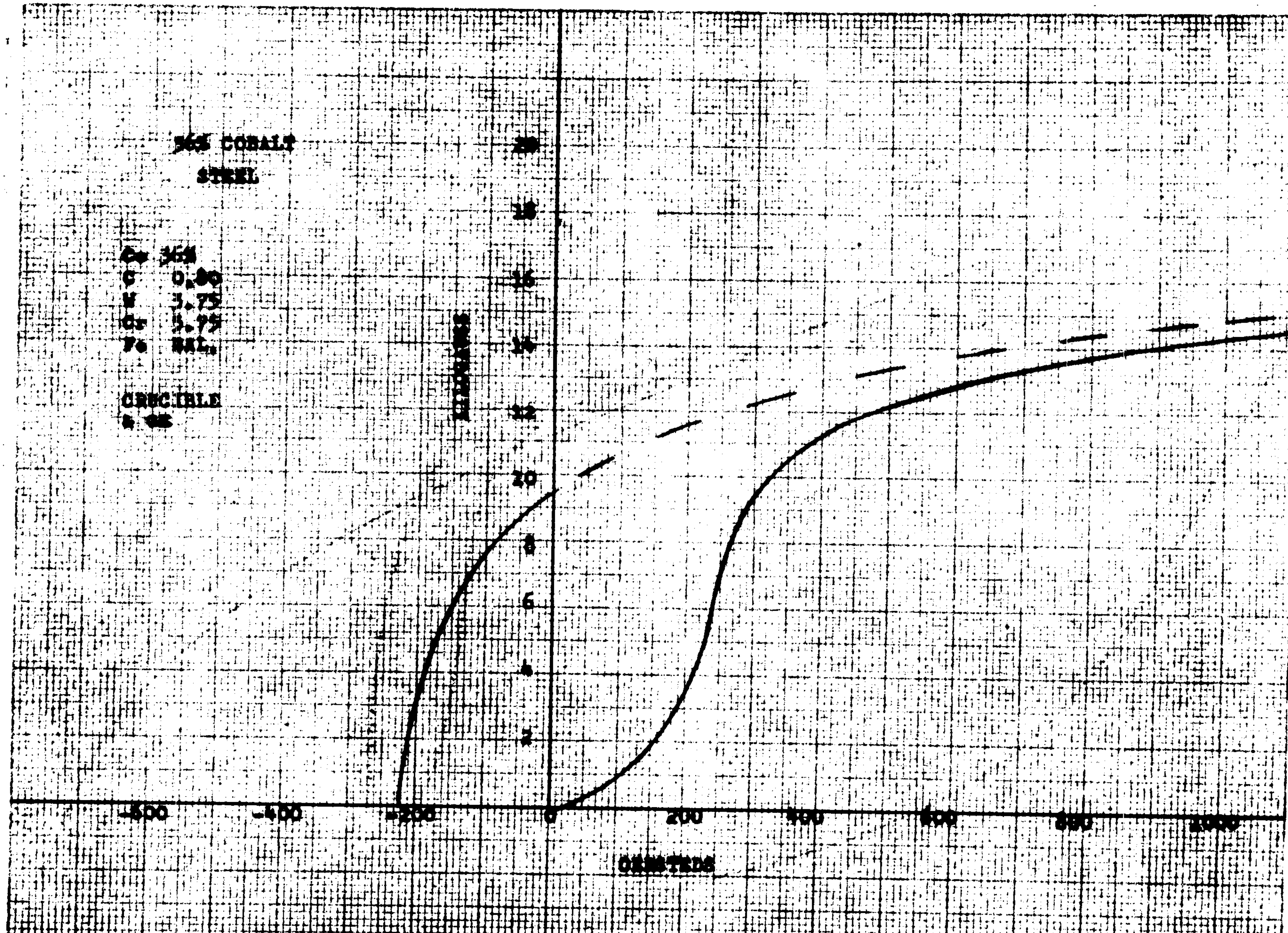
COBALT
STEEL
C 0.80
3.75
CRUCIBLE
-600
-400
0
200
400
600
2
4
6
8
10
12
14
16
18

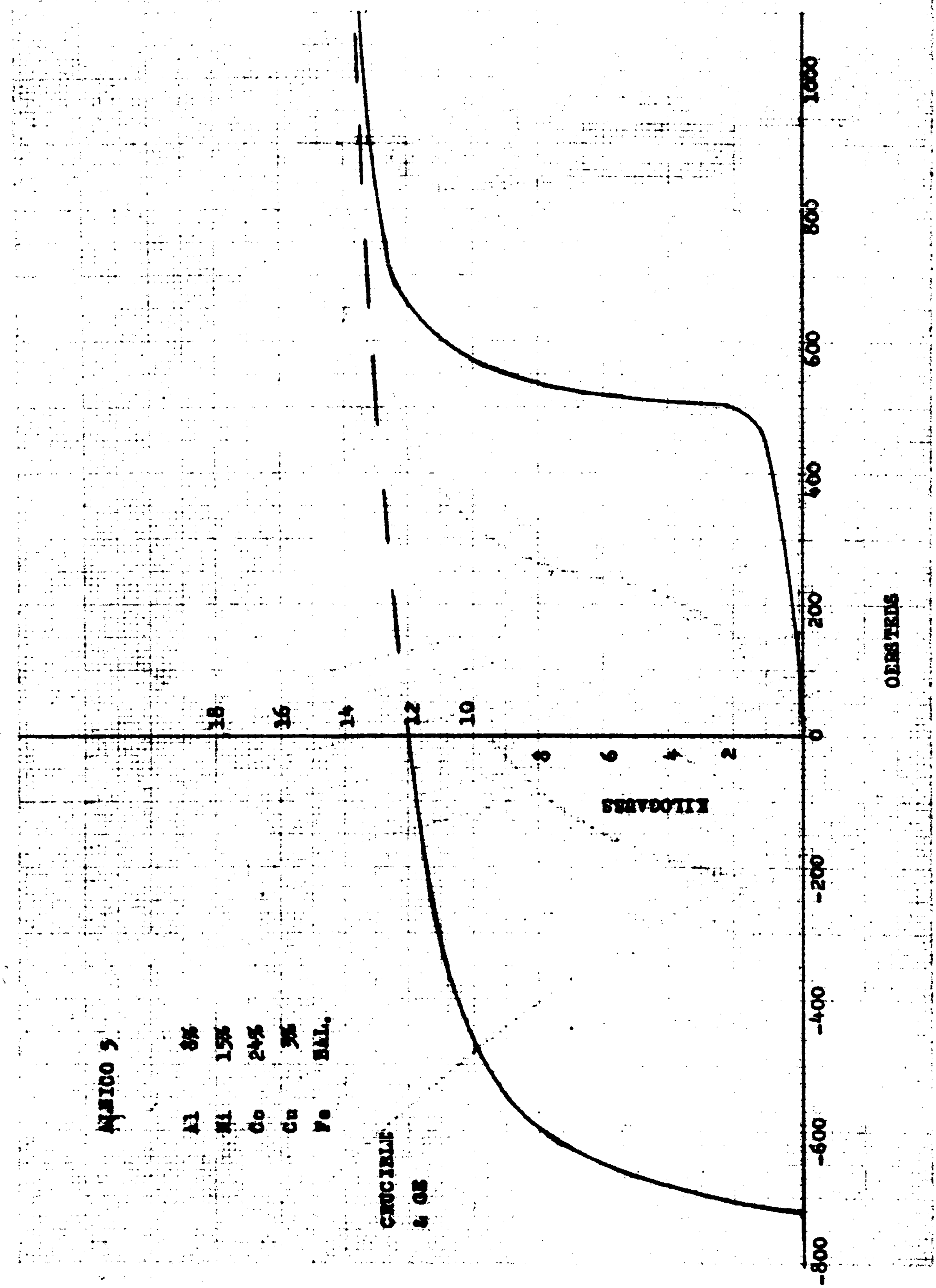
ALNICO 5
Al 8%
Ni 15%
Co 24%
Cu 3%
Fe BAL.
CRUCIBLE
& GE
KILOGAUSS
OERSTEDS
18
16
14
12
10
8
6
4
2
-800
-600
-400
-200
0
200
400
600
800
1000

ALNICO 6

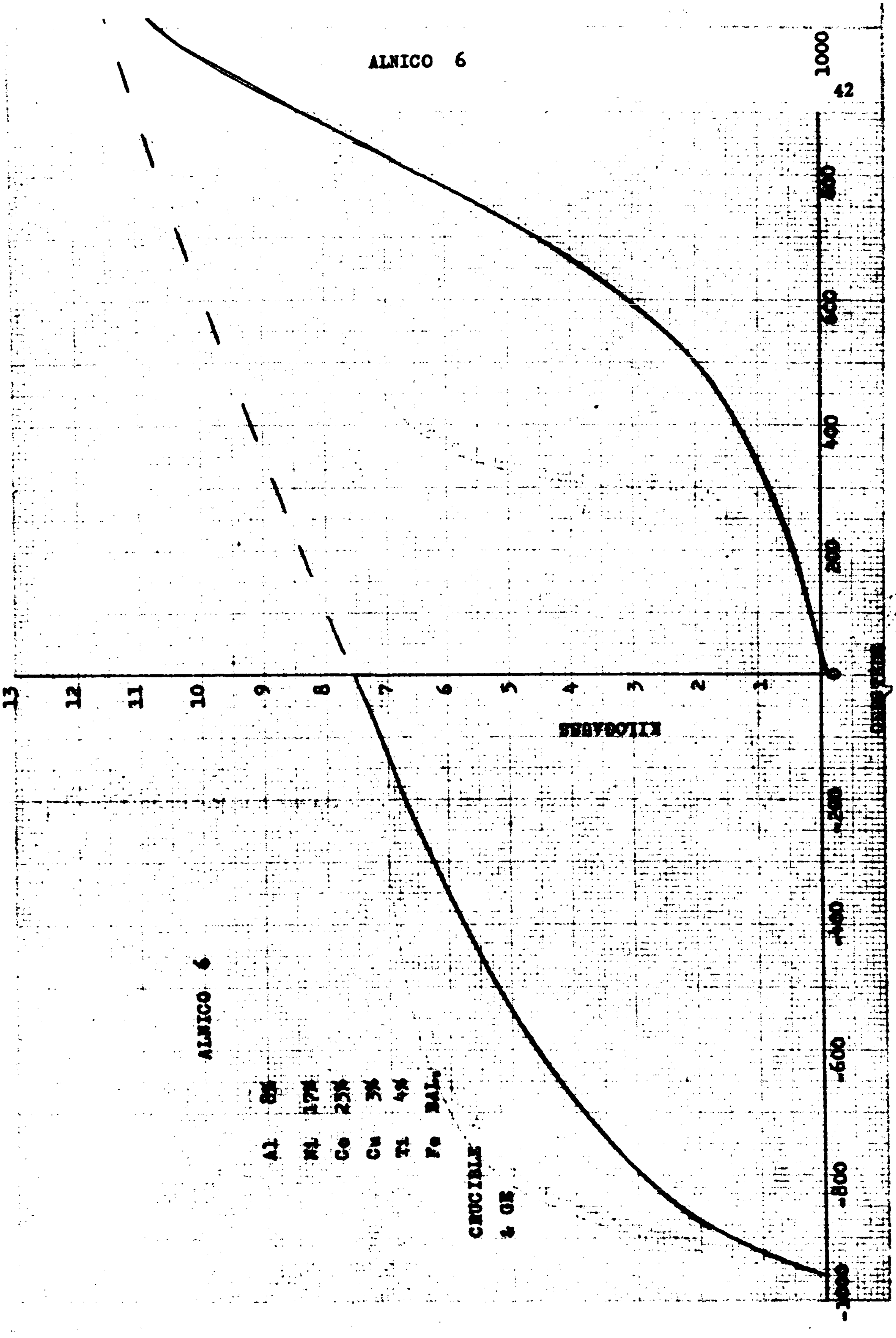
ALNICO 6
Al 8%
Ni 17%
Co 25%
Cu 3%
Ti 4%
Fe BAL.
CRUCIBLE
KILOGAUSS
OERSTEDS
13
12
11
10
9
8
7
6
5
4
3
2
1
0
-1000
-800
-600
-400
-200
200
400
600
800
1000

The following list of cobalt steels known as "hard" magnetic steels was taken from Cobalt No. 4 Sept., 1959, the publication of the Cobalt Information Center in Brussels.

Cobalt Steels		Composition	B_r Gauss
2% Cobalt Steel (G. B.) Co 040) 16/120/48) WH) K2)	Germany	4 Cr 2 Co 1 C 0.6 W	9800
3% Cobalt Steel (G. B.) Co 045) 18/97/47) Kobalt 100) HA 1 (Belgium) KS 4 (Japan)	Germany	9 Cr 3 Co 1.5 MO 1 C	7200
6% Cobalt Steel (G. B.) Co 050) 20/68/44) Kobalt 125) K 6) HA 2 (Belgium) MS 6 (Switzerland)	Germany	9 Cr 6 Co 1.5 MO 1 C	7800
9% Cobalt Steel (G. B.) Co 160) 25/51/43) KS 3 (Japan)	Germany	9 Co 9 Cr 1.5 MO 1 C	8000
11% Cobalt Steel) Co 060) K 11)	Germany	11 Co 8.5 Cr 1.5 MO 1 C	8400
15% Cobalt Steel (G. B.) Co 070 Kobalt 200 28/46/43 K 16 HA 3 (Belgium) MS 15 (Switzerland) KS 2 (Japan)		15% Co 9 Cr 1.5 MO 1 C	8500

List of Cobalt Steels (Cont)

Cobalt Steels		Composition	B_r Gauss
17% Cobalt Steel (USA)		17 Co 8 W 2.5 Cr 0175 C	9500
20% Cobalt Steel (G. B.)		20 Co 9 Cr 1.5 MO 1 C	9000
30% Cobalt Steel Co 090 K 30	Germany	30 Co 4.5 Cr 4.5 W 0.9 C	8600
35% Cobalt Steel (G. B.) KS-1 (Japan)			
Co 100 Kobalt 300 40/35/42	Germany	35 Co 6 Cr 5 W 0.9 C	9000
Hi-Cobalt (USA) HA-4 (Belgium) MS-35 (Switzerland) Ergit Max 1 (Hungary)			
36% Cobalt Steel (USA)		36 Co 5 W 4 Cr 0.7 C	9500
38% Cobalt Steel (USA)		38 Co 5 W 4 Co 0.7 C	10000

DERIVATIONS

DERIVATION OF FORMULAS AND DESIGN NOTES

CONTENTS

GROUPING OF FRACTIONAL SLOT WINDINGS

When the stator is comprised of a winding having fractional slots per pole, the grouping of the coils can be determined by the following method.

Express the ratio of the number of slots to the number of poles as an improper fraction reduced to its lowest terms. The denominator will then represent the number of poles in a repeatable section and the numerator will then be the number of slots in a repeatable section. If the number of slots in a repeatable section is not divisible by the number of phases a balanced polyphase winding cannot be obtained.

The maximum number of parallel paths in the winding is found by dividing the number of poles of the machine by the number of poles in a repeatable section. This gives the maximum possible number of parallels.

To determine the grouping lay out a table having as many horizontal divisions as there are slots per repeatable section, and as many vertical divisions as there are poles per repeatable section. Divide the horizontal divisions into m number of phases and using a pitch of y = poles per repeatable section lay out the winding.

As an example consider a 3 phase, 20 pole, 84 slot machine, then 84/20 = 21/5 = (slots per repeatable section)/(poles per repeatable section). The maximum number of parallels possible = 20/5 = 4, and the available number of parallels will then be 4 and 2. Lay out the table as follows with y = 5 and throw = 1-6.

	1	2	3	4	5	6	7	8	9	10	11	12	13	14	15	16	17	18	19	20	21
1	x					x					x					x					x
2					x					x					x					x	
3				x					x					x					x		
4			x					x					x					x			
5		x					x					x					x				

Phase a **Phase c** **Phase b**

The grouping will thus be 21211-21211 = 21211 = and repeat 3 x 4 = 12 times. The coils will then be placed as follows:

Slot No.	1	2	3	4	5	6	7	8	9	10	11	12	13	14	15	16	17	18	19	20	21
Phase of Coil	+ a	+ a	- c	+ b	+ b	- a	+ c	- b	- b	+ a	- c	- c	+ b	- a	+ c	+ c	- b	+ a	+ a	- c	+ b
Grouping	2		1	2		1	1	2		1	2		1	1	2		1	2		1	1

Another way of accomplishing the same result as that given above is as follows:

Since there are 5 poles per repeatable section and 21 slots per repeatable section there must be 7 slots per phase in each repeatable section with these 7 slots occupying positions over 5 poles. The coils in a section may be arranged in any order but the best arrangement in general is that which gives the largest distribution factor. Usually the most symmetrical arrangement of the coils is best, or in this case 12121. Laying out the winding of the previous example for the 12121 arrangement gives:

Slot No.	1	2	3	4	5	6	7	8	9	10	11	12	13	14	15	16	17	18	19	20	21
Phase of Coil	+ a	- c	- c	+ b	- a	- a	+ c	- b	+ a	+ a	- c	+ b	+ b	- a	+ c	- b	- b	+ a	- c	- c	+ b
Grouping	1	2		1	2		1	1	2		1	2		1	1	2		1	2		1

which is the same as that arrived at previously with the exception that it is displaced several slots.

THE SLOT STAR

The two above methods of grouping can be verified by the slot star method.

In general let the number of slots per phase per pole q be represented as $q = N/B = a + b/B$. where a is an integer. Then the winding repeats itself after each B poles and the number of recurrent groups is equal to P/B. Each

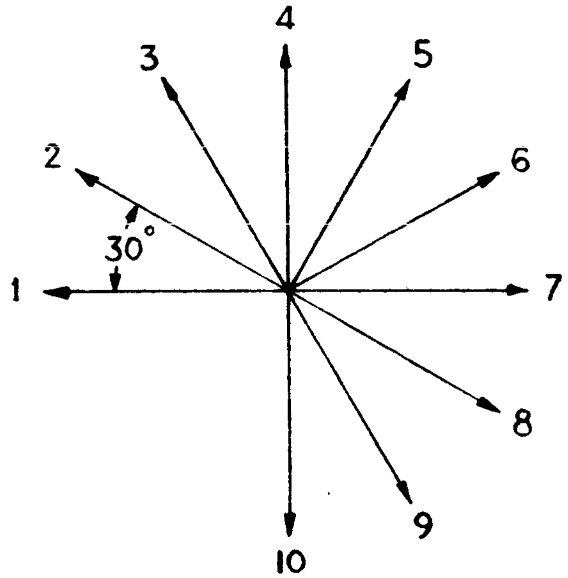

FIGURE 1

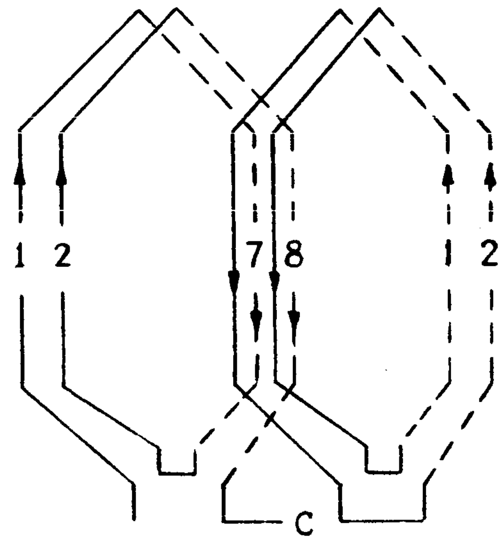

FIGURE 2

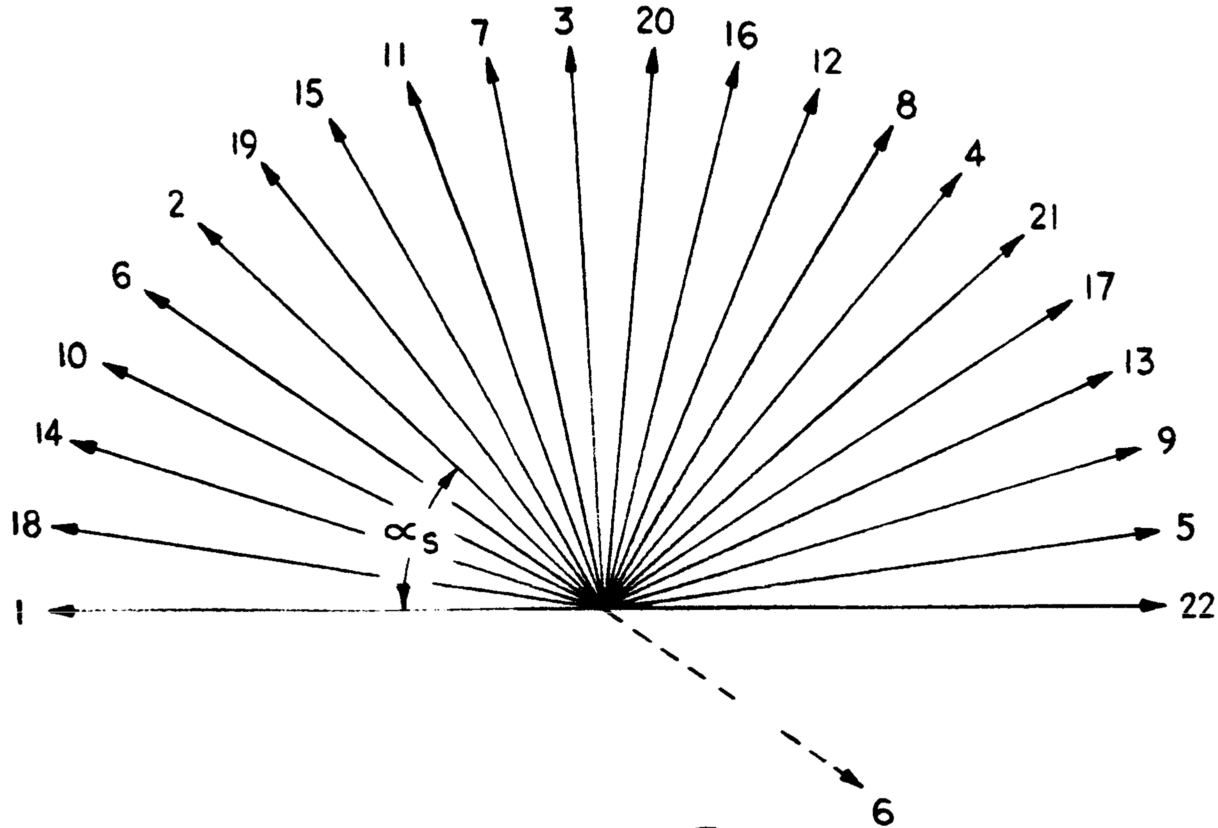

FIGURE 3

phase has N slots in B poles. Further, each phase has B - b coil groups with a coils and b coil groups with a + 1 coils in B poles. If B/m equals an integer there cannot be a perfectly balanced fractional slot winding.

Apply the above rules to the 3 phase, 20 pole, 84 slot example gives q = 84/(20 x 3) = 7/5 = 1 + 2/5. Thus the winding repeats itself after each 5 poles the number of recurrent groups is 20/5 = 4. Each phase has 7 slots in 5 poles and each phase had 5 - 2 = 3 coil groups with 1 coil and 2 coil groups with 1 + 1 = 2 coils in 5 poles.

The slot star of a 2 pole, 3 phase integral slot winding with q equals two is shown in Figure 1. The angle between two adjacent slots is $\alpha_s = 180^\circ/mq = 30^\circ$.

Two adjacent vectors correspond to two adjacent slots and thus slots 1, 2, 7, and 8 belong to phase I, slots 3, 4, 9, and 10 belong to phase II and so on. Vector 7 with which the second pole starts is shifted 180° with respect to vector 1, and the same applies for vectors 2 and 8, 3 and 9, etc. Therefore the bottom half of the slot star is the same as the top half except that their vectors are shifted by 180°.

The four coils of phase 1 are shown in Figure 2 with the solid lines representing the tops of the slots and the dotted lines representing the bottom. The connector C takes care that all the emfs add together and thus the slot star of this example is completely represented by only half of the circle.

The above type of star will then apply to the integral slot windings in general.

In the fractional slot winding, B poles make the recurrent group and just as for the integral slot winding the slot star of B poles is represented by half of a circle.

Figure 3 shows the slot star of the 20 pole, 3 phase, 84 slot example. There are 5 poles in B with 7 x 3 = 21 slots per recurrent group. $\alpha_s = 180/(3 \times 1.4)$

= 42 and 6/7°. Thus the angles which correspond to the slots are:

Slot No.	1	2	3	4	5	6
α_s -	0	42 6/7	85 5/7	128 4/7	171 3/7	214 2/7 = 34 2/7 etc.

Since the largest distribution factor for the fundamental is obtained when the slots belonging to each group are closest together, the first seven slots in the slot star will be assigned to phase a. The second seven to phase c, and the last seven to phase b. Thus slots 1, 18, 14, 10, 6, 2, and 19 are phase a; 15, 11, 7, 3, 20, 16, and 12 are phase c; and 8, 4, 21, 17, 13, 9, and 5 are phase b.

The grouping then becomes

<table>
<tr><td>Slot No.</td><td>1</td><td>2</td><td>3</td><td>4</td><td>5</td><td>6</td><td>7</td><td>8</td><td>9</td><td>10</td><td>11</td><td>12</td><td>13</td><td>14</td><td>15</td><td>16</td><td>17</td><td>18</td><td>19</td><td>20</td><td>21</td></tr>
<tr><td>Phase of
Coil</td><td>+
a</td><td>+
a</td><td>-
c</td><td>+
b</td><td>+
b</td><td>-
a</td><td>+
c</td><td>-
b</td><td>-
b</td><td>+
a</td><td>-
c</td><td>-
c</td><td>+
b</td><td>-
a</td><td>+
c</td><td>+
c</td><td>-
b</td><td>+
a</td><td>+
a</td><td>-
c</td><td>+
b</td></tr>
<tr><td>Grouping</td><td colspan="2">2</td><td>1</td><td colspan="2">2</td><td>1</td><td>1</td><td colspan="2">2</td><td>1</td><td colspan="2">2</td><td>1</td><td>1</td><td colspan="2">2</td><td>1</td><td colspan="2">2</td><td>1</td><td>1</td></tr>
</table>

This is identical with the grouping of the first method and therefore verifies its accuracy.

In the integral slot winding the beginnings of the phases are displaced by 120 and 240 electrical degrees. Also in the fractional slot windings the distances between the beginnings of the phases can be made 120 and 240°. This will be the case when the beginnings are placed in slots 1, 1 + N, and 1 + 2N when B is an even number, and in slots 1, 1 + 2N, and 1 + (1 + m) N, when B is an odd number. This arrangement of the beginnings of the phases will place them far apart from each other mechanically while it is often desirable to have them near to each other. In order to place the beginnings of the phases near to each other the beginnings can be placed approximately 120 and 240 electrical degrees apart and the windings still will be balanced. This is due to the fact that in the fractional slot winding the emfs of the consecutive coil groups are not in phase and the sequence of the geometric addition of the single emfs is of no influence on the resultant phase emf. So in the ~~example~~ considered the beginnings of the phases can be placed in slot 1 for phase a, slot 4 for phase b, and slot 7 for phase c. The angles between the beginnings are then 128 and $4/7^{\circ}$, and 257 and $1/7^{\circ}$.

DISTRIBUTION FACTOR

The voltages induced in the separate coils of a distributed winding are not in exact phase and their resultant is therefore less than would be produced in a concentrated winding having the same number of turns. The ratio of the voltages produced by distributed and concentrated windings having the same number of turns is called the distribution factor. In the case of integral slots per phase per pole it can be derived as follows:

$$\theta = \text{electrical angle per phase group}$$

$$\theta = q\,\alpha_s$$

$$\sin\frac{\alpha_s}{2} = \frac{e/2}{r} = \frac{e}{2r}$$

$$r = \frac{e}{2\sin\frac{\alpha_s}{2}}$$

$$\sin\frac{\theta}{2} = \sin\frac{q\,\alpha_s}{2} = \frac{E}{2r}$$

$$E = 2r\sin\frac{q\,\alpha_s}{2} = 2\left(\frac{e}{2\sin\frac{\alpha_s}{2}}\right)\sin\frac{q\,\alpha_s}{2} = \frac{e\sin\frac{q\,\alpha_s}{2}}{\sin\frac{\alpha_s}{2}}$$

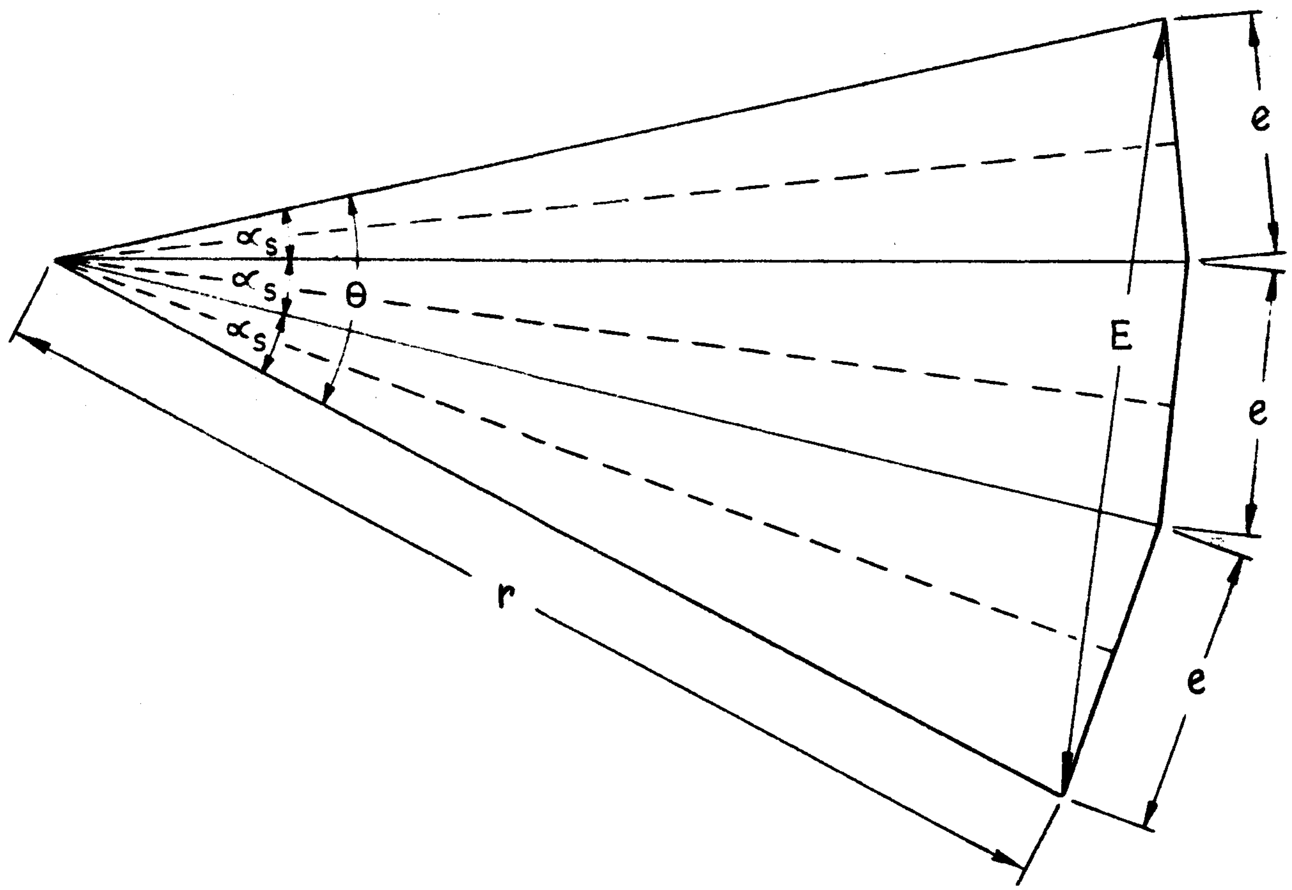

e
e
e
E
θ
α_s
α_s
α_s
r

$$\text{Thus } K_d = \left(\frac{e \sin \frac{q\alpha_s}{2}}{\sin \frac{\alpha_s}{2}} \right) \div qe = \frac{\sin \frac{q\alpha_s}{2}}{q \sin \frac{\alpha_s}{2}}$$

Since a displacement of α_s between the slots is $n\alpha_s$ for the nth harmonic,

K_{dn} for the nth harmonic is $K_{dn} = \dfrac{\sin \frac{qn\alpha_s}{2}}{q \sin \frac{n\alpha_s}{2}}$

FRACTIONAL SLOT DISTRIBUTION FACTOR

Refer to the slot star shown in Figure 3 of the section titled "Grouping of Fractional Slot Windings" and it will be noted that to determine K_d for a fractional slot winding it is necessary to distinguish between the angle between two slots α_s and the angle between two vectors α_m. This latter angle is the magnetic field angle between the slots of the recurrent group and this angle determines the phase difference between the vectors. The magnetic field angle is $\alpha_m = 180^\circ/Nm$ where N is the same as in "Grouping of Fractional Slot Windings".

It can be seen from the slot star that the fractional slot winding thus behaves like a winding with N slots per phase per pole shifted with respect to each other by the magnetic field angle α_m. Therefore the distribution factor is

$$K_d = \frac{\sin \frac{N\alpha_m}{2}}{N \sin \frac{\alpha_m}{2}}$$

The general effect of distributing a winding is to smooth out the wave form by diminishing the amplitude of the harmonics with respect to the fundamental. The distribution of the armature copper loss is also improved.

The distribution factor of the three phase winding is greater than that of the two phase winding and for this reason the three phase winding is used where there is a free choice of the number of phases. The distribution factor of the single phase winding is much smaller than that of either 3 or 2 phase windings because the winding is distributed over a larger arc.

In general only 2/3 of the slots per pole are used in winding single phase machines. The reason for this can be best shown by an example. Let the number of slots per pole equal 9, and if all slots were wound then $\alpha_s = 180^o/9 = 20^o$, and

$$K_d = \frac{\sin\left(9 \times \frac{20}{2}\right)}{9 \times \sin 10^o} = \frac{1}{1.563} = .640$$

If only 6 slots are wound

$$K_d = \frac{\sin (6 \times 10)}{6 \times \sin 10} = .832$$

Thus, for 9 slots the number of effective turns is only $\frac{9 \times .640}{6 \times .832} = 1.15$ times the number of effective turns obtained when using 6 slots, and therefore by using 50% more copper with its additional 50% more loss, only 15% more voltage has been obtained.

SKEW FACTOR

It can be noted in the table of distribution factors that some harmonics have the same distribution factor as the fundamental. These harmonics are called the slot harmonics and their orders are

$$n = \left[K (2mq)\right] \pm 1 = K\left(\frac{Q}{p/2}\right) \pm 1 \quad \text{where K is an integer}$$

The slot harmonics which correspond to K = 1 (slot harmonics of the first order) are among the most troublesome harmonics in AC machines. Their influence, as well as the influence of other harmonics of higher order, can be reduced by skewing and for this reason stator or rotor slots are sometimes skewed. The skewing also reduces the flux variation in the fringing of the flux at the pole tips due to the slots entering and leaving the polar region. Such a flux variation oftentimes contributes to noise.

Skewing has the same effect as the distribution of a winding over a larger zone because it reduces the interlinkages between the field and stator windings. This distribution factor due to skewing is called the skew factor.

For slots that have a large number of slots per coil group the path of the vectors being added approaches the arc of a circle, and when this happens the distribution factor can be expressed as the ratio of the chord AE to the arc AE and

$$\sin\frac{q\alpha_s}{2} = \frac{1/2 \text{ chord AE}}{R}$$

$$\text{chord AE} = 2R\sin\frac{q\alpha_s}{2}$$

$$\text{arc AE} = Rq\alpha_s$$

$$K_d = \frac{2R\sin\frac{q\alpha_s}{2}}{Rq\alpha_s} = \frac{\sin\frac{q\alpha_s}{2}}{\frac{q\alpha_s}{2}}$$

If Z is the arc which the coil group occupies per pole and t_p is the pole pitch then

$$\frac{q\alpha_s}{2} = \frac{Z\pi}{t_p 2} \text{ and } K_d = \frac{\sin\frac{Z\pi}{t_p 2}}{\frac{Z\pi}{t_p 2}}$$

Let t_{sk} be the slot skew in inches for a length equal to the core length of the machine and the skew factor K_{sk} is

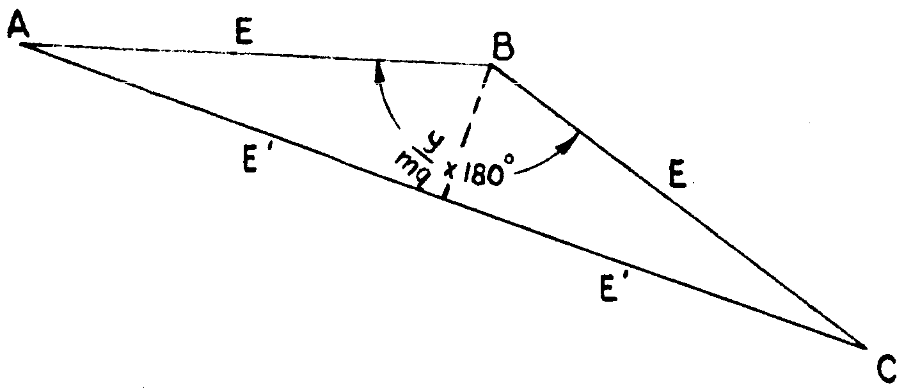
A
E
B
E'
E
E'
C

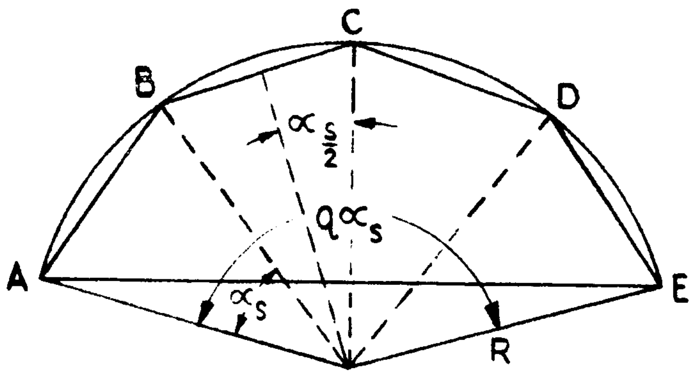
C
B
D
A
E
R

$$K_{sk} = \frac{\sin \frac{t_{sk}\pi}{2t_p}}{\frac{t_{sk}}{t_p}\frac{\pi}{2}} \text{ (fundamental) } \& \; K_{nsk} = \frac{\sin n\frac{t_{sk}\pi}{2t_p}}{n\frac{t_{sk}\pi}{2t_p}} \text{ (nth harmonic)}$$

The influence of skewing is nigligible for the fundamental, small for the harmonics of low order, and very considerable for the harmonics of higher order. A skew which is equal to one stator slot pitch makes the influence of the dangerous slot harmonics almost negligible.

PITCH FACTOR

Fractional pitch windings decrease the length of end connections, reduce slot reactance, and provide a means for improving the wave form. They can be used to eliminate any one harmonic from the voltage wave as well as to reduce other harmonics. However, they require a few more turns or a greater flux for the same voltage than a full pitch winding.

Since the two sides of a coil of a fractional pitch winding do not lie under the centers of adjacent poles at the same instant the voltages induced in them are not in phase when considered around the coil. The voltage produced is therefore less than that which would be produced in a full pitch winding. The voltage generated in any single turn is the vector difference of the voltages generated in the two inductors which form the active sides of the turn. If the throw in slots is y, then $(y/mq) \times 180^\circ$ will be the angle of phase difference between the turns and K_p is then derived as follows:

AB = BC = E; since AB = BC, angle C = angle A, and the bisector of $(y/mq) \times 180^\circ$ will be perpendicular to AC and will bisect AC into two equal parts E'; thus

$$K_p = 2E'/2E = E'/E = \sin\left[(y/mq) \times (180^\circ/2)\right] = \sin\left(\frac{y}{mq} \times 90^\circ\right)$$

Since the displacement for any harmonic such as the nth is n times the phase displacement of the fundamental, K_p for any harmonic n is

$$K_p = \sin\left(\frac{ny}{mq} \times 90^\circ\right)$$

Any harmonic can be eliminated by choosing a pitch that makes the pitch factor zero for that harmonic. Thus to eliminate the nth harmonic it is only necessary to select a pitch such that $n(y/mq) \times 90^\circ$ equals 180°, 360°, 540°, etc. (any multiple of 180°). Eliminating any one harmonic also reduces other harmonics and the fundamental by different amounts. A pitch of 5/6 will give minimum fifth and seventh harmonics and should theoretically give a minimum additional rotor surface loss under load conditions.

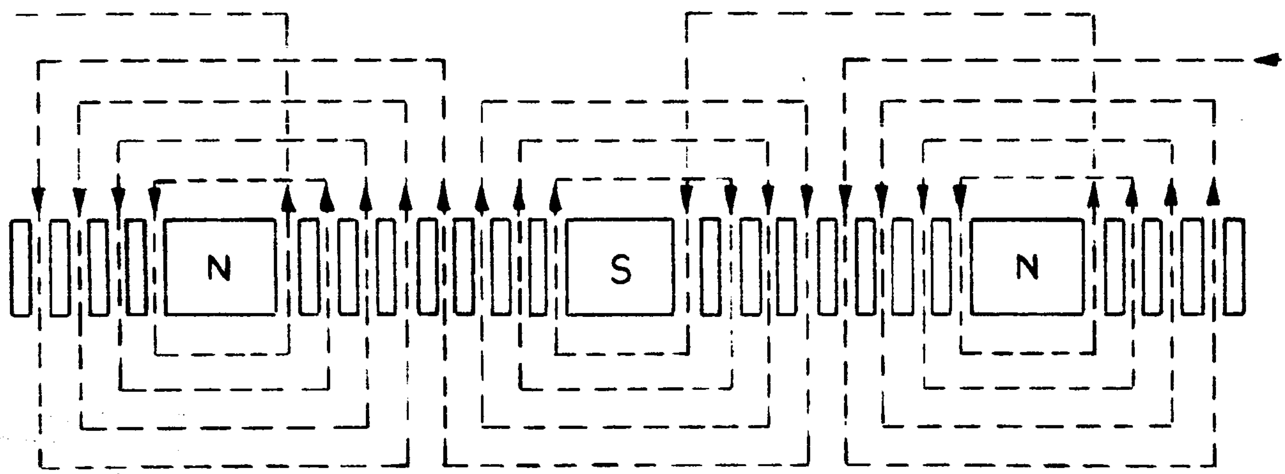
N
S
N

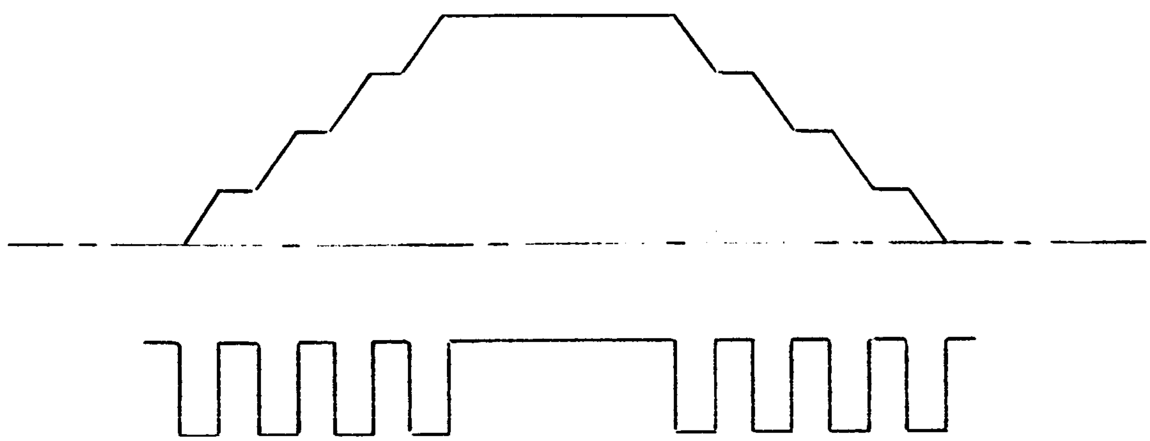

FUNDAMENTAL OF THE FIELD FORM

The field winding of a round rotor machine is generally made in spiral fashion as shown. It is distributed in such a manner that an approximate sinusoidal distribution of flux is obtained. The distribution of MMF produced by the winding is shown in the lower part of the figure. The center portion of the pole can either be left solid as in the figure or can be slotted with the slots left unwound. For the same reason as in the single phase winding the field winding is usually distributed over about 2/3 of the pole pitch of the rotor.

C_1 BASED ON A ROTOR WITH SOLID CENTER SECTION

Assume that the distribution of MMF is trapezoidal in shape instead of stepped and let $\alpha = Q_r/Q_r'$ = number of rotor slots wound/number of slot pitches on rotor surface; K_r = Carter's coefficient for the rotor slots; K_s = Carter's coefficient for the stator slots; g = actual value of the single air gap; $g_e = K_s g$; and r = the radius of the stator bore.

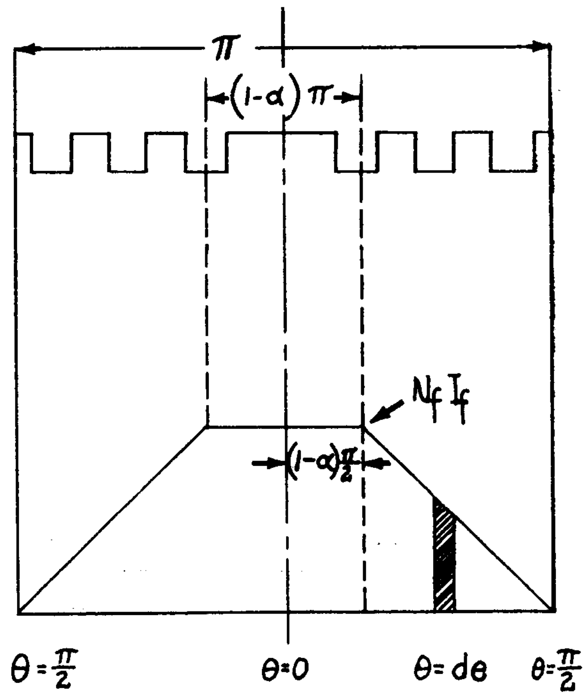

Assume that the field current is one ampere and then the ampere turns at the solid center portion of the pole will be N_f where N_f is the number of field turns per pole. The flux density B_{pc} at the solid portion is thus:

$$B_{pc} = \frac{\phi}{a} = \frac{MMFa}{\ell a} = \frac{3.19N_f}{ge}$$

At the slotted portion of the rotor, the air gap will be increased by an amount K_r and the field ampere turns will vary as a straight line from 0 to N_f. The equation of a straight line is $mx + b$ where m is the slope of the line and thus $N_f = m\theta + b$. The slope m is calculated to be

$$m = \frac{y_2 - y_1}{x_2 - x_1} \text{ where } y_2 = N_f;\ y_1 = 0;\ x_2 = -\left[\frac{\pi}{2} - (1 - \alpha)\frac{\pi}{2}\right];\ x_1 = 0$$

$$m = \frac{N_f}{-\frac{\pi}{2} + \frac{\pi}{2} - \alpha\frac{\pi}{2}} = \frac{N_f}{-\alpha\frac{\pi}{2}} \quad \text{and } N_f = \frac{N_f\theta}{\alpha\frac{\pi}{2}} + b$$

Substituting for the condition $N_f = 0$ at $\theta = \pi/2$ gives

$$0 = -\frac{N_f\frac{\pi}{2}}{\alpha\frac{\pi}{2}} + b \quad \text{and} \quad b = \frac{N_f}{d}$$

Thus $$N_f = -\frac{N_f\theta}{\alpha\frac{\pi}{2}} = \frac{N_f}{\alpha} = \frac{N_f}{d}\left(1 - \frac{2\theta}{\pi}\right)$$

The flux density at the slotted portion of the pole then becomes

$$B_{rs} = \frac{3.19\frac{N_f}{\alpha}\left(1 - \frac{2\theta}{\pi}\right)}{K_r\, g_e} = \frac{3.19N_f}{K_r\, g_e\, \alpha}\left(1 - \frac{2\theta}{\pi}\right)$$

The equation for the Fourier coefficient A_1 (the maximum fundamental) is

$$A_1 = \frac{4}{\pi}\int_0^{\pi/2} f(\theta)\cos\theta d\theta$$

$$A_1 = \frac{4}{\pi}\int^{(1-\alpha)\pi/2} \frac{3.19N_f}{g_e}\cos\theta d\theta + \frac{4}{\pi}\int_{(1-\alpha)\pi/2}^{\pi/2} \frac{3.19N_f}{K_r\, g_e\, \alpha}\left(1 - \frac{2\theta}{\pi}\right)\cos\theta d\theta$$

$$A_1 = \frac{4}{\pi}\,\frac{3.19N_f}{g_e}\,(\sin\theta)_o^{(1-\alpha)\,\pi/2} + \frac{4}{\pi}\,\frac{3.19N_f}{K_r g_e\,\alpha}\int_{(1-d)\,\pi/2}^{\pi/2} \cos\theta d\theta - \frac{4}{\pi}$$

$$\frac{3.19N_f\,2}{K_r g_e\,\alpha}\int_{(1-\alpha)\,\pi/2}^{\pi/2} \theta\cos\theta d\theta$$

$$\int x\cos x\,d\,x = \cos x + x\sin x$$

$$A_1 = \frac{4}{\pi}\,\frac{3.19N_f}{g_e}\sin(1-\alpha)\,\frac{\pi}{2} + \frac{4}{\pi}\,\frac{3.19N_f}{K_r g_e\,\alpha}(\sin\theta)_{(1-\alpha)\,\pi/2}^{\pi/2}$$

$$-\frac{8}{\pi 2}\,\frac{3.19N_f}{K_r g_e\,\alpha}(\cos\theta + \theta\sin\theta)_{(1-\alpha)\,\pi/2}^{\pi/2}$$

$$A_1 = \frac{4}{\pi}\,\frac{3.19N_f}{g_e}\sin(1-\alpha)^{\pi/2} + \frac{4}{\pi}\,\frac{3.19N_f}{K_r g_e\,\alpha} - \frac{4}{\pi}\,\frac{3.19N_f}{K_r g_e\,\alpha}\sin(1-\alpha)^{\pi/2}$$

$$+\frac{8}{\pi 2}\,\frac{3.19N_f}{K_r g_e\,\alpha}\cos(1-\alpha)^{\pi/2} - \frac{8}{\pi 2}\,\frac{3.19N_f}{K_r g_e\,\alpha}\,\frac{\pi}{2}$$

$$+\frac{8}{\pi 2}\,\frac{3.19N_f}{K_r g_e\,\alpha}(1-\alpha)\,\frac{\pi}{2}\sin(1-\alpha)^{\pi/2}$$

$$A_1 = \sin (1 - \alpha)\frac{\pi}{2} \left[\frac{4}{\pi} \frac{3.19N_f}{g_e} - \frac{4}{\pi} \frac{3.19N_f}{K_r g_e \alpha} + \frac{4}{\pi} \frac{3.19N_f}{K_r g_e \alpha} (1 - \alpha) \right]$$

$$+ \frac{4}{\pi} \frac{3.19N_f}{K_r g_e \alpha} - \frac{4}{\pi} \frac{3.19N_f}{K_r g_e \alpha} + \frac{8}{\pi 2} \frac{3.19N_f}{K_r g_e \alpha} \cos (1 - \alpha) \frac{\pi}{2}$$

$$\sin (x - y) = \sin x \cos y - \cos x \sin y$$

$$\cos (x - y) = \cos x \cos y + \sin x \sin y$$

$$\sin (1 - \alpha) \frac{\pi}{2} = \sin \left(\frac{\pi}{2} - \frac{\pi\alpha}{2} \right) = \sin \frac{\pi}{2} \cos \frac{\pi\alpha}{2} - \cos \frac{\pi}{2} \sin \frac{\pi\alpha}{2}$$

$$= \cos \frac{\pi\alpha}{2}$$

$$\cos (1 - \alpha) \frac{\pi}{2} = \cos \left(\frac{\pi}{2} - \frac{\pi\alpha}{2} \right) = \cos \frac{\pi}{2} \cos \frac{\pi\alpha}{2} + \sin \frac{\pi}{2} \sin \frac{\pi\alpha}{2}$$

$$= \sin \frac{\pi\alpha}{2}$$

$$A_1 = \cos \frac{\pi\alpha}{2} \left[\frac{4}{\pi} \frac{3.19N_f}{g_e} - \frac{4}{\pi} \frac{3.19N_f}{K_r g_e \alpha} + \frac{4}{\pi} \frac{3.19N_f}{K_r g_e \alpha} - \frac{4}{\pi} \frac{3.19N_f}{K_r g_e} \right]$$

$$+ \sin \frac{\pi\alpha}{2} \left(\frac{8}{\pi 2} \frac{3.19N_f}{K_r g_e \alpha} \right)$$

$$A_1 = \frac{4}{\pi} \frac{3.19N_f}{g_e} \cos \frac{\pi\alpha}{2} \left[1 - \frac{1}{K_r} \right] + \sin \frac{\pi\alpha}{2} \left(\frac{8}{\pi 2} \frac{3.19N_f}{K_r g_e \alpha} \right)$$

C_1 is the ratio of A_1 to the actual maxium of the wave

$$C_1 = \frac{A_1}{B_{pc}} = \frac{\frac{4}{\pi}\,\frac{3.19N_f}{g_e}\cos\frac{\pi\alpha}{2}\left[\frac{K_r - 1}{K_r}\right] + \frac{8}{\pi^2 Kr\,\alpha}\,\frac{3.19N_f}{g_e}\sin\frac{\pi\alpha}{2}}{\frac{3.19N_f}{g_e}}$$

$$C_1 = \frac{4}{\pi}\cos\frac{\pi\alpha}{2}\left[\frac{K_r - 1}{K_r}\right] + \frac{8}{\pi^2 Kr\,\alpha}\sin\frac{\pi\alpha}{2}$$

C_1 BASED ON A ROTOR WITH SLOTTED CENTER SECTION

When the center is slotted instead of solid the K_r applies to the complete rotor. Therefore, by making K_r equal to unity in the above equation we will get an answer that is independent of the effect of rotor slots and

$$C_1 = \frac{8}{\pi^2\alpha}\sin\frac{\pi\alpha}{2}$$

When using this value of C_1 it is necessary to include K_r in g_e and

$$g_e = K_r K_s g$$

TOTAL FLUX IN THE AIR GAP

When a synchronous alternator operates at no load the only MMF acting is that of the field winding. The flux produced by this winding depends only upon the current it carries, the number of turns and their arrangement, and the total reluctance of the path through which the MMF acts. Neglecting the effect of stator and rotor slots the distribution of the no load air gap flux depends upon the distribution of the field winding. The voltage induced in the stator coils under this open circuit condition can thus be calculated as follows:

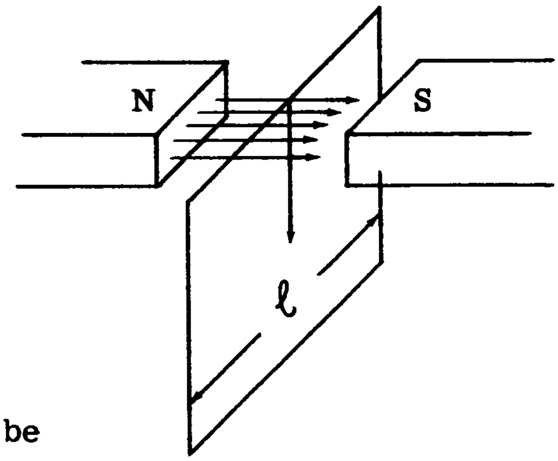

Consider a closed loop rectangular conductor moving down between two poles as shown in the figure. If it moves a distance dx in a time dt the flux interlinkage is;

$$d\phi = (\text{lines/cm}^2)\ (\text{cm}^2) = -B\ell dx$$

and the voltage induced in the coil will be

$$e = -\frac{d\phi}{dt}10^{-8} = B\ell\frac{dx}{dt}10^{-8} = B\ell v 10^{-8} \quad \text{where } v = \text{cm/sec.}$$

If English units of B = lines/in.^{2}, ℓ = inches, and v = ft./min are used

$$e = \left(\frac{B}{2.54^2}\right)(\ell \times 2.54)\left(\frac{v \times 12 \times 2.54}{60}\right) = \frac{1}{5}B\ell v 10^{-8} \text{ volts/coil}$$

The maximum voltage induced per coil in a generator then becomes

$$E \text{ max/coil} = \frac{1}{5} n_s \, Bm\ell\frac{\pi d \text{ RPM}}{12} \; 10^{-8} \text{ volts}$$

where Bm is the maximum fundamental flux density at the stator bore and equals C_1B_g. Thus

$$E_{max/phase} = \left(E_{max/coil}\right)\frac{Q}{m}K_pK_d = \frac{n_s Bm\ell\pi d\text{RPM } 10^{-8} K_pK_dQ}{60m}$$

$$E_{RMS/phase} = Eph = \frac{E_{max/phase}}{\sqrt{2}}$$

$$E_{RMS/line} = E = \frac{E}{Eph} \times Eph = \frac{E}{Eph} \times \frac{n_s C_1 B_g \ell \pi d RPM K_p K_d Q 10^{-8}}{\sqrt{2}\ 60m}$$

$$C_w = \frac{E}{Eph} \frac{C_1 K_d}{\sqrt{2}\, m} \text{ and } n_e = Qn_s K_p$$

$$E = \frac{Cw\, n_e B_g \ell \pi d RPM}{60 \times 10^8} \text{ and } B_g = \frac{6000E\, 10^6}{Cw\, n_e RPM \pi d \tau}$$

$$\phi_T = \pi d \tau B_g = \frac{6000E\, 10^6}{Cw\, n_e RPM}$$

POLE CONSTANT

C_p BASED ON A ROTOR WITH A SOLID CENTER SECTION

The pole constant is defined as the ratio of the average value of the field form to the maximum value of the field form. This constant determines the actual value of flux in the machine.

Refer to the section showing the derivation of the fundamental of the field form and use the same assumptions and wave shape as was used there. The average height of the one half trapezoid will be the area of the curve divided by the base. Since the base of the one half trapezoid is $\pi/2$ the average height is:

Average height =

$$\left[\int_{o}^{(1-\alpha)\,\pi/2} \frac{3.19N_f}{g_e}\, d\theta + \int_{(1-\alpha)\,\pi/2}^{\pi/2} \frac{3.19N_f}{K_r g_e\, \alpha}\left(1 - \frac{2\theta}{}\, d\theta\right)\right] \div \frac{\pi}{2}$$

$$= \frac{2}{\pi}\,\frac{3.19N_f}{g_e}(1-\alpha)\,\frac{\pi}{2} + \frac{2}{\pi}\,\frac{3.19N_f}{K_r g_e\, \alpha}\left[\frac{\pi}{2} - (1-\alpha)\,\frac{\pi}{2}\right] - \left[\frac{2}{\pi}\,\frac{2}{\pi}\,\frac{3.19N_f\theta^2}{K_r g_e\, \alpha\, 2}\right]_{(1-\alpha)\,\pi/2}^{\pi/2}$$

$$= \frac{3.19N_f}{g_e} - \frac{\alpha\, 3.19N_f}{g_e} + \frac{2}{\pi}\,\frac{3.19N_f}{K_r g_e\, \alpha}\left[\frac{\pi}{2} - \frac{\pi}{2} + \frac{\pi\alpha}{2}\right]$$

$$- \frac{2}{\pi\, 2}\,\frac{3.19N_f\pi^2}{K_r g_e\, \alpha\, 4} + \frac{2}{\pi\, 2}\,\frac{3.19N_f\pi^2}{K_r g_e\, \alpha\, 4}(1-\alpha)^2$$

$$= \frac{3.19N_f}{g_e} - \frac{3.19N_f\alpha}{g_e} + \frac{3.19N_f}{K_r g_e} - \frac{3.19N_f}{2K_r g_e\, \alpha} + \frac{3.19N_f}{2K_r g_e\, \alpha}$$

$$- \frac{3.19N_f 2\,\alpha}{2K_r g_e\, \alpha} + \frac{3.19N_f\,\alpha}{2K_r g_e} = \frac{3.19N_f}{g_e}(1-\alpha) + \frac{3.19N_f\,\alpha}{2K_r g_e}$$

C_p is the ratio of the average to the maximum and

$$C_p = \left[\frac{3.19N_f}{g_e}(1-\alpha) + \frac{3.19N_f\,\alpha}{2K_r g_e}\right] \div \frac{3.19N_f}{g_e}$$

$$C_p = 1 - \alpha + \frac{\alpha}{2K_r}$$

C_p BASED ON A ROTOR WITH SLOTTED CENTER SECTION

When the center is slotted instead of solid K_r is included in the effective gap and K_r becomes unity in the C_p equation.

$$C_p = 1 - \alpha + \frac{\alpha}{2} = 1 - \frac{\alpha}{2}$$

EFFECTIVE RESISTANCE AND EDDY FACTOR

When an electric circuit carries an alternating current eddy current losses will occur in neighboring conducting media and in the conductor itself. These losses cause an increase in the energy component of the voltage drop through the circuit for a given current, which is equivalent to an apparent increase in the resistance of the circuit.

When a conductor in air carries an alternating current the distribution of the current over the cross section of the conductor is not uniform. Less current is carried by the central portions of the conductor than by the outer portions. Since the loss in any element of a conductor is proportional to the square of the current it carries any lack of uniformity in the distribution of current over its cross section increases its power loss and in this way increases its apparent resistance. This is the ordinary skin effect. It is much exaggerated when the conductor is partially surrounded by iron, as in the case of the stator conductor of a generator. The difference between the current density at the top and at the bottom of a conductor in the stator slot may be great unless something is done to prevent it, especially when the cross section of the conductor is large and it is in a narrow, deep slot.

Consider the slot shown in Figure 4. The flux density will vary linearly with the depth of the slot and will be a maximum at the top. The flux-linkages will vary as a squared value and will be a maximum at the bottom. The flux produced by the element in the bottom of the slot surrounds this element. It passes across the slot above the element and returns in the iron below it. Only a negligible amount of this return flux passes through the slot below the element because of the high reluctance of the air path as compared with that of the iron. The flux produced by the next element passes across the slot above the element and returns in the iron below the slot. All of the flux produced by both elements surrounds or links all the elements below it. As a result the number of flux-linkages with elements increases in passing from the top to the bottom of the slot. For this reason the reactance of the elements also increases in going from the top to the bottom of the slot, and since the current in the elements will divide between them inversely as their impedances, more current will be carried by the upper elements than by the lower ones. This condition thus leads to additional losses in the upper strands and the ratio of the total losses in the slot to the conventional I^2R loss is defined as the eddy factor.

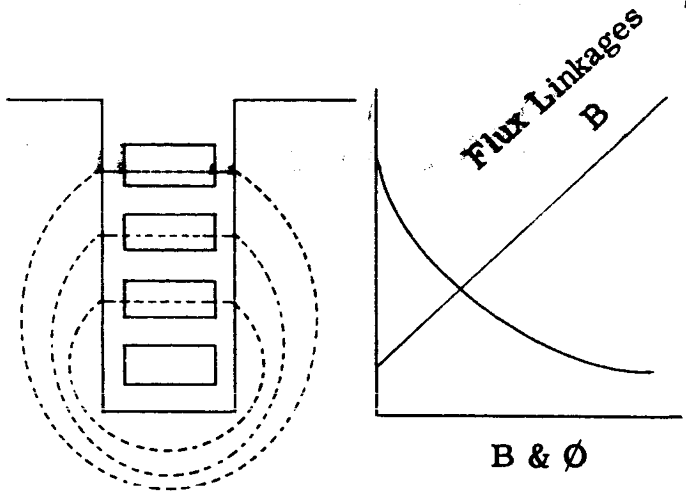

Figure 4

The formula for the losses in a thin sheet of material, neglecting end effects and circulating currents between strands, is given by Puchstein and Lloyd as

$$\text{Watts/in}^3 = \frac{\pi^2 h_{st} f^2 (Bm)^2}{6\rho 10^{16}}$$

where ρ = resistivity in ohm-inches

B_m = maximum value of sine wave density in lines/sq. in.

f = frequency in cycles/sec.

h_{st} = height of uninsulated strand (Figure 5)

Since $B = \frac{3.19NI}{\text{length}}$; $B = \frac{3.19\sqrt{2}\, n_s Ic}{b_s}$; where n_s = conductors per slot and Ic = amperes per conductor. B_m being a straight line function will give a density at the middle of conductor 1 of (Figure 5).

$$B_{m1} = B_m\left(\frac{n_s - \frac{1}{2}}{n_s}\right) = B_m\left(\frac{8 - \frac{1}{2}}{8}\right) \approx B_m \frac{n_s}{n_s}$$

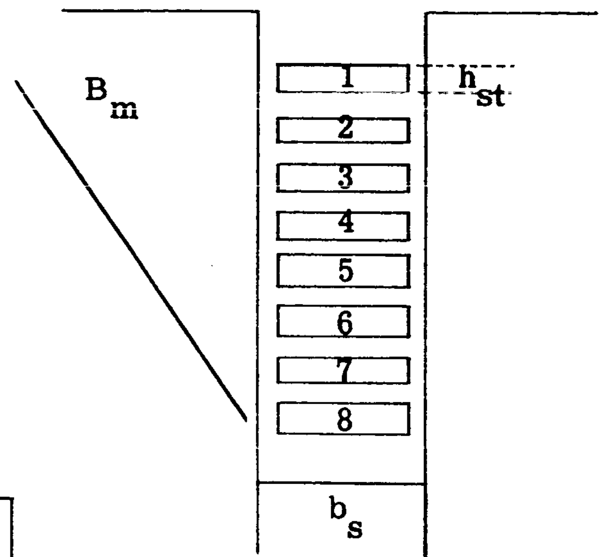

Figure 5

At the middle of conductor 2

$$B_{m2} = B_m\left(\frac{n_s - 1.5}{n_s}\right) \approx B_m\left(\frac{n_s - 1}{n_s}\right)$$

And at the middle of the nth conductor from the top

$$B_{mn} = B_m\left[\frac{n_s - (n - \frac{1}{2})}{n_s}\right] = B_m\left[\frac{n_s - \left(\frac{2n-1}{2}\right)}{n_s}\right]$$

$$\approx B_m\left(\frac{n_s - n}{n_s}\right)$$

Thus for the nth conductor

$$B_{mn} = \frac{3.19\sqrt{2}\ I_c n_s}{b_s}\left[\frac{n_s - \left(\frac{2n-1}{2}\right)}{n_s}\right]$$

and the AC Loss/in.^{3} $= \frac{\pi^2 h_{st} f^2}{6\rho 10^{16}} \times \frac{3.19^2 (\sqrt{2})^2 I_c^{\ 2} n_s^{\ 2}}{b_s^{\ 2}}\left[\frac{n_s - \frac{2n-1}{2}}{n_s}\right]^2$

Rewriting and making the approximation $\left[\frac{n_s - \left(\frac{2n-1}{2}\right)}{n_s}\right] = \frac{n_s - n}{n_s}$

$$\text{WATTS/STRAND} = \frac{9.86\,h_{st}^2 f^2}{6\rho 10^{16}} \times \frac{20.38\,I_c^2 n_s^2}{b_s^2} \left[\frac{n_s - n}{n_s}\right]^2 \ell a_{st}$$

where a_{st} = strand area and ℓ = core length

$$\text{WATTS/STRAND} = \frac{3.35\,h_{st}^2 f^2 I_c^2 n_s^2 \ell a_{st} (n_s - n)^2}{\rho 10^{15} b_s^2 n_s^2}$$

EDDY FACTOR is defined as $\dfrac{\text{AC Eddy Loss} + \text{DCI}^2\text{R Loss}}{\text{DCI}^2\text{R Loss}}$

$$\text{E.F.} - 1 = \frac{\text{AC Eddy Loss}}{\text{DC Loss}} + 1 - 1 = \frac{\text{AC Eddy Loss}}{\text{DC Loss}}$$

$$\text{DC Loss per strand} = I^2 R = I_c^2 \rho \frac{\ell}{a_{st}}$$

$$\text{Thus E.F.} - 1 = \left(\frac{3.35 h_{st}^2 f^2 I_c^2 n_s^2 \ell a_{st} \left[n_s - n\right]^2}{\rho 10^{15} b_s^2 n_s^2}\right. \frac{a_{st}}{I_c^2 \rho \ell} = \frac{3.35}{10^{15}}$$

$$\left[\frac{f^2 h_{st}^2 n_s^2 a_{st}}{b_s^2 \rho^2}\right] \frac{(n_s - n)^2}{n_s^2}$$

This equation gives the eddy factor for the nth strand from the top of the slot. Therefore, calculating the values of EF-1 for the different positions gives:

$$\text{EF-1} = K\,(n_s^2 - 2nn_s + n^2) \text{ where } K = \frac{3.35 f^2 h_{st}^2 n_s^2 a_{st}^2}{10^{15} b_s^2 \rho^2 n_s^2}$$

= K (64 - 16 + 1) = 49K for the first strand

= K (64 - 32 + 4) = 36K for the second strand

= K (64 - 48 + 9) = 25K for the third strand

= K (64 - 64 + 16) = 16K for the fourth strand

= K (64 - 80 + 25) = 9K for the fifth strand

= K (64 - 96 + 36) = 4K for the sixth strand

= K (64 - 112 + 49) = 1K for the seventh strand

= K (64 - 128 + 64) = 0 for the eighth strand

Plotting these values of EF-1 vs. strands in depth gives:

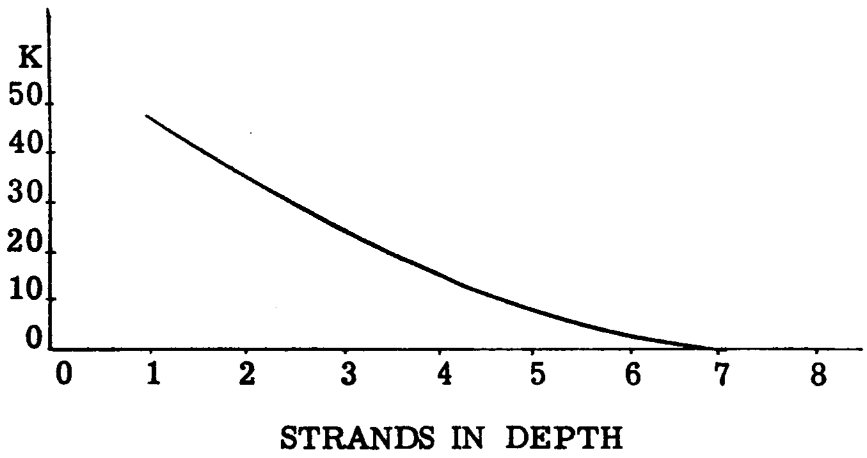

Integrating this curve and dividing by the base will give the average EF-1 of the slot

$$(EF\text{-}1)_{avg} = \frac{1}{n_s} \times \frac{3.35}{10^{15}} \left[\frac{f^2 h_{st}^2 n_s^2 a_{st}^2}{b_s^2 \rho^2}\right] \frac{1}{n_s^2} \int_o^{n_s} (n_s^2 - 2nn_s + n^2)\, dn$$

$$= \frac{3.35}{10^{15}} \left[\frac{f^2 h_{st}^2 n_s^2 a_{st}^2}{b_s^2 \rho^2}\right] \frac{1}{n_s^3} \left[n_s^2 n - \frac{2n^2 n_s}{2} + \frac{n^3}{3}\right]_o^{n_s}$$

$$= \frac{3.35}{10^{15}}\left[\frac{f^2 h_{st} n_s^{2} a_{st}^{2}}{b_s^{2}\rho^2}\right]\frac{1}{n_s^{3}}\left(n_s^{3} - \frac{2n_s^{3}}{2} + \frac{n_s^{3}}{3}\right)$$

$$= \frac{1}{3}\left[\frac{3.35}{10^{15}}\left(\frac{f^2 h_{st}^2 n_s^{2} a_{st}^{2}}{b_s^{2}\rho}\right)\right]$$

For the general case $EF\text{-}1 = K\left[\frac{3.35}{10^{15}}\left(\frac{f^2 h_{st}^2 n_s^{2} a_{st}^{2}}{b_s^{2}\rho}\right)\right]$

Thus it can be seen that the average eddy factor for the slot is 1/3 of the maximum, and in a similar manner it can be shown that the constant K in the general case will be equal to the following values for other parts of the slot.

EF-1	K
Top strand	1.00
Top 1/2 of slot	.584
Bottom 1/2 of slot	.0833
Bottom strand	.000
Average over slot	.333

The above derivation will give the eddy factor when each conductor in the slot consists of a single strand, but sometimes this type of coil will result in eddy currents of large value. If the eddy factor is large it can be reduced most effectively by laminating the conductor into several strands per conductor. When this is done, however, it will cause circulating currents to flow through the strands due to the differences in flux density in the various depths of the slot.

Consider Figure 6 which represents the slots containing a two conductor coil with two strands in parallel for each conductor. Any flux which links one strand and not the other will generate a net EMF around the loop of the strands which are shorted at the ends of the coil. This will cause a circulating current to flow. The density between any two strands of a conductor will be

$B_m\left(\frac{2n_s - n}{2n_s}\right)$ where n is the number of strands from the top of the slot.

In the usual diamond type of coil the A strand is always above the B strand in one slot and always below the B strand in the other. Since the strand which is on top will be in a higher flux density than the one in the bottom, A will have a higher induced voltage in it in one slot and a lower one in the other slot. These two effects tend to cancel each other so that the total flux tending to circulate a current is the difference between the sum of the fluxes in each slot, and the total flux causing circulation will be

$$\left[\sum B_m \text{ between A and B}\right] \times \left[\text{area between the } \mathcal{C} \text{ of the strands}\right]$$

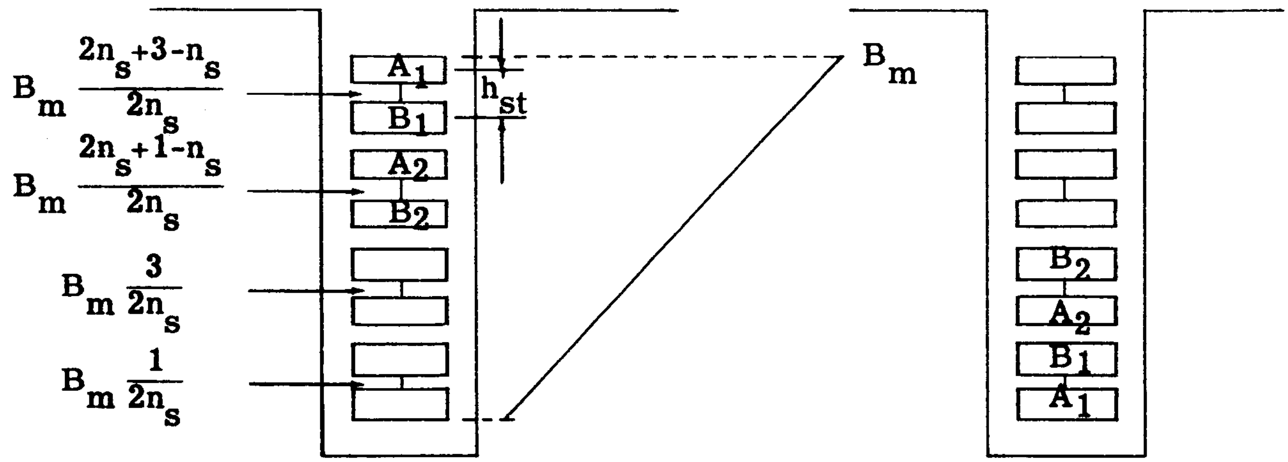

Figure 6

Assume that the density found between conductors will remain constant over the upper strand. Then the flux tending to circulate current in the coil when it is in the top of the slot will be

$$B_m\left(\frac{2n_s + 1 - n_s}{2n_s} + \frac{2n_s + 3 - n_s}{2n_s}\right)$$

and the flux when the coil is in the bottom of the slot equals

$$B_m\left(\frac{1}{2n_s} + \frac{3}{2n_s}\right)$$

Thus $\sum B_m$ between A and B is

$$B_m\left[\left(\frac{2n_s + 1 - n_s}{2n_s} + \frac{2n_s + 3 - n_s}{2n_s}\right) - \left(\frac{1}{2n_s} + \frac{3}{2n_s}\right)\right]$$

$$= B_m\left[\frac{1}{2} + \frac{1}{2n_s} + \frac{1}{2} + \frac{3}{2n_s} - \frac{1}{2n_s} - \frac{3}{2n_s}\right] = B_m\left(\frac{1}{2} + \frac{1}{2}\right)$$

It is to be noted that the factor 1/2 appears $n_s/2$ times, and this will be true for all cases of two strands per conductor. Therefore the total flux causing circulation will be

$$\phi_m = B_m \frac{n_s}{2} \times \frac{1}{2} \times h'_{st} \times \ell = \frac{B_m n_s h'_{st} \ell}{4}$$

Since $$B_m = \frac{3.19\sqrt{2}\ I_c n_s}{b_s}$$

$$\phi_m = \frac{3.19\sqrt{2}\ I_c n_s^2 h'_{st} \ell}{4b_s}$$

The formula for voltage generated is $E_{RMS} = \dfrac{4.44 f \phi_m N}{10^8}$ where N is the number of turns. Since the ϕ_m just derived is the total flux causing circulation in a single coil the N in the voltage formula becomes unity because the coil as a unit has been under consideration. Substituting ϕ_M in the voltage formula gives the voltage tending to circulate current and

$$E_{RMS} = \frac{\sqrt{2}\ f}{10^8}\ \frac{I_c n_s^2 h'_{st}\ 3.19\sqrt{2}}{4b_s}$$

The resistance of the loop will be the sum of the strand resistances in series because all of the strands contribute resistance to the circulating current and

$$R_{loop} = \rho \frac{\ell}{a} = \rho \frac{(2\ell_t)(N_{st/2})}{a_{st}} = \rho \frac{2\ell_t n_s}{a_{st}}$$

where N_{st} = number of strands per slot = $2n_s$

The total eddy current loss due to circulating currents will thus be

$$\text{Eddy Current Loss} = \frac{E^2}{R} = \left[\frac{3.19\pi f I_c n_s^2 h'_{st} \ell}{2b_s 10^8}\right] \frac{a_{st}}{2\rho \ell_t n_s}$$

$$= \frac{3.19^2 \pi^2 f^2 I_c^2 n_s^3 h'^2_{st} \ell^2 a_{st}}{8\ _t b_s^2\ 10^{16}}$$

$$\text{EF-1} = \frac{\text{AC Eddy Loss}}{\text{DC Loss}} = \left[\frac{3.19^2 \pi^2 f^2 I_c^2 n_s^3 h'^2_{st} \ell^2 a_{st}}{8\ell_t b_s^2 \rho 10^{16}}\right] x \frac{1}{I_c^2 R_c}$$

where R_c = conductor resistance $= \rho \frac{2n_s \ell_t}{4a_{st}} = \rho \frac{n_s \ell_t}{2a_{st}}$

$$\text{EF-1} = \frac{3.19^2 \pi^2 f^2 n_s^3 h'^2_{st} \ell a_{st}}{8\ell_t b_s^2 \rho 10^{16}} x \frac{2a_{st}}{\rho \ell_t n_s} = \frac{3.19^2 \pi^2}{4x10^{16}} \left[\frac{f^2 n_s^2 h'^2_{st}}{\ell_t^2 \rho^2 b_s^2}\right] \ell^2 a_{st}^2$$

since $a_c = 2a_{st}$

$$\text{EF-1} = \frac{100.4}{4x10^{16}} \left[\frac{f^2 n_s^2 h'^2_{st} a_c^2}{\ell_t^2 \rho^2 b_s^2 4}\right] \ell^2$$

Multiply by $\dfrac{3h_{st}^2}{3h_{st}^2}$ and

$$EF-1 = \frac{3.35}{10^{15}} \times \frac{3}{16}\left[\frac{f^2 n_s^2 h_{st}^2 a_c^2}{\rho^2 b_s^2}\right]\left[\frac{\ell^2 h'^2_{st}}{\ell_t^2 h_{st}^2}\right]$$

The above derivation has been based upon a conductor with two strands in depth and the 3/16 component of the resultant equation is for this case only. By Kirchoff's laws it can be shown that for the general case this part is equal to $\dfrac{N_{st}^2 - 1}{16}$ where N_{st} is the number of strands per conductor in depth.

For example, with the two strands per conductor case the loss per strand will be:

$$I_1 = \frac{E}{2R}$$

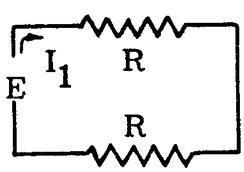

$$\text{Total loss} = I_1^2 R = \frac{E^2}{4R^2} \times 2R = \frac{E^2}{2R}$$

Loss per strand $= \dfrac{E^2}{4R}$ and by the

$\dfrac{N_{st}^2 - 1}{16}$ formula the loss is multiplied by the

factor $\dfrac{3}{16}$

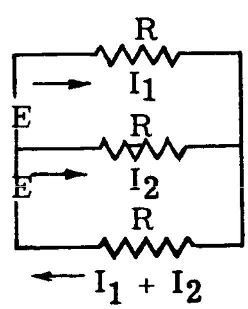

With three strands per conductor

$E + I_1R - I_2R = 0$ and $E = I_2R - I_1R$

$E + I_2R + (I_1 + I_2)R = 0$

and $I_2R - I_1R + I_2R + I_1R + I_2R = 0$

from which $I_2 = 0$

$$\text{Total loss} = I_1^2R + 0 + I_1^2R = 2I_1^2R$$

$$I_1 = \frac{2E}{2R} = \frac{E}{R}$$

$$\text{Total loss} = 2\frac{E^2}{R^2}R = \frac{2E^2}{R}$$

$$\text{Loss per strand} = \frac{2E^2}{3R}$$

Comparing the loss per strand for the two strand and three strand cases gives

$$\text{Ratio of } \frac{3 \text{ strand loss}}{2 \text{ strand loss}} = \frac{2E^2}{3R} \times \frac{4R}{E^2} = \frac{8}{3}$$

and similarly, by the expression $\frac{N_{st}^2 - 1}{16}$ the ratio between the cases is 8/3.

By similar comparison with any number of strands in depth the designated relationship can be proven and therefore the circulating current component of the eddy loss is

$$EF-1 = \frac{3.35}{10^{15}}\left(\frac{N_{st}^2 - 1}{16}\right)\left(\frac{\ell h'_{st}}{\ell_t h_s t}\right)^2\left(\frac{fn_s a_c h_{st}}{\rho\, b_s}\right)^2$$

The total eddy factor is the sum of the eddy loss and the circulating current components.

$$EF-1 = K\left(\frac{3.35}{10^{15}}\right)\left(\frac{fh_{st}a_c n_s}{b_s\,\rho}\right)^2 + \left(\frac{3.35}{10^{15}}\right)\left(\frac{N^2_{st} - 1}{16}\right)\left(\frac{\ell h'_{st}}{\ell_t h_{st}}\right)^2\left(\frac{fn_s a_c h_{st}}{\rho\, b_s}\right)^2$$

$$EF-1 = 1 + \left[K + \left(\frac{N_{st}^2 - 1}{16}\right)\left(\frac{\ell h'_{st}}{\ell_t h_{st}}\right)^2 \right]\left(\frac{3.35}{10^{15}}\right)\left[\frac{f h_{st} a_c n_s}{b_s \rho}\right]^2$$

DEMAGNETIZING AMPERE TURNS AND DEMAGNETIZING FACTOR

When a generator is loaded an MMF is produced by the stator current which modifies the flux that the field current is producing. Part of the flux produced by this stator current combines with the flux due to the field winding and gives a resultant flux which links both the stator and field windings. This component of the stator current MMF is known as armature reaction and only this part is under discussion in this section.

The field winding of a round rotor generator is always distributed and produces an MMF that is nearly sinusoidal in its space distribution. Likewise, a distributed stator winding also produces an approximate sine wave of MMF, the wave more nearly becoming sinusoidal as the number of slots and phases increases. If the harmonics in both MMF waves are neglected the two waves will always add to give a resultant wave which has a sinusoidal space distribution. This follows from the fact that any two space sinusoidal waves of the same wave length always add to give a resultant wave which is a sinusoid and is of the same wave length as the components.

Since the air gap of a round rotor machine is uniform, except for the effects of slots, the shape of the resultant MMF wave is independent of the direction of the armature reaction with respect to the field axis. Therefore, the armature reaction produces little field distortion. It affects only the resultant field strength and displaces the axis of the resultant field from the axis of the field poles.

The demagnetizing ampere turns are defined as the field ampere turns necessary to balance out the MMF of the stator winding. It is therefore necessary to calculate the fundamental of the stator MMF and convert this value to terms of field MMF. To calculate the fundamental of the stator MMF first consider a single phase, two pole generator with a concentrated stator winding. The MMF of the stator winding under this condition is constant in its space distribution over the coil area and can be represented by a rectangular wave. The amplitude of the fundamental of the Fourier series which represents a rectangular wave is $4/\pi$ times the amplitude of the rectangular wave.

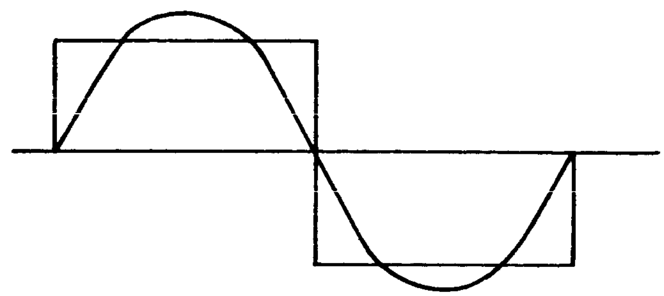

Both the rectangular wave and the fundamental vary sinusoidally in magnitude with time but they are stationary in space with respect to the stator coil. The fundamental of the wave can be represented by an oscillating vector which lies along the axis of the coil and which has a maximum length equal to the maximum value of the fundamental.

Let the oscillating vector be replaced by two equal and oppositely rotating component vectors. These two oppositely rotating vectors represent oppositely rotating MMF waves, each of which has a constant amplitude equal to one-half the amplitude of the original MMF wave. Both of the vectors revolve at synchronous speed with respect to the stator, with one vector stationary with respect to the field poles, and the other at double speed with respect to the poles.

The amplitude of the rotating components will thus be

$$F_{DM_{ph}} = \frac{1}{2}\,\frac{4}{\pi}\,\frac{ne_{ph} I_M K_d}{2P} \quad \text{ampere turns per pole/phase}$$

where I_M = max. current, and ne_{ph} = total eff. conductors/phase

Since $I_M = 2$ Iph (turns $= \frac{\text{conductors}}{2}$)

$$F_{DM_{ph}} = \frac{1}{2}\,\frac{4}{\pi}\,\frac{ne_{ph}}{2p}\sqrt{2}\,\text{Iph}\,K_d = \frac{.45\,ne_{ph}\,\text{Iph}\,K_d}{P}$$

In a polyphase generator under balanced load it is found that the forward rotating parts of the space fundamental mmf of armature reaction add directly, while the backward rotating parts of the fundamental cancel one another. The net fundamental mmf of armature reaction is thus a purely rotating wave whose amplitude is 3 $F_{DM_{ph}}$. Thus for polyphase machines

$$F_{DM} = \frac{.45 n_e \text{Iph} K_d}{P}$$

The amplitude of the resultant fundamental sinusoidal component of the MMF produced by the distributed field winding is

$$F_f = \frac{4}{\pi} N_f I_f K_{df} K_{pf} \quad \text{ampere turns per pole}$$

where K_{df} and K_{pf} are the pitch and distribution factors of the field winding. Since the field has a spiral winding the axes of all field coils for any given pole coincide, and in this case the distribution factor is unity.

Thus

$$F_f = \frac{4}{\pi} N_f I_f K_{pf}\ \text{avg.}$$

where K_{pf} avg = the average pitch factor for the field coils.

The same result is obtained if the field winding is assumed to be replaced by a full pitch distributed lap winding with Q/p slots in a belt of conductors.

In this case

$$F_f = \frac{4}{\pi} N_f I_f K_{df}$$

Therefore, to obtain the value of demagnetizing ampere turns due to armature reaction, in terms of field ampere turns, it is necessary to multiply F_{DM} by the factor $\frac{\pi}{4K_{df}}$, and this factor is known as C_M, the demagnetizing factor.

Thus

$$F_{DM} = \frac{.45\, n_e C_M Iph K_d}{P}$$

The factor C_M can either be obtained by (1) calculating the average field pitch factor, or (2) the field distribution factor, or (3) by using the formula (from Kilgore's paper)

$$C_M = \frac{\pi^2}{8} \quad \frac{\alpha}{\sin \frac{\pi a}{2}}$$

To illustrate the calculation of C_M by the various methods consider the following example:

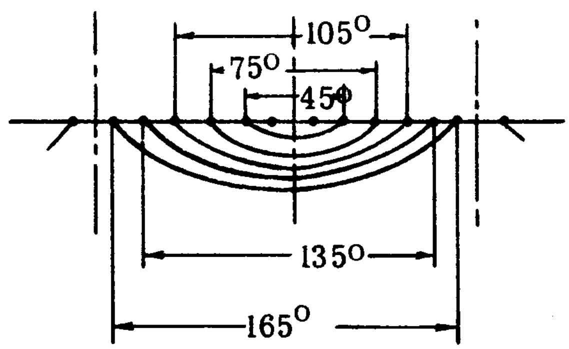

Number of rotor slots = 48;

Number of slots wound = 40;

Poles = 4

(3) $C_M = \frac{\pi^2}{8} \times \frac{.833}{\sin 75^o} = 1.061$

(2) $K_{df} = \dfrac{\sin \frac{n\alpha}{2}}{n \sin \frac{\alpha_s}{2}}$ (where α_s = angle between slots

$$K_{df} = \frac{\sin - \left(10 \times \frac{15}{2}\right)}{10 \sin 7.5^o} = \frac{.966}{1.305} ; \quad C_M = \frac{\pi}{4 \times .740} = 1.061$$

(1)

Coil Spreads	Pitch Factor
45^o	$\sin(1/2 \times 45^o) = .383$
75^o	$\sin(1/2 \times 75^o) = .609$
105^o	$\sin(1/2 \times 105^o) = .794$
135^o	$\sin(1/2 \times 135^o) = .924$
165^o	$\sin(1/2 \times 165^o) = .991$
	3.701

$$\text{Average } K_{pf} = \frac{3.701}{5} = .7402$$

$$C_M = \frac{\pi}{4 \times .7402} = 1.061$$

The effect on the field of a given number of ampere turns of armature reaction for any fixed load and power factor depends upon the ratio of the ampere turns of armature reaction to the no load field ampere turns. To reduce the effect of armature reaction this ratio must be decreased. This may be accomplished by increasing the radial length of the air gap or by increasing the saturation of the magnetic circuit. Neither of the changes affects the armature ampere turns for a given load but both decrease the permeance of the magnetic circuit and make an increase in the field ampere turns necessary in order to maintain the same flux. The higher the degree of saturation the less is the effect of a given number of ampere turns of armature reaction, but high saturation in the field circuit increases the field pole leakage. Increasing the length of the air gap has a similar effect so far as armature reaction is concerned, but it does not increase the field leakage to so great an extent as does increasing the degree of saturation of the magnetic circuit.

For unbalanced load conditions it is important to note that the armature reaction is neither fixed in magnitude nor in direction with respect to the poles.

LEAKAGE REACTANCE

In addition to the demagnetizing action of armature reaction there also exists a voltage drop due to the leakage fluxes. The lines of leakage flux go partly across the slot from one wall to the other (slot leakage), partly from tooth top to tooth top, (tooth tip), partly from phase belt to phase belt (zig zag), and partly in the end windings (end leakage). Each of the leakage fluxes is directly proportional to the current which produces it because its reluctance is principally in air.

Consider first the slot leakage flux. This flux includes all the flux which links the portion of the conductors that are embedded in the iron, but which does not enter the air gap. Assume an integral slot, full pitched winding, and assume that the flux passes directly across the slot. The effect of the notches at the wedge will be neglected and the current density in the conductors will be assumed constant. Also, for simplification, the distance between the top and bottom coil will be assumed negligible.

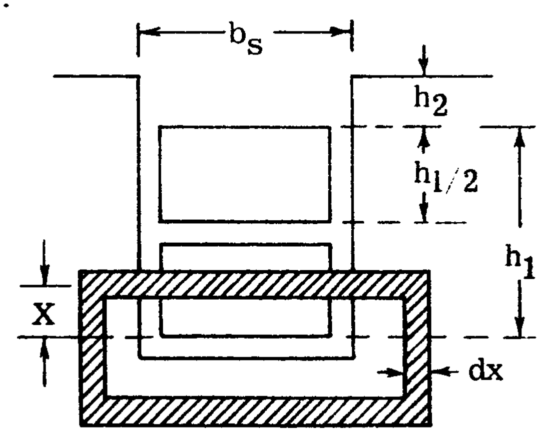

The flux produced by the element in the bottom of the slot will surround this element. It passes across the slot above the element and returns in the iron below it. The flux will thus encircle part of the coil plus all of the slot above the coil. For the part above the coil the flux will proportion itself equally over the distance $h_{1/2} + h_2$, and since the inductance L equals $\dfrac{3.19n_s^2 a}{4\ell 10^8}$ the L per slot per inch of core length for this part is:

$$L = \frac{3.19n_s^2 (h_{1/2} + h_2)}{4b_s 10^8}$$

For the inductance of the part of the coil itself consider the element dx enclosing part of the conductor. The L per slot per inch of core length for this part will be equal to $\frac{3.19}{10^8}\sum\frac{N_x^2}{R_x}$ and since $N_x = \frac{x}{h_{1/2}}\ \frac{n_s}{2}$ and $R_x = \frac{b_s}{dx}$ then

$$L = \frac{3.19}{10^8}\int_0^{L_{1/2}} \frac{x^2 n_s^2 dx}{h_{1/2}^2\, 4b_s} = \frac{3.19 n_s^2 h_{1/2}^3}{10^8 h_{1/2}^2 4b_s 3} = \frac{3.19 n_s^2}{4b_s 10^8} \times \frac{h_{1/2}}{3}$$

and the total inductance of the bottom coil side is

$$L_B = \frac{3.19 n_s^2}{4b_s 10^8}\left(h_{1/2} + h_2 + \frac{h_{1/2}}{3}\right) = \frac{3.19 n_s^2}{10^8}\left(\frac{h_{1/2}}{3b_s} + \frac{h_2}{4b_s}\right)$$

In the same manner the inductance of the top coil side will be that due to its own current plus that due to the flux in the part h_2 above the coil and thus:

$$L_T = \frac{3.19 n_s^2}{4b_s 10^8}\left(\frac{h_{1/2}}{3} + h_2\right) = \frac{3.19 n_s^2}{10^8}\left(\frac{h_{1/2}}{12b_s} + \frac{h_2}{4b_s}\right)$$

Since a full pitched winding has been assumed, the currents of both coil sides will be in phase in all slots and the mutual inductance in the top coil due to the current in the bottom coil will be equal to that in the bottom coil due to the current in the top. Thus L_M in the top coil due to i in the bottom coil will be

$$L_M = \frac{3.19 n_s^2}{4\ell 10^8}\sum \text{ current in the top coil enclosed by the flux from}$$

the bottom

At the distance x the current enclosed is

$$\left(\frac{x}{h_{1/2}}\right) dx \text{ and } L_M = \frac{3.19n_s^2}{4b_s 10^8 h_{1/2}} \int_o^{h_{1/2}} x\, dx = \frac{3.19n_s^2}{10^8}\left(\frac{h_{1/2}}{8b_s}\right)$$

For the portion above the slot

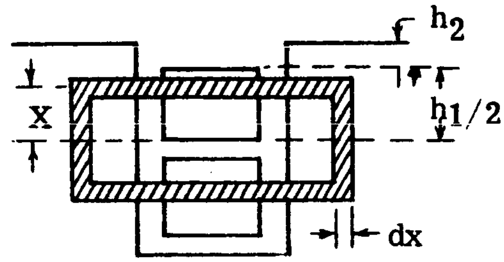

$$L_M = \frac{3.19n_s^2}{10^8}\left(\frac{h_2}{4b_s}\right)$$

as in the previous cases.

Therefore, since total inductance is L_T L_B $2L_M$ the total inductance per slot per inch of core length is

$$L = \frac{3.19n_s^2}{10^8}\left(\frac{h_{1/2}}{12b_s} + \frac{h_2}{4b_s} + \frac{h_{1/2}}{3b_s} + \frac{h_2}{4b_s} + \frac{2h_{1/2}}{8b_s} + \frac{2h_2}{4b_s}\right) = \frac{3.19n_s^2}{10^8}\left(\frac{2h_{1/2}}{3b_s} + \frac{h_2}{b_s}\right)$$

Since the portion of the slot between the coils has been neglected it can now be included by making $h_{1/2}$ in the above derivation equal to

$\frac{h_1}{2}$ and the formula for L will then be:

$$L = \frac{3.19n_s^2}{10^8}\left(\frac{h_1}{3b_s} + \frac{h_2}{b_s}\right)$$

The tooth tip and zigzag leakage components have been derived by Kilgore with flux plotting methods and these have been determined to be

$$\frac{b_t^2 n_s^2 3.19}{16t_s g 10^8} \quad \text{and} \quad \frac{.35b_t n_s^2 3.19}{t_s 10^8}$$

Adding these to the slot leakage portion gives

$$L = \frac{3.19n_s^2}{10^8}\left(\frac{h_1}{3b_s} + \frac{h_2}{b_s} + \frac{b_t^2}{16t_s g} + \frac{.35b_t}{t_s}\right)$$

The above derivation has been based upon a full pitched integral slot winding. When the winding is chorded, however, as is usually the case in polyphase machines, the currents in the two coil sides in a certain number of slots will be out of phase and the coefficient of self inductance will be smaller than for the full pitch case. For the slots in which both the bottom and top layer belong to the same phase the conditions are the same as for full pitch. Both coil sides carry currents of the same phase and the phase angle between the currents is zero. In the slots in which the bottom layer and top layer belong to different phases, the phase angle β between the currents is not zero and the mutual inductance between the two layers will be reduced. The reduction factor is equal to $\cos\beta$.

Two reduction factors have to be used: K_{xco} for the slot part in which the conductors lie, and K_{xt} for the part above the conductors. Thus L becomes

$$L = \frac{3.19n_s^2}{10^8}\left[K_{xco}\left(\frac{h_1}{3b_s}\right) + K_{xt}\left(\frac{h_2}{b_s}\right) + \frac{b_t^2}{16t_s g} + \frac{.35b_t}{t_s}\right]$$

The factors K_{xco} and K_{xt} will vary according to the percent pitch and when they are derived they are found to be independent of the number of slots per phase per pole. Hence, since they depend solely upon the percent pitch, they have been combined into a single factor K_x which is reasonably accurate for most machines. It is determined as follows:

$$K_x = \frac{1}{4}\left(\frac{3y}{mq} + 1\right) \quad \text{for three phase machines}$$

$$K_x = \frac{y}{mq} \quad \text{for two phase machines}$$

Therefore the leakage inductance per slot finally becomes

$$L = \frac{3.19 n_s^2}{10^8} K_x \left(\frac{h_2}{b_s} + \frac{h_1}{3b_s} + \frac{b_t^2}{16 t_s g} + \frac{.35 b_t}{t_s} \right)$$

and the per unit reactance per phase will be

$$X_s = 2\pi f L \frac{Q\ell}{m} \frac{Iph}{Eph} \qquad \text{where}$$

$$Iph = \frac{A\pi d}{Q K_p n_s}$$

$$Eph = \frac{1}{\sqrt{2}} n_s C_1 B_g \ell \frac{\pi d RPM}{60} 10^{-8} \frac{Q}{m} K_p K_d$$

(see total flux derivation)

$$X_s = \frac{2\pi p RPM\, 3.19 n_s^2 K_x Q A \pi d \sqrt{2}\; 60\; 10^8 m \ell}{m\, 120\; 10^8 Q K_p n_s n_s C_1 B_g \ell \pi d RPM Q K_p K_d} \left(\frac{h_2}{b_s} + \frac{h_1}{3b_s} + \frac{b_t}{16 t_s g} + \frac{.35 b_t}{t_s} \right) \frac{\sqrt{2}}{\sqrt{2}}$$

Substituting $Q = pmq$

$$X_s = \frac{20 p A m K_x}{m^2 q p K_p^2 C_1 B_g K_d \sqrt{2}} \left(\frac{h_2}{b_s} + \frac{h_1}{3b_s} + \frac{b_t^2}{16 t_s g} + \frac{.35 b_t}{t_s} \right) \frac{K_d}{K_d}$$

$$\text{Let } C_x = \frac{K_x}{K_p^2 K_d^2} \qquad \text{and since } \mathfrak{X} = \frac{A K_d}{\sqrt{2}\, C_1 B_g}$$

$$X_s = \mathfrak{X} C_x \frac{20}{mq} \left(\frac{h_2}{b_s} + \frac{h_1}{3b_s} + \frac{b_t^2}{16 t_s g} + \frac{.35 b_t}{t_s} \right)$$

Many attempts have been made to determine accurate formulas for the end winding leakage reactance, but the one that appears to be most promising for small machines is the one proposed by E. C. Barnes in AIEE Volume 70-1951. Expressed in per cent notation this formula will be:

$$\% X_E = 6.28f \left(\frac{n_s}{C}\right)^2 q^2 K_p^2 \, pm \left[\frac{\phi_E L_E}{2n}\right] \frac{Iph}{Eph} \; K_E 10^{-6}$$

where $\frac{\phi_E L_E}{2n}$ is proportional to the pole pitch and is taken from Graph No. 1 and K_E is proportional to the ratio of the calculated L_E to the L_E of Graph No. 1.

$$K_E = \sqrt{\frac{\text{calculated } L_E}{L_E \text{ from Graph \#1}}} \qquad \text{(for d below 8'' diameter)}$$

$$\text{and } K_E = \frac{\text{calculated } L_E}{L_E \text{ from Graph \#1}} \qquad \text{(for d above 8'' diameter)}$$

$$\text{Since } Iph = \frac{CA\pi d}{QK_p n_s} \quad \text{and } Eph = \frac{n_s C_1 B_g \ell \pi d \, RPM \, QK_p K_d}{\sqrt{2} \; C60M10^8}$$

$$\% X_E = 6.28f \left(\frac{n_s}{C}\right)^2 q^2 K_p pm \left[\frac{\phi_E L_E}{2n}\right] K_E \frac{\sqrt{2}}{\sqrt{2}} \left[\frac{CA\pi d}{QK_p n_s} \; \frac{\sqrt{2}\; 60 \; 10^8 mc}{n_s C_1 B_g \ell \pi d \, RPM \, QK_p K_d \; 10^6}\right]$$

Multiplying by $\frac{K_d}{K_d}$ and substituting $f = \frac{p\,RPM}{2 \times 60}$; $X = \frac{100AK_d}{\sqrt{2}\, C_1 B_g}$; $q = \frac{Q}{pm}$

gives

$$\% X_E = X \; \frac{6.28 \, p \, RPM}{2 \times 60} \; \frac{Q^2 pm}{p^2 m^2} \left|\frac{Q_E L_E}{2n}\right| K_E \; \frac{2 \times 60m}{Q^2 \ell \, RPM \, K_d^2}$$

$$\% X_E = X \; \frac{6.28}{\ell K_d^2} \left[\frac{Q_E L_E}{2n}\right] K_E$$

REACTANCE OF ARMATURE REACTION

Since the shape of the resultant MMF wave is independent of the direction of armature reaction the effect produced by the MMF's of the field and stator windings can be found by treating the two forces as if they each acted alone, and thus the forces may be replaced by the voltages they would cause if acting separately. If this substitution is made the voltage due to armature reaction may be considered as being a voltage drop due to a fictituous reactance X_{ad}, and this is called the reactance of armature reaction. It is not an actual reactance but under steady operating conditions may be considered as such in order to simplify the methods of calculation. It is in phase with the voltage drop due to leakage reactance $I_{ph}X_{\ell}$, and the sum of these two reactances is the synchronous reactance X_d.

If the effect of saturation is neglected the saturation curve becomes a straight line, and then any change in flux with its corresponding change in voltage, produced by any change in MMF is proportional to the change in MMF. Thus, if an unsaturated condition is assumed, the reactance of armature reaction in per unit value can be seen to be the ratio of the MMF of armature reaction to the MMF required by the field to force the flux across the air gap, or

$$X_{ad} = \frac{F_{DM}}{F_g} \quad \text{(percent)}$$

$$\text{Since } F_{DM} = \frac{\sqrt{2}\, n_e C_M I_{ph} K_d}{\pi p} \quad \text{and } F_g = \frac{B_g g_e}{3.19}$$

$$X_{ad} = \frac{\sqrt{2}\, n_e C_M I_{ph} K_d \, 3.19}{\pi p B_g g_e} \times \frac{\sqrt{2}\, C_1}{\sqrt{2}\, C_1} = \frac{6.38\, n_e C_M I_{ph} K_d C_1}{\sqrt{2}\, \pi p B_g g_e C_1}$$

$$I_{ph} = \frac{A \pi d}{Q n_s K_p} = \frac{A \pi d}{n_e} \left(\text{from } A = \frac{I_{ph} n_s K_p}{t_s} \text{ and } t_s = \frac{\pi d}{Q} \right)$$

$$\lambda_a = \frac{6.38\,d}{Pg_e} \quad \text{and} \quad X = \frac{A K_d}{\sqrt{2}\, C_1 B_g}$$

$$X_{ad} = \frac{6.38\, dA\, \pi n_e C_M C_1 K_d}{\sqrt{2}\, n_e \pi P g_e B_g C_1} = X \lambda_a C_M C_1$$

ROTOR SLOT FLUX

Consider the rotor of Figure 7, and since ϕ_T is the total flux that would exist if the gap density were uniform and equal to the maximum density, the portion of the total flux leaving each pole center will be

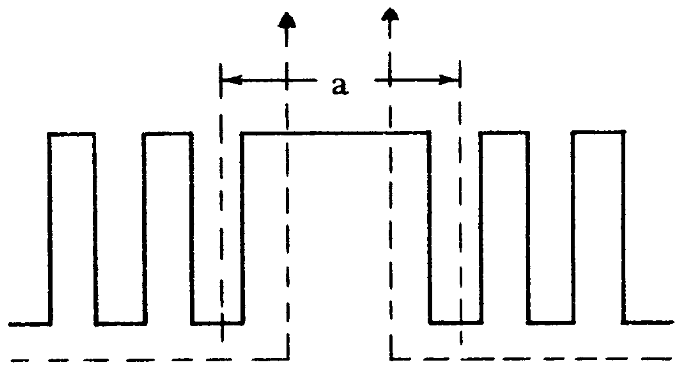

FIGURE 7

$$\frac{Q_r' - Q_r + P}{Q_r} \times \frac{\phi_T}{P} = \phi_{gp}$$

Consider the slot in Figure 8 and assume that the flux density will vary directly with the depth of the slot, being a maximum at the bottom of the bottom conductor. The permeance of the leakage flux paths per inch of core length per slot will then be

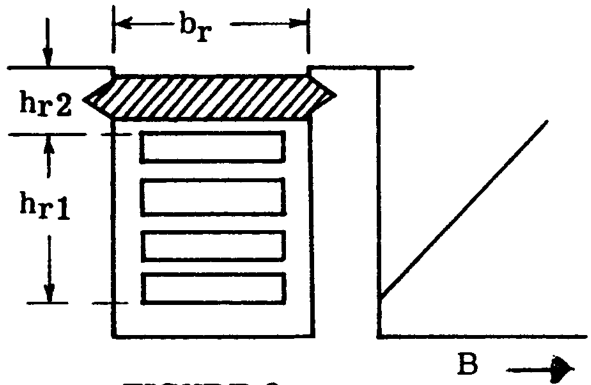

FIGURE 8

$\frac{h_{r2}}{b_r}$ for the depth h_{r2}, and $\frac{1}{2}\,\frac{h_{r1}}{b_r}$ for the depth h_{r1}. Including Kilgore's factors for tooth tip and zigzag leakage gives

$$\lambda_r \text{ per slot } = \left[\frac{h_{r2}}{b_r} + \frac{h_{r1}}{2b_r} + \frac{.35b_{tr}}{t_{rs}} + \frac{g}{2t_{rs}}\right] 3.19$$

Since there are two leakage paths per pole, with one half of the slots per pole in each path, the total permeance per pole is two times the permeance of one of the paths. Permeances in series are added the same as resistances in parallel and thus

$$\lambda_r \text{ per path} = \frac{1}{\dfrac{1}{\lambda r/\text{slot}} + \dfrac{1}{\lambda r/\text{slot}} + \cdots} = \frac{1}{\dfrac{1}{2}\dfrac{Q_r}{P/\lambda r/\text{slot}}} = \frac{2p\lambda_r/\text{slot}}{Q_r}$$

and the total leakage permeance is

$$\lambda rs = \frac{2 \times 2p}{Q_r} \times 3.19 \left[\frac{h_{r2}}{b_r} + \frac{h_{r1}}{2b_r} + \frac{.35b_{tr}}{t_{rs}} + \frac{g}{2t_{rs}}\right]$$

The MMF acting across the leakage paths is the sum of the gap and stator ampere turns and the slot leakage flux per pole becomes

$$\phi_{\ell s} = \left[F_g + F_s\right] \lambda rs\,\ell r$$

and the total flux per pole is then $(\phi_{gp} + \phi_{\ell s})$

DERIVATION OF FLUX DISTRIBUTION CONSTANT C_f

C_f is the ratio of the interlinkages with the field to that which would be produced with a uniform gap and a concentrated field winding.

$$C_f = \frac{\text{Rotor interlinkages with its own flux}}{\text{Max. interlinkages of a concentrated field winding}}$$

C_f BASED ON A ROTOR WITH SOLID CENTER SECTION

Assume that the field current is one ampere and then for a concentrated field winding the flux will be

$$\phi = (\text{MMF})\left(\frac{\text{Area}}{\text{gap}}\right) = 3.19N_f \frac{\pi r \ell}{K_s g}$$

and the maximum number of flux linkages at the unslotted pole center are

$$\text{Concentrated } \phi N_f = \frac{3.19\pi r \ell N_f^2}{K_s g}$$

In the solid pole center portion of the machine the flux will be equal to

$$\phi = \frac{3.19\pi r \ell N_f}{K_s g}(1 - \alpha)$$

and the flux linkages will total

$$\phi N_f = \frac{3.19\pi r \ell N_f^2}{K_s g}(1 - \alpha)$$

For the slotted portion of the rotor refer to the derivation of the constant C_1 and note that the ampere turns acting $= \frac{N_f}{\alpha}\left(1 - \frac{2\theta}{\pi}\right)$. Thus at an element where $\theta = d\theta$ the flux will be

$$d\theta = \frac{3.19 r \ell d\theta}{K_s K_r g} \frac{N_f}{\alpha}(1 - \frac{2\theta}{\pi})$$

and the sum of the flux linkages for a complete pole pitch will then be

$$\Sigma \phi N_f = 2 \int_{(1-\alpha)\pi/2}^{\pi/2} \frac{3.19 r \ell d\theta}{K_s K_r g} \left[\frac{N_f}{\alpha}\left(1 - \frac{2\theta}{\pi}\right)\right]^2$$

$$= \frac{6.38 r \ell N_f}{K_s K_r g \alpha^2} \int_{(1-\alpha)\pi/2}^{\pi/2} \left(1 - \frac{4\theta}{\pi} + \frac{4\theta^2}{\pi 2}\right) d\theta$$

$$\Sigma \phi N_f = \frac{6.38 r \ell N_f^2}{K_s K_r g \alpha^2} \left[\frac{\pi}{2} - (1 - \alpha)\,\pi/2 - \frac{4}{2\pi}\left(\frac{\pi^2}{4} - \frac{\pi^2}{4}\left\{1 - \alpha\right\}^2\right)\right.$$

$$\left. + \frac{4}{3\pi^2}\left(\frac{\pi^3}{8} - \frac{\pi^3}{8}\left\{1 - \alpha\right\}^3\right)\right]$$

$$\Sigma \phi N_f = \frac{6.38 r \ell N_f^2}{K_s K_r g \alpha^2} \left[\frac{\pi}{2}(1 - 1 + \alpha) - \frac{2\pi^2}{4\pi}(1 - 1 + 2\alpha - \alpha^2)\right.$$

$$\left. + \frac{4}{3\pi^2}\,\frac{\pi^3}{8}(1 - 1 + 3\alpha - 3\alpha^2 + \alpha^3)\right]$$

$$\Sigma \phi N_f = \frac{6.38 r \ell N_f^2}{K_s K_r g \alpha^2} \left[\frac{\pi\alpha}{2} - \frac{\pi\alpha}{2}(2 - \alpha) + \frac{\pi\alpha}{6}(3 - 3\alpha + \alpha^2)\right]$$

$$\Sigma \phi N_f = \frac{6.38 r \ell N_f^2}{K_s K_r g \alpha^2} \left[\frac{\pi\alpha}{2}(1 - 2 + \alpha) + \frac{\pi\alpha}{6}(3 - 3\alpha + \alpha^2)\right]$$

$$\Sigma \phi N_f = \frac{6.38 r \ell N_f^2}{K_s K_r g \alpha^2} \left[\frac{\pi\alpha}{6} \left(-3 + 3\alpha + 3 - 3\alpha + \alpha^2 \right) \right] .$$

$$\Sigma \phi N_f = \frac{6.38 r \ell N_f^2}{K_s K_r g \alpha} \frac{\pi}{6} \alpha^2 = \frac{3.19 \pi r \ell N_f^2}{g K_s} \cdot \frac{\alpha}{3K_r}$$

The total flux linkages for the solid and slotted portions is thus

$$\text{Total } \phi N_f = \frac{3.19 \pi r \ell N_f^2}{g K_s} (1 - \alpha) + \frac{3.19 \pi r \ell N_f^2}{g K_s} \cdot \frac{\alpha}{3K_r}$$

$$= \frac{3.19 \pi r \ell N_f^2}{g K_s} \left(1 - \alpha + \frac{\alpha}{3K_r} \right)$$

$$C_f = \frac{Kg}{3.19 \pi r \ell N_f^2} \times \frac{3.19 \pi r \ell N_f^2}{K_s g} \left(1 - \alpha + \frac{\alpha}{3K_r} \right)$$

$$C_f = 1 - \alpha + \frac{\alpha}{3K_r}$$

C_f BASED ON A ROTOR WITH SLOTTED CENTER SECTION

When the center is slotted instead of solid K_r is included in the effective gap and K_r becomes unity in the C_f equation.

$$C_f = 1 - \alpha + \frac{\alpha}{3} = 1 - \frac{2\alpha}{3}$$

SYNCHRONOUS REACTANCE

When a generator operates on a steady state symmetrical short circuit condition its terminal voltage is zero and its saturation is negligible. Since there is no terminal voltage the net stator linkage must be zero, and thus the stator linkage due to its current acting alone must be exactly equal and opposite in direction to the stator linkage due to the field current acting alone. If the field current were acting alone with the stator open-circuited a certain terminal voltage would exist, and since the armature linkage has the same value as the field linkage, the voltage which must be applied to produce the stator current must be exactly the same as the terminal voltage induced under open circuit. Therefore the unsaturated synchronous impedance is the ratio of the phase voltage on open circuit resulting from a certain field current to the steady state short circuit stator current resulting from the same field current. Further, since the value of the effective resistance is usually very small in comparison with the reactance it can be neglected, and the impedance and reactance are then equal. Thus

$$X_d = \frac{E \text{ (open circuit)}}{I \text{ (short circuit)}} \text{ ohms}$$

and since the voltage drop due to the stator current is due to the fictituous reactance X_{ad} and the actual reactance $X\ell$

$$X_d = X_{ad} + X\ell$$

TRANSIENT AND SUBTRANSIENT REACTANCES AND TIME CONSTANTS

Figure 9 shows the short circuit current in one phase of a three phase alternator that has had all three phases shorted when operating at no load. The line ef drawn midway between the two sides of the envelope is called the direct current component and has different magnitudes in the three phases. The envelope of the alternating component is redrawn in Figure 10 with its axis horizontal, i.e., with the direct current component eliminated. The alternating components are the same in all three phases. When an alternating voltage is short circuited through an inductance and a resistance in series, the short circuit current will consist of two components. These components are the unidirectional or DC component which decreases logarithmically to zero, and an alternating component which is fixed by the voltage, the resistance, and the reactance of the circuit, and is constant when the resistance and reactance are constant.

In the short circuited generator the reactance is not constant until the condition equivalent to synchronous reactance is reached. When a sudden change occurs in the stator current the armature reactance is no longer constant, and under this condition voltages are induced by the changing armature reaction in the field winding, and in any other closed windings on the field structure. As the stator current builds up the voltages of the field structure will build up simultaneously, tending to maintain constant the total number of ampere turns acting on the magnetic circuit. These voltages cause transient currents in these parts.

In a polyphase generator the alternating components of the short circuit stator currents produce armature reaction which is fixed in direction with respect to the poles but decreases from an initial value to a final value fixed by the steady state short circuit currents. To balance this increase in armature reaction there must be an increase in the field current. This increase in field current is in the same direction as the initial field current since the armature reaction caused by lagging currents is demagnetizing. The change in field current decreases and becomes zero, when steady state conditions are reached.

The DC components in the stator currents produce a resultant MMF which is fixed with respect to the stator but has fundamental frequency with respect to the field. To balance this the field current must contain an alternating component of fundamental frequency. This alternating component in the field current produces an MMF of fundamental frequency in the air gap which is fixed in direction with respect to the field poles. This MMF can be resolved into two oppositely rotating components, each of which rotates at synchronous speed

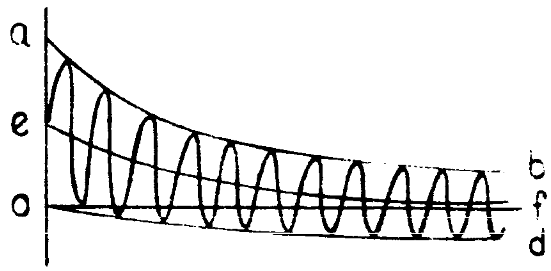

FIGURE 9

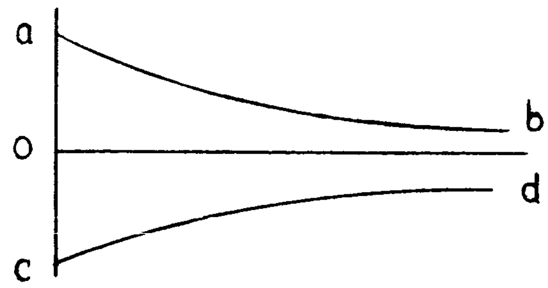

FIGURE 10

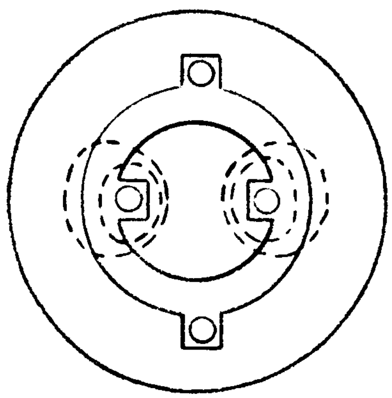

FIGURE 11

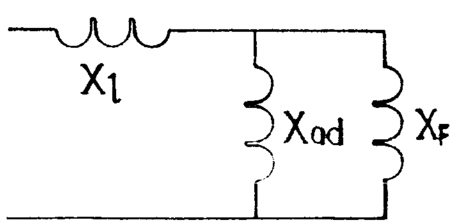

FIGURE 12

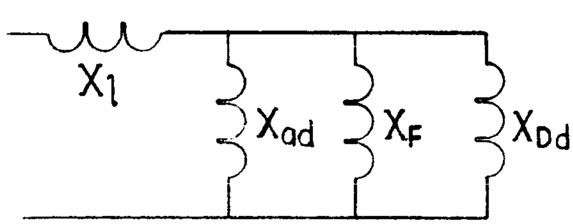

FIGURE 13

with respect to the stator. The component which rotates in the direction of the stator balances the stator MMF caused by the DC components in the stator currents. The oppositely rotating component rotates at double synchronous speed with respect to the stator winding and must be balanced by second harmonic components in the transient stator currents. All except the fundamental alternating components decrease to zero when steady state conditions have been reached and the fundamental alternating components become the steady state short circuit currents.

Consider the elementary generator shown in Figure 11. The stator winding is open and the rotor winding is excited by a DC current of magnitude I_f. At the time $t = 0$, when the axes of both windings are perpendicular to each other, the stator winding is suddenly short circuited. As stated previously the total flux interlinked with each winding under this condition will remain constant. Thus the total flux interlinked with the field winding at $t = 0$ will consist of two parts; one part going through the path of the main flux, and the other part going through the leakage path of the rotor. The total flux interlinked with the armature at $t = 0$ is zero.

During the time t the rotor moves through an angle $a = wt$ and this produces a current i_a in the stator winding and also forces a current i_f to flow in the field winding in order to sustain the field flux interlinkage. The transient currents i_a and i_f are determined by the angle a as well as the leakage fluxes of both windings and they become a maximum when $a = \pi/2$, a quarter period after the short circuit occurred.

It can be shown that the maximum transient stator current is determined by the equivalent circuit of Figure 12, and the reactance that corresponds to this circuit is the direct axis unsaturated transient reactance, X'_{du}. The field reactance, X_F, is given in Kilgore's paper as

$$X_F = X \frac{4}{\pi} C_M^2 \lambda F$$

and therefore the unsaturated transient reactance becomes

$$X'_{du} = X\ell + X_F\left(\frac{X_{ad}}{X_F + X_{ad}}\right)$$

The saturated transient reactance has been determined empirically and is approximately 88% of the unsaturated value.

In the determination of the transient reactance only the field winding of the rotor was considered. If there is a damper winding in the poles, or if eddy currents are possible in the rotor iron, subtransient currents similar to the transient currents of the field winding are induced in these circuits. These circuits will support the field winding for a few cycles and therefore they have to be considered as acting in parallel with the field winding. The equivalent circuit for this case is shown in Figure 13. X_{Dd} is the leakage reactance of the damper winding and eddy current circuits together in the direct axis, and per Kilgore's paper

$$X_{Dd} = X\lambda_{Dd}$$

where $$X_{Dd} = \frac{3.19p}{d}\left[g + \delta_d + h_{r2}\right]$$

δ is a depth of penetration factor and varies as $\sqrt{\frac{1}{f}}$. It is equal to 1.2 at 60 cycles and $\left(\sqrt{\frac{60}{400}}\right)(1.2)$ at 400 cycles. The subtransient reactance is therefore

$$X''_d = X\ell + X_{Dd}$$

The rate of decrease of the transient and subtransient currents will be determined by the time constants of the windings involved. The damper winding and eddy current circuits have much larger ratios of resistance to leakage reactance than the field winding and therefore their influence will be much shorter in duration than that of the field winding. As a matter of fact, the damper winding and eddy current circuits influence the currents only during the first few cycles. The field winding determines the decrease of the amplitudes for a much longer time. The change of the ~~amplitudes during the short~~ circuit period is such that the amplitudes are determined first by the subtransient reactance X''_d, then by the transient reactance X'_d, and finally by the synchronous reactance X_d.

The total self inductance of the field winding is

$$L_f = \frac{N_f^2 p \ell_r}{10^8}\left[C_F\left(3.19\,\frac{t_p}{g_e}\right) + \lambda_F\right]$$

where C_f is the ratio of the interlinkages of the field with its own flux to the maximum interlinkages that would be produced with a uniform gap and a concentrated field winding.

The time constant is the time in seconds required for the particular component to decay to 36.8% of its initial value. The time constant T'_{do} is the time constant of the field winding with the armature circuit open and with negligible external resistance and inductance in the field circuit. Therefore, the open circuit time constant is

$$T'_{do} = \frac{L_f}{R_f}$$

The armature time constant is the time constant of the DC component and is

$$T_a = \frac{X_2}{2\pi f r_a} \qquad \text{where } r_a = \frac{\text{stator } I^2R\ (\text{KW})}{\text{rated KVA}}$$

The transient time constant T'_d is the time constant of the transient reactance component of the alternating wave and with good approximation is

$$T'_d = \frac{X'_d}{X_d}\,T'_{do}$$

The subtransient time constant T''_d is the time constant of the subtransient reactance component of the alternating wave and is approximately .005 second for 400 cycle machines. (from tests of 60 cycle machines $T''_d \approx .035$ second or 2.1 cycles).

POTIER REACTANCE

The terminal voltage of an alternator under load differs from its open circuit voltage at the same field excitation. This difference is due to a voltage drop through the armature caused by leakage reactance, armature effective resistance, and armature reaction. The relative importance of the three factors depends upon the power factor of the load. With a reactive load at zero power factor the decrease in the terminal voltage is due almost entirely to the armature reaction and the armature leakage reactance. Under this condition the effective resistance drop is in quadrature with the terminal voltage, and since it is small in magnitude, it has little influence on the change in the terminal voltage caused by a change in load. Likewise, the resultant field F_{NL} is almost exactly equal to the algebraic difference between F_{NL} and F_{DM}, and the terminal voltage E is nearly equal to the algebraic difference between E_g and IphX. Under these conditions the armature reaction subtracts almost directly from the impressed field and the armature leakage reactance drop subtracts almost directly from the generated voltage. It follows from this that if an open circuit characteristic OB, and a curve CD are plotted as in Figure 14, showing the variation in the terminal voltage with excitation for the condition of constant stator current at a reactive power factor of zero, the two curves are so related that any two points, as E and F, which correspond to the same degree of saturation and consequently to the same generated voltage, are displaced from each other horizontally by an amount equal to the armature reaction and vertically by an amount equal to the leakage reactance drop.

GF represents the armature reaction in equivalent field amperes and GE represents the leakage reactance drop in volts. The armature leakage reactance per phase for a Y connected generator is thus $X = {}^{EG}/\sqrt{3}\ I$ and this reactance is called the Potier reactance. The triangle EJF is known as the Potier Triangle.

If the leakage reactance is constant and the increase in field current necessary to balance a given number of ampere turns of armature reaction is independent of the saturation of the magnetic circuit, Potier triangles drawn between the open circuit saturation curve and the zero power factor curve at points corresponding to different degrees of saturation would be identical. Under these conditions the zero power factor curve would have the same shape as the open circuit saturation curve but would be displaced from the open circuit curve by a distance equal to the length of the hypotenuse of the Potier triangle. Actually, the field pole leakage increases somewhat with an increase in saturation, and for this reason the number of field ampere turns which are necessary to balance a fixed number of ampere turns of armature reaction is not quite constant. In spite of this change in field pole leakage, the curves have nearly enough the same shape for practical purposes and are assumed to have the same shape when determining generator performance.

In order to make use of the Potier method to construct a zero power factor curve it is necessary to locate two points on the Potier triangle. Figure 14 shows how the method is applied. A triangle OCL is constructed with OC equal to the amperes corresponding to short circuit ampere turns ($F_{sc} = X_d F_g$). The altitude LT is made equal to IX_{pl} where Potier's reactance is calculated by a partly empirical method and

$$Xp = X\ell + \left[\frac{F_{TR} + F_{CR}}{F_{TR} + F_{CR} + F_T + F_C}\right] X_{FS}$$

$$X_{FS} = \left(\frac{\lambda rs}{\frac{2d}{Pg_e} + \lambda rs}\right) X_d$$

As the point L of the triangle is moved along the no load saturation curve, point C traces the zero power factor saturation curve.

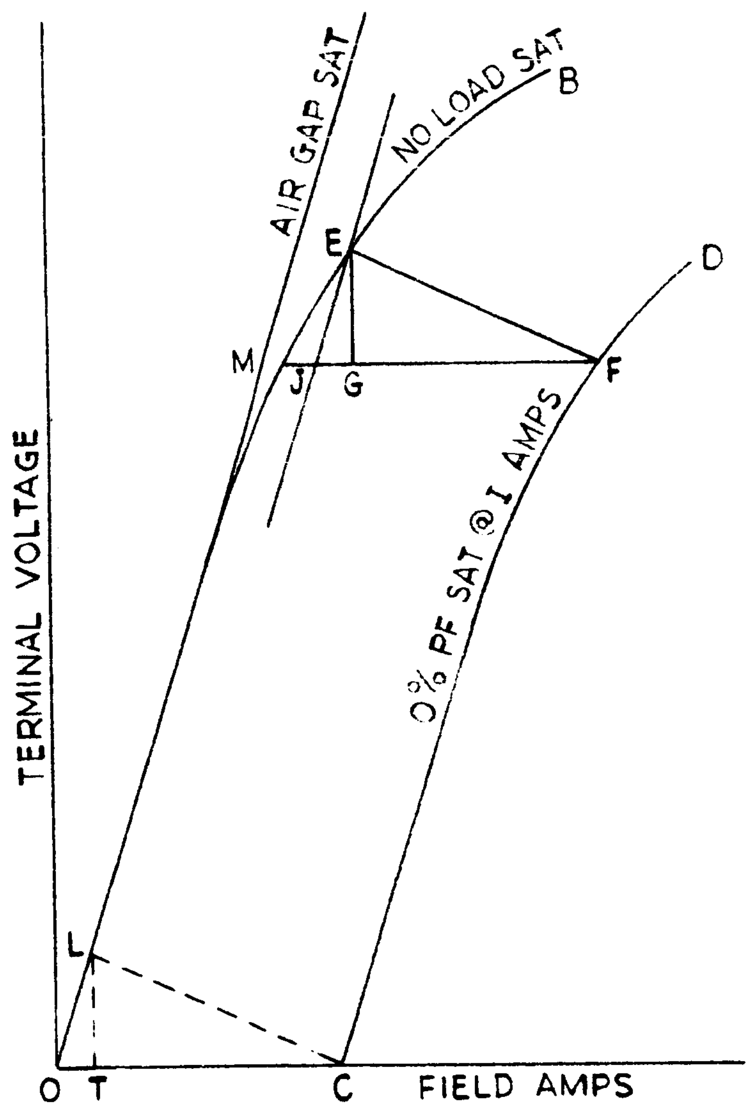
AIR GAP SAT
NO LOAD SAT
B
E
D
M
J
G
F
0% PF SAT @ I AMPS
TERMINAL VOLTAGE
L
O
T
C
FIELD AMPS

FIGURE 14

VECTOR DIAGRAM OF A ROUND ROTOR GENERATOR

All currents and all voltages on the vector diagrams of generators must be per phase. The MMF of armature reaction must always be for all phases because the reactions of all phases combine to modify the resultant field and affect the voltages of all phases alike. All MMFs are expressed in ampere turns per pole.

VECTOR DIAGRAM OF A ROUND ROTOR GENERATOR

Referring to the figure, Iph r_e is the effective resistance drop and Iph X_ℓ is the leakage reactance drop. Adding these drops vectorially to Eph gives E_g, which is the voltage rise generated by the air gap flux ϕ_g. This is the flux which is produced by the combined action of the impressed field and the armature reaction and is called the resultant field. It must lead the voltage rise E_g in the armature by 90^o in time. To illustrate this, assume that the two active sides of a coil are 180 electrical degrees apart. Under this condition, when the coil is directly over a pole and contains a maximum flux its two active sides are midway between the poles and are in zero fields. They are cutting no flux and the voltages induced in them are zero. When the coil has moved forward 90 electrical degrees the flux through it becomes zero but the inductors are now directly under the centers of opposite poles and are in the strongest part of the field. The voltages induced in the two coil sides have maximum values and thus the voltage in the coil is in quadrature with respect to the flux through it.

Let F_{NL} be the resultant MMF required to produce the flux ϕ_g. If it were not for armature reaction F_{NL} would be the MMF of the impressed field. The armature reaction is in phase with the current and is shown by F_{DM} on the diagram. On account of the armature reaction the impressed field must have a component $-F_{DM}$ to balance it. Adding F_{NL} and $-F_{DM}$ vectorially gives the field MMF, F_{FL}, which is required to produce the terminal voltage Eph. This

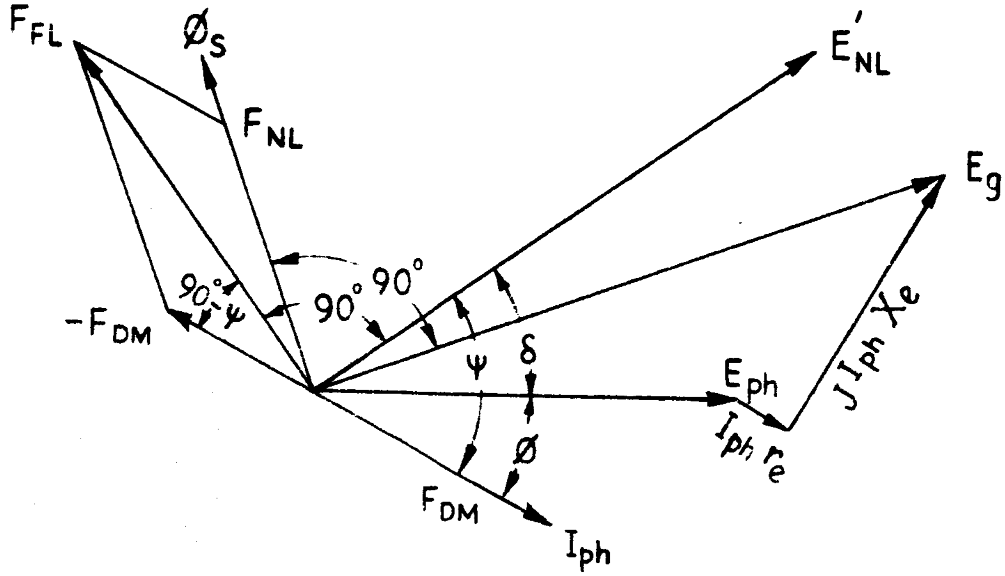

F_{FL}
ϕ_S
F_{NL}
E'_{NL}
E_g
$90°$
$90°$
$90°$
$90°-\psi$
$-F_{DM}$
ψ
δ
E_{ph}
$jI_{ph}X_e$
$I_{ph}r_e$
ϕ
F_{DM}
I_{ph}

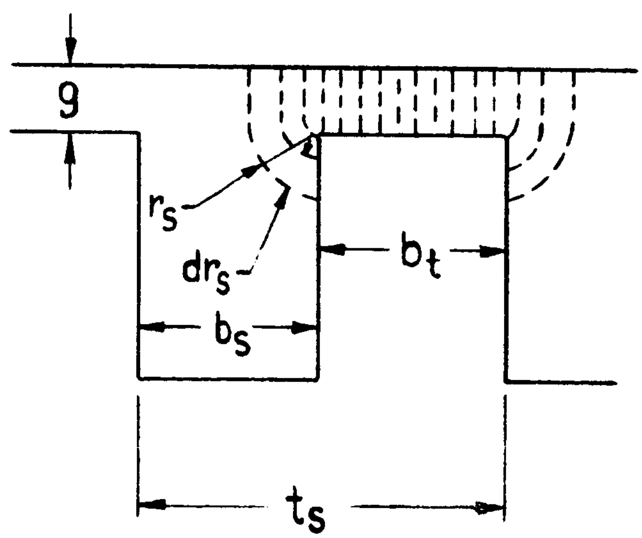

g
r_s
dr_s
b_t
b_s
t_s

assumes that the coefficient of field leakage is unaffected by a change in load. It also assumes that the air gap is uniform. The effect of the change in the leakage coefficient can be taken into account by making use of an open circuit saturation curve which has been corrected for field leakage. The open circuit voltage when the load is removed is the voltage E'_{NL} corresponding to the excitation F_{FL} on the open circuit characteristic. It lags F_{FL} by 90 degrees.

CARTER'S COEFFICIENTS

Carter's coefficients are factors that take into account the increase in the reluctance of the magnetic circuit due to the presence of slots, air gaps, etc. For convenience in calculating these coefficients it is assumed that there is no saturation in the teeth and the teeth are considered as having parallel sides. Also, the path of the flux is assumed to follow a straight line across the length of the gap g, and then to curve at a radius r into the side of the tooth. Under these conditions the permeance of the gap per inch of core length will be made up of two parts; (a) the permeance $P_1 = b_{t/g}$ between the pole face and the top of the tooth and (b) the permeance $2P_2$ where P_2 is the permeance between the pole face and one side of the tooth. The permeance of any small section dr_s is

$$dP_2 = \frac{dr_s}{g + \frac{\pi rs}{2}} = \frac{2dr_s}{(2g + \pi r_s)\frac{\pi}{\pi}} = \frac{2}{\pi} \frac{dr_s}{\frac{2g}{\pi} + r_s}$$

$$P_2 = \frac{2}{\pi} \int_0^{b_{s/2}} \frac{dr_s}{\frac{2g}{\pi} + r_s}$$

$$\text{Since} \int \frac{dx}{a + bx} = \frac{1}{b} \log_e (a + bx)$$

$$P_2 = \frac{2}{\pi}\left[\log_e\left(\frac{2g}{\pi} + r_s\right)\right]_o^{b_s/2} = \frac{2}{\pi}\left[\log_e\left(\frac{2g}{\pi} + \frac{b_s}{2}\right) - \log_e \frac{2g}{\pi}\right]$$

$$\log_e a - \log_e b = \log_e \frac{a}{b}$$

$$P_2 = \frac{2}{\pi} \log_e \left(1 + \frac{\pi b_s}{4g}\right)$$

The average permeance over the slot pitch is therefore

$$P_{avg} = \frac{b_s}{t_s}(2P_2) + \frac{b_t}{t_s}(P_1) = \frac{b_s\left[\frac{4}{\pi} \log_e \left(1 + \frac{\pi b_s}{4g}\right)\right] + \frac{b_t^2}{g}}{t_s}$$

and the reciprocal of this quantity is the reluctance which corresponds to that of the equivalent gap. This reluctance compared to that of a smooth surface is the Carter coefficient.

Since the flux does not behave exactly as given in the above derivation it has become necessary to obtain the equivalent gap by empirical means. When this has been done the various Carter's coefficients have been determined as indicated in the following:

(a) OPEN SLOTS

$$K = \frac{t_s (5g + b_s)}{t_s (5g + b_s) - b_s^2}$$

(b) PARTIALLY CLOSED SLOTS

$$K = \frac{t_s (4.44g + 0.75b_o)}{t_s (4.44g + 0.75b_o) - b_o^2}$$

THE EFFECT OF VARYING THE POLE EMBRACE IN ELECTROMAGNETIC GENERATORS

Salient-pole, wound-pole, synchronous generators have for many years been made with pole embraces of 70% to 75%. The 70% (approx.) pole embrace is a compromise since the amount of field winding that can be supported on a pole of a wound-pole generator depends in part on the pole head overhang and thus on the pole embrace. Too great a pole embrace results in excessive flux leakage and too small a pole embrace would not allow enough field winding so the best pole embrace is in most cases 70-75%. That value has come to be regarded as the best to use for synchronous salient-pole machines in general.

None of the brushless, rectifierless generators have field windings on their poles and the best pole embrace for these machines to use can be determined by the efficiency of the magnetic circuit. The best pole embrace should result in the maximum output per pound of machine weight.

The length of the rotor and stator of most brushless, rectifierless generators is limited by the flux that can be carried through the rotor. In all Lundell generators and in the axial-gap homopolar inductor, the flux is carried axially through a shaft section. The limiting feature of the design of any of these machines is the amount of flux that can be carried through these shaft sections. As a result, the maximum rating that can be built for any specified stator bore diameter depends upon the efficiency with which the machine utilizes its rotor flux.

In all the variations of the Lundell type generators and homopolar inductors, the easiest and most practical pole shape to use is concentric with the stator bore. For this reason, the concentric pole has been used to study the effect of varying the pole embrace. Curves of C_1 and C_p versus pole embrace can be taken from David Ginsberg "Design Calculations for A-C Generators" - Trans. AIEE, Vol. 69, pp 1274-80, 1950. The curves of C_1 and C_p can also be obtained by integrating a square wave over the pole embrace. C_p is the average over the pole pitch and is identical in value to the pole embrace. C_1 values are derived later in this article.

Summary

A study of pole embrace variation for concentric poles in synchronous generators shows that:

1. Narrow poles make most efficient use of pole flux in conventional wound-pole, salient-pole machines, and in all Lundell type machines.

2. Best pole width for homopolar inductor generators varies with the level of interpolar leakage. For high values of interpolar leakage, wider poles should be used. Narrow poles are best for low leakage inductors.

3. In most machines, a pole embrace of about 50% should give good utilization of pole flux.

Discussion

The voltage generated in any electromagnetic generator can be expressed by the equation:

$$E_{LL} = \frac{\phi_T \, RPM \, C_W Ne}{60 \times 10^5}$$

Where:

$$C_W = \text{The Winding Constant}$$

$$= \frac{E_{LL}}{E_{ph}} \times \frac{1}{m} \times \frac{C_1 K_d}{\sqrt{2}}$$

m = No. of Phases

Ne = No. of Effective Conductors in Machine

K_d = Distribution Constant

ϕ_T = Bg Ag = Gap Density over pole head x area of the air gap

This equation can be shown to be equivalent to any other voltage equation used in machine design.

If C_1 is inserted directly into the voltage equation:

$$E_{LL} = \phi_T \left[f_n (C_1) \right] \text{ for any given machine at a fixed RPM}$$

The flux in the pole of a generator is:

$$\phi_p = \frac{\phi_T}{P} \times C_p$$

Where:

P = No. of Poles

C_p = Pole Constant = $\frac{\text{Average Field Form}}{\text{Max. of Field Form}}$

If E_{LL} and RPM are constant and all machine parameters are fixed except the pole embrace, C_1, C_p and ϕ_p will vary with changes in pole head width.

In the following tables, ϕ_p is tabulated for various pole embraces and various levels of interpolar flux leakage.

Case I is the case for salient pole generators such as the conventional synchronous generator and Lundell generators.

Case II is a study of homopolar inductors with various levels of interpolar flux leakage.

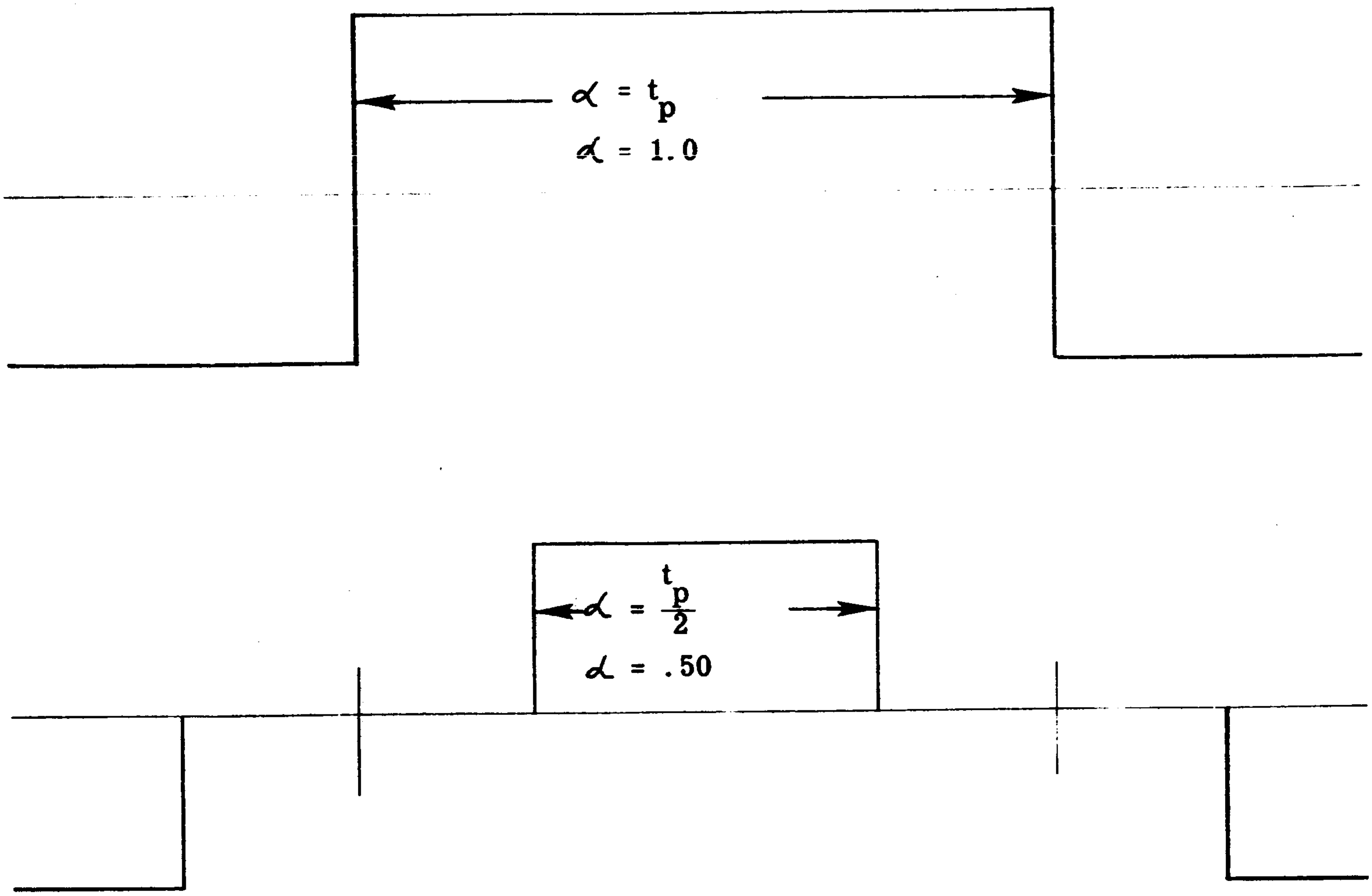

Vary α from 1.0 to 0.3

Case I -- No Interpolar Flux Leakage -- This is the Case for a Conventional Synchronous Generator and for Lundell-Type Generators

C_1 = "The Fundamental of the Field Form". It is the ratio:

$$\frac{\text{Maximum Fundamental Flux}}{\text{Actual Maximum Value of the Field Form}}$$

$$C_1 = \frac{2}{N}\int_0^N Y_N \cos\alpha$$

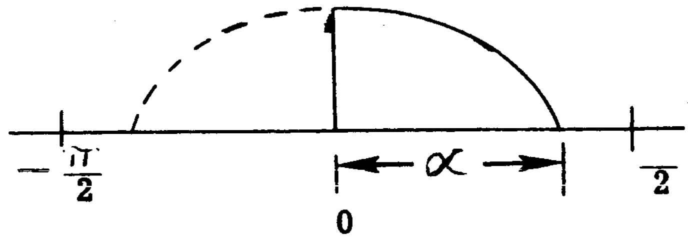

$$C_1 = \frac{4}{\pi}\int_0^{\frac{\pi}{2}} (1)\cos\alpha = \frac{4}{\pi} = 1.27 \text{ for 100\% Pole Emb.}$$

$$C_1 = \frac{4}{\pi}\int_0^{\frac{\pi}{2}(.5)} (1)\cos\alpha = \frac{4}{\pi}\ .707 = .90 \text{ for 50\% Pole Emb.}$$

α	C_1 (No Leakage)
1.0	1.27
.9	1.26
.8	1.21
.7	1.14
.6	1.03
.5	.90
.4	.75
.3	.58

C_p = "The Pole Constant". It is the ratio of the average to the maximum of the field form.

$$C_p = \frac{1}{N}\int_0^N Y_N$$

For a uniform gap, the field form is a square wave and the pole constant is equal to the pole embrace.

CASE I

Pole Embrace	C_1	Per Unit Total Flux To Generate 1.0 P.U. Volts	C_p	Per Unit Pole Flux To Generate 1.0 P.U. Volts = C_p x P.U. ØT
1.0	1.27	1.0	1.0	1.0
.9	1.26	1.01	.9	.909
.8	1.21	1.045	.8	.835
.7	1.14	1.11	.7	.777
.6	1.03	1.23	.6	.738
.5	.90	1.41	.5	.705
.4	.75	1.70	.4	.68
.3	.58	2.19	.3	.658

This case represents the wound-pole synchronous generator, and the Lundell-Type generators, both axial-gap and radial-gap.

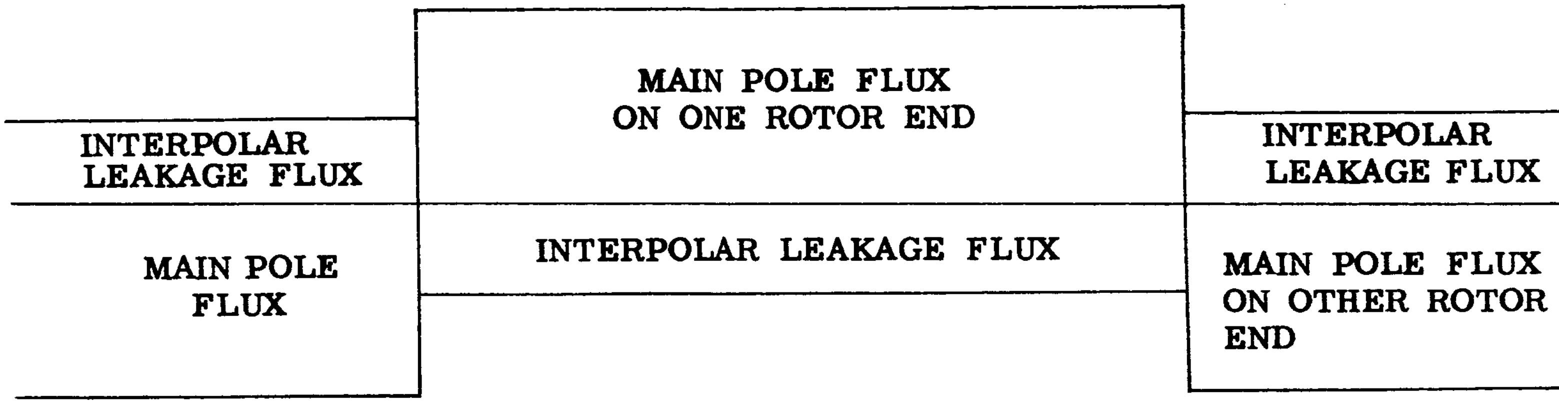

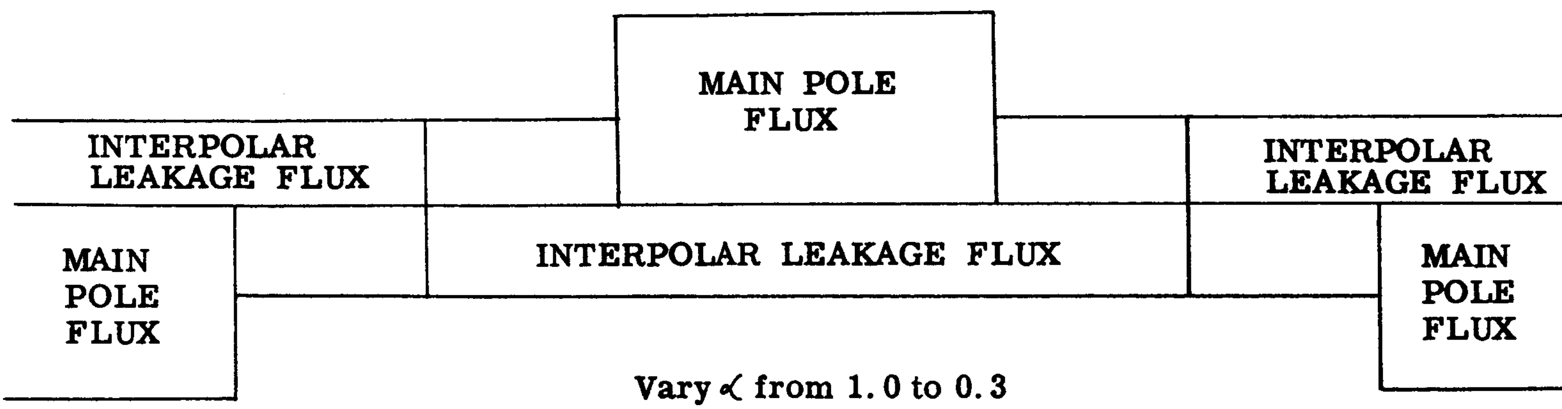

Vary α from 1.0 to 0.3

Case II -- Interpolar Leakage Flux Varies from 5% to 25% of the Maximum

Value of the Actual Pole Flux Wave (Field Form)

CASE II

5% LEAKAGE

Pole Embrace	C_1 for Square Wave	C_1 Reduced to 95%	P.U. Total Flux to Generate 1.0 P.U. Volts	C_p Increased 5%	P.U. Pole Flux to Generate 1.0 P.U. Volts = $C_p/1.05 \times$ P.U. ϕ_T
1.0	1.27	1.21	1.0	1.05	1.0
.9	1.26	1.20	1.01	.95	.913
.8	1.21	1.15	1.05	.85	.85
.7	1.14	1.08	1.12	.75	.80
.6	1.03	.98	1.23	.65	.76
.5	.90	.855	1.41	.55	.74
.4	.75	.71	1.70	.45	.73
.3	.58	.55	2.20	.35	.733

CASE II

10% LEAKAGE

Pole Embrace	C_1 for Square Wave	C_1 Reduced to 90%	P.U. Total Flux to Generate 1.0 P.U. Volts	C_p Increased 10%	P.U. Pole Flux to Generate 1.0 P.U. Volts = $C_p/1.10 \times$ P.U. ϕ_P
1.0	1.27	1.14	1.0	1.10	1.0
.9	1.26	1.135	1.01	1.0	.92
.8	1.21	1.09	1.045	.90	.856
.7	1.14	1.025	1.11	.80	.81
.6	1.03	.93	1.225	.70	.78
.5	.90	.81	1.41	.60	.77
.4	.75	.675	1.69	.50	.77
.3	.58	.52	2.19	.40	.80

CASE II

20% LEAKAGE

Pole Embrace	C_1 for Square Wave	C_1 Reduced to 80%	P.U. Total Flux to Generate 1.0 P.U. Volts	C_p Increased 20%	P.U. Pole Flux to Generate 1.0 P.U. Volts = $C_p/1.20 \times$ P.U. ϕ_T
1.0	1.27	1.015	1.0	1.20	1.0
.9	1.26	1.005	1.01	1.10	.93
.8	1.21	.97	1.05	1.0	.875
.7	1.14	.91	1.12	.90	.84
.6	1.03	.825	1.23	.80	.82
.5	.90	.72	1.41	.70	.822
.4	.75	.60	1.69	.60	.845
.3	.58	.463	2.2	.50	.917

CASE II

25% LEAKAGE

Pole Embrace	C_1 for Square Wave	C_1 Reduced to 75%	P.U. Total Flux to Generate 1.0 P.U. Volts	C_p Increased 25%	P.U. Pole Flux to Generate 1.0 P.U. Volts = $C_p/1.25 \times$ P.U. ϕ_T
1.0	1.27	.95	1.0	1.25	1.0
.9	1.26	.94	1.01	1.15	.93
.8	1.21	.91	1.04	1.05	.875
.7	1.14	.855	1.11	.95	.845
.6	1.03	.77	1.23	.85	.835
.5	.90	.675	1.41	.75	.845
.4	.75	.56	1.7	.65	.882
.3	.58	.435	2.18	.55	.96

CASE II

40% LEAKAGE

Pole Embrace	C_1 for Square Wave	C_1 Reduced to 60%	P. U. Total Flux to Generate 1.0 P. U. Volts	C_p Increased 40%	P. U. Pole Flux to Generate 1.0 P. U. Volts = $C_p/1.4 \times$ P. U. ϕ_T
1.0	1.27	.763	1.0	1.4	1.0
.9	1.26	.756	1.01	1.3	.94
.8	1.21	.73	1.05	1.2	.9
.7	1.14	.685	1.11	1.1	.875
.6	1.03	.62	1.23	1.0	.88
.5	.90	.54	1.41	.9	.91
.4	.75	.45	1.7	.8	.97
.3	.58	.347	2.24	.7	1.12

BEST POLE EMBRACE V.S. INTERPOLAR LEAKAGE FOR HOMOPOLAR INDUCTOR GENERATORS

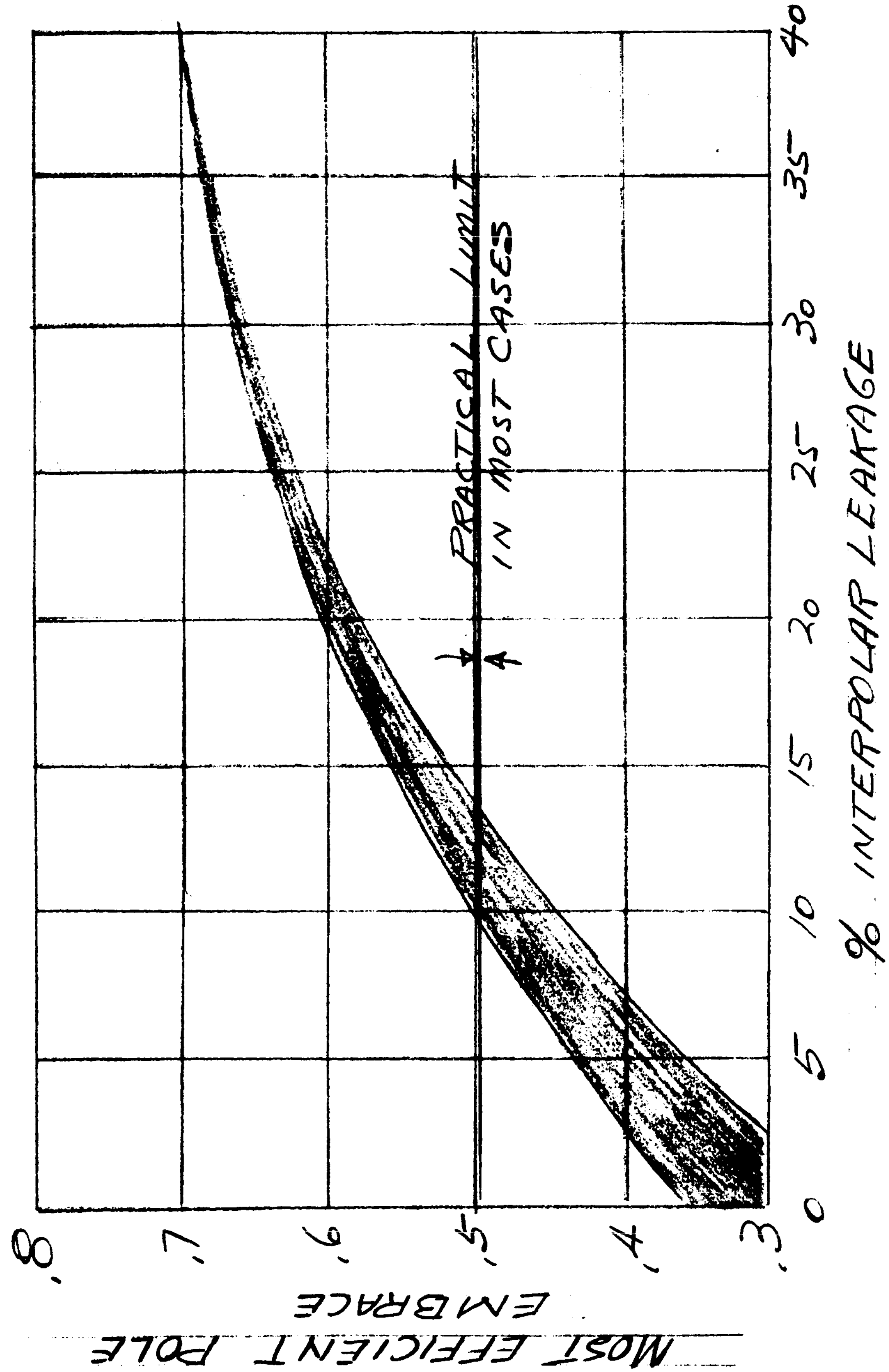

Conclusion

The brief study shows that the narrower poles are most efficient for machines with no interpolar leakage. In most cases, .5 pole embrace would represent an extreme since the flux density in the teeth for .5 embrace is 27% higher than for an embrace of .70.

The best pole embrace for homopolar inductors depends upon the level of interpolar leakage but in a practical design with 10% leakage or less, a 50% pole embrace will allow greater output than will a wider pole.

FLUX-PLOTTING

GRAPHICAL FLUX ANALYSIS

Graphical flux analysis is the quickest and most direct solution to many field problems. Irregular or complex fields that yield slowly to mathematical analysis, if at all, can be solved graphically. Manual plots are used to solve heat-flow, air-flow, dielectric field, and flux field problems.

In this study, only flux field distributions are mapped, and only the simplest case is considered -- that is, the case where the iron surfaces are equipotential surfaces and the space between the iron surfaces has the permeability of air. The same total field potential exists across the air space regardless of any change in dimension or configuration.

The permeability of air is constant, so if the field gradient per unit of linear measurement (ampere turns per inch) across the air space changes, the flux density must change by the same ratio.

In making flux plots, the flux is considered to consist of tubes of flux. In a three dimensional field, a single tube is conceived of as looking like this:

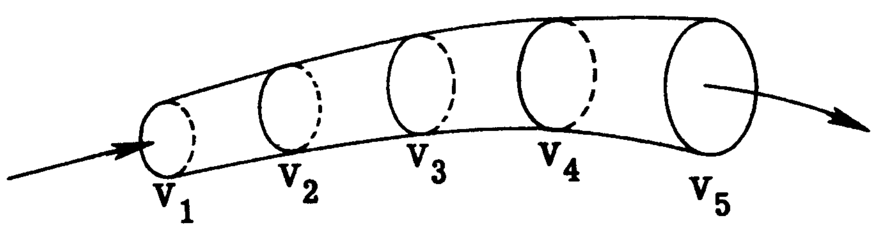

In a two dimensional field, the depth of the tube is constant and the tube looks like this:

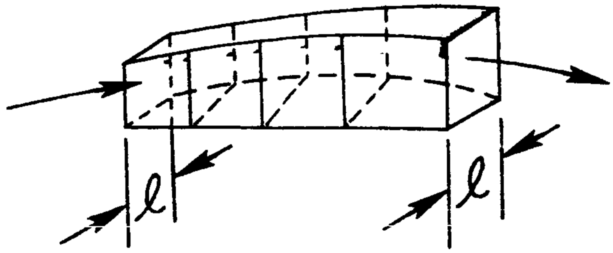

If the number of lines of flux in a tube is held constant, and the depth of the tube is constant, the sides of the tube of flux must converge or diverge in direct ratio to the change in field gradient.

By choosing the scale of field gradient and flux density, the area of flux tube enclosed by the sides of the tube and the equipotential field gradient lines become a square.

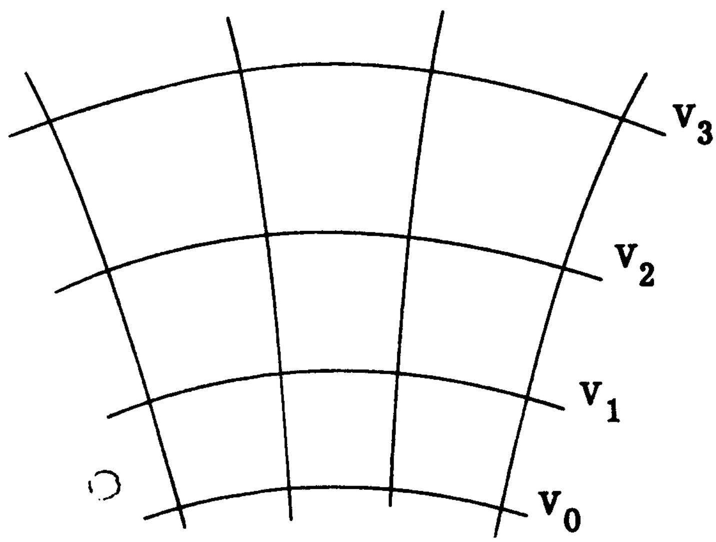

The lines of flux must cross equipotential lines at right angles and enter the iron at right angles. The corners of the areas so defined are right angles and if the squares are successfully divided into fourths, the smaller squares become more closely true squares. In any of the squares, the two dividing lines used to divide the square into four squares will be closely equal in length.

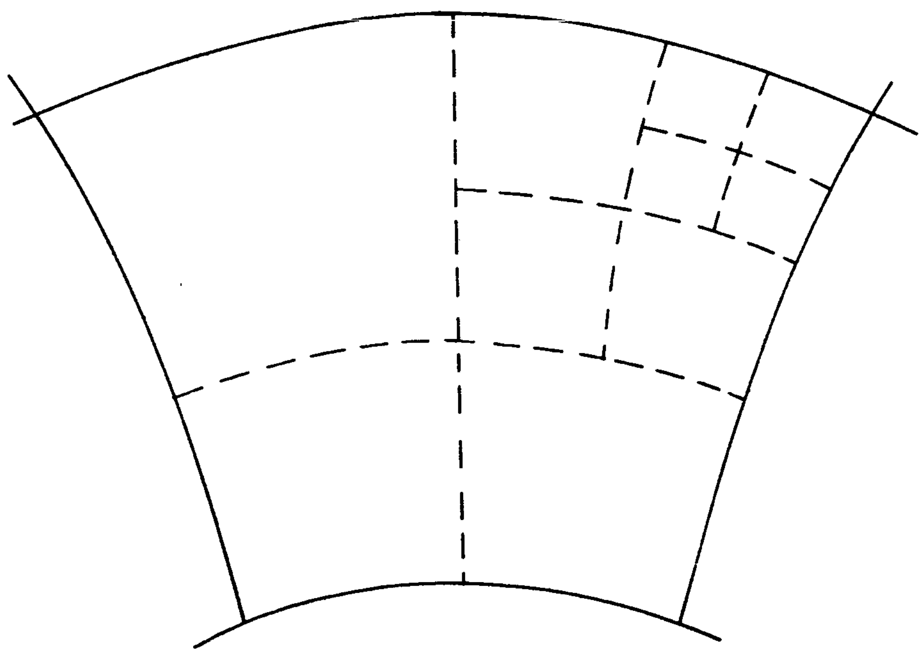

To start a map or flux plot, draw the area to be mapped as large in scale as practical. Ink the boundaries of the iron so erasures will not remove them. Also, ink in the lines of symmetry.

Draw in the middle an equipotential line and then start the plot in the most irregular region or at a corner and a line of symmetry.

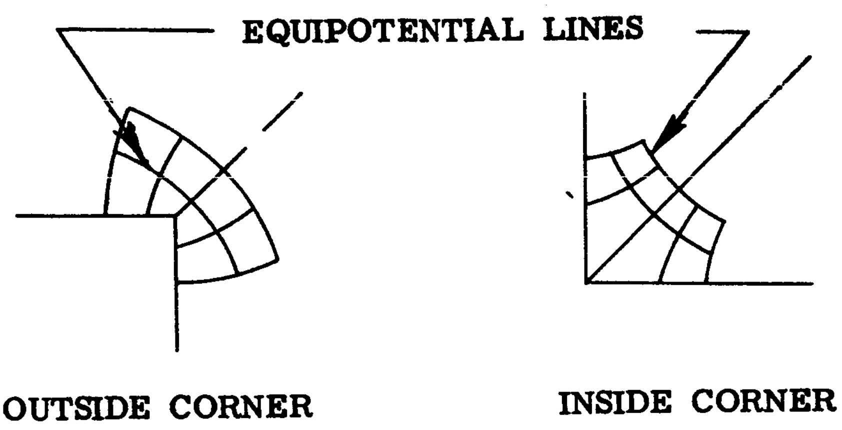

Start the maps with large sweeping curves and close the map before trying to perfect the detailed areas.

Use 2H pencil for easy erasures with minimum smudging.

Make large squares and divide only where necessary to check map accuracy or to obtain accurate density.

Intersections between flux lines and equipotential lines must be right angles at all times or the map can not be made accurately.

When the tubes of equal flux are divided, they are most easily divided into multiples of two.

A map can not be forced. However, useable accuracy can be obtained without a precise map, and the operator should exercise his own judgment as to the accuracy required.

To move lines a small amount, try widening the line with pencil and removing the unwanted portion with a sharp-pointed eraser.

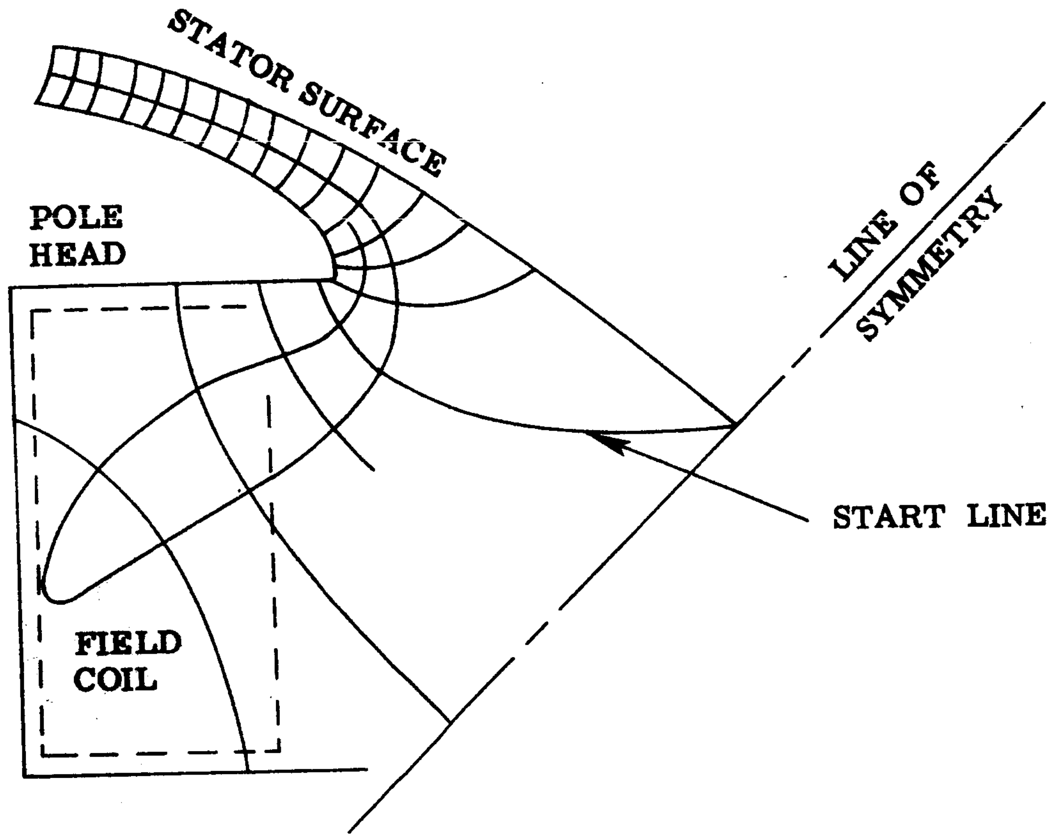

To determine, by means of a freehand flux plot, the no load field form of an electromagnetic machine:

1. Make the flux plot in the manner described in the literature, with all intersections of flux lines and equipotential lines at right angles and with all curvilinear squares capable of being divided into smaller, curvilinear squares.

2. The distance from centerline between poles to the centerline of the pole is 90 electrical degrees. Divide this arc on the stator surface into 10° increments.

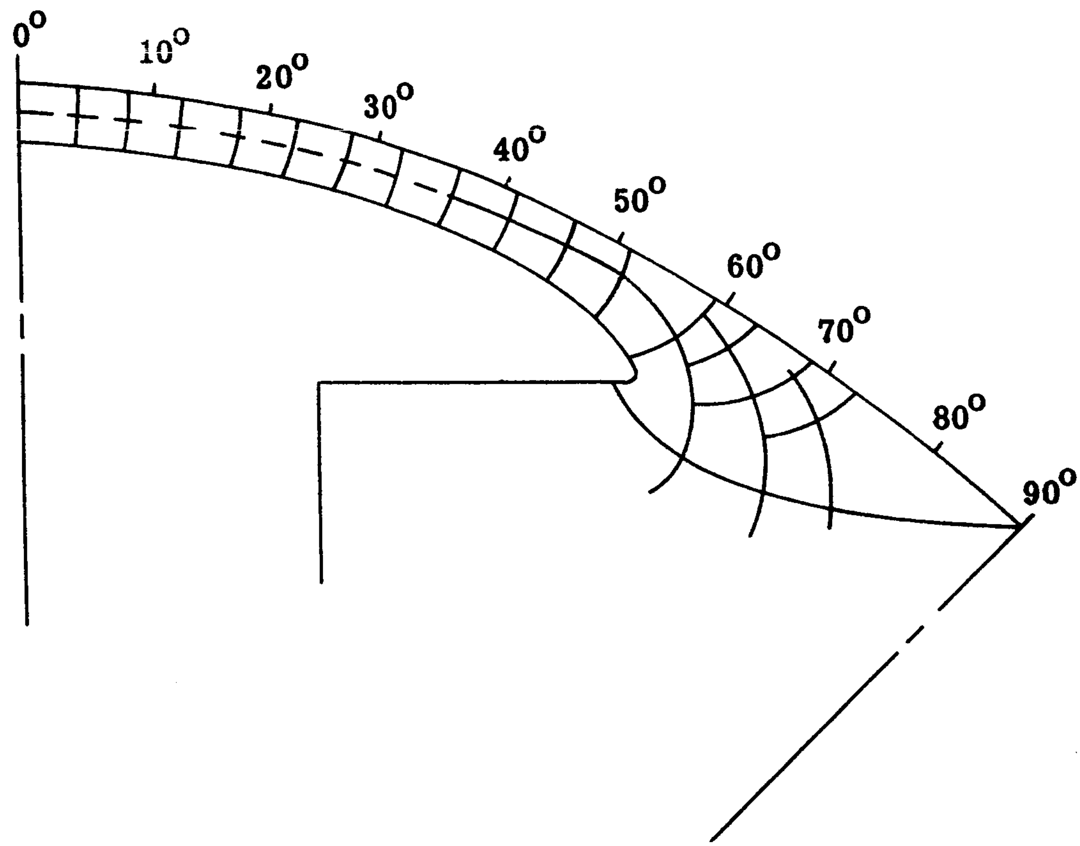

3. At any point on the stator surface, the distance from the surface to the first equipotential line is proportional to the flux density at that point. A plot of flux density, therefore, is a plot of the ratio of distance from the stator surface to the first equipotential line. Where the equipotential lines have been further divided, the distance ratios increase proportionately.

4. The maximum density (usually at the pole head centerline) can be used as a one per unit; 1.0 or 100%.

$$C_1 = \text{Ratio } \frac{\text{Fundamental}}{\text{Actual}} = \frac{2}{\pi}\int_0^{\pi} f(\theta)\sin\theta\, d\theta$$

$$\text{or } \frac{4}{\pi}\int_0^{\pi/2} f(\theta)\cos\theta\, d\theta$$

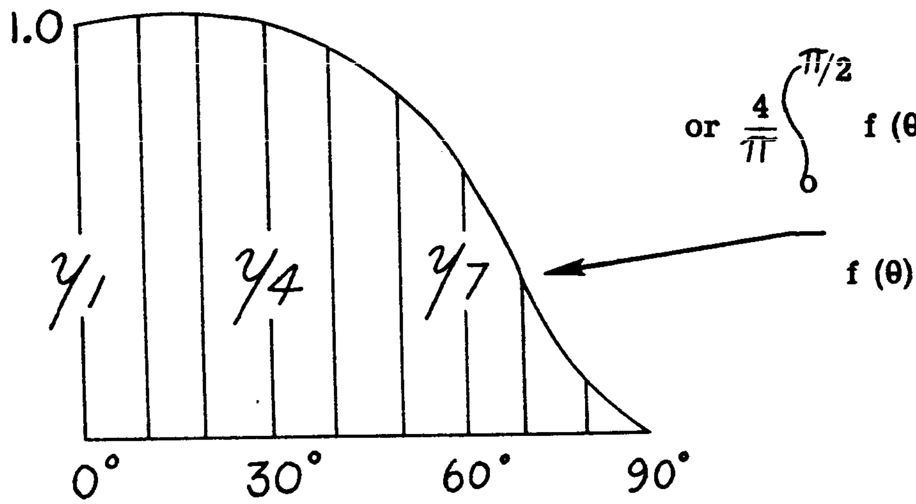

Cos 0° = 1.000	Y1	(.5)	=
Cos 10° = .985	Y2	(.985)	=
Cos 20° = .940	Y3	(.940)	=
Cos 30° = .866	Y4	(.866)	=
Cos 40° = .766	Y5	(.766)	=
Cos 50° = .643	Y6	(.643)	=
Cos 60° = .500	Y7	(.500)	=
Cos 70° = .342	Y8	(.342)	=
Cos 80° = .173	Y9	(.173)	=
Cos 90° = .000			

$9\overline{\big)\sum_{Y_i}^{1/9}}$

C_1 =

Ref: Mathematics of Modern Engineering, Vol 1, pp 73-92, Doherty and Keller.

References to use for a study of Flux-Mapping techniques are:

"Graphical Flux Analysis in Transformer Design", M.G. Leonard, Electro-Technology, Oct., 1961, pp 122-128.

"Fundamentals of Electrical Design", A.D. Moore, McGraw-Hill Book.

"Electromagnetic Devices", H.C. Roters, John-Wiley & Sons Book.

Notes on Air-Gap and Interpolar Induction, F.W. Carter, IEE Proc. (British), Vol 29, 1900, p 925.

Air Gap Induction, F.W. Carter, El. World, Vol. 38, p 884.

Sketches of Magnetic Fields in Iron, Th. Lehmann, Rev. Gen. El., Vol. 17, 1926

Mapping Magnetic and Electrostatic Fields, A.C. Moore, El. J., Vol. 23, 1926, p 355.

Fundamental Theory of Flux Plotting, A.R. Stevenson, G. E. Rev., Vol. 29, 1926, p 797.

Graphical Determination of Magnetic Fields, R.W. Wieseman, AIEE Trans., Vol. 46, 1927, p 430.

Graphical Determination of Magnetic Fields, E.E. Johnson and C.H. Green, AIEE Trans., Vol. 46, 1927, p 136.

Graphical Determination of Magnetic Fields, A.R. Stevenson and R.H. Park, AIEE Trans., Vol. 46, 1927, p 112.

The Interpolar Fields of Saturated Circuits, T. Lehmann, AIEE Trans., Vol. 46, 1927, p 1411.

A Practical Application of Graphical Flux Mapping, J.F. Calvert, El. J., Vol. 24, 1927, p 543.

Graphical Flux Mapping, J.F. Calvert and A.M. Harrison, El. J., Vol. 25, 1928. Theory and General Discussion, p 147; Fields of Non-Salient Pole Synchronous Machines, p 179; D-C Motors and Generators, p 399; D-C Motor, Salient Pole Synchronous Machine, Universal Motor, etc., p 510.

Analytical Determination of Magnetic Fields, B.L. Robertson and I.A. Terry, AIEE Trans., Vol. 48, 1929, p 1242.

Magnetic Fields in Machinery Windings, J.F.H. Douglas, AIEE Trans., Vol. 54, 1935, p 959.

SYMBOLS

LIST OF SYMBOLS

A, a

A	ampere-conductors per unit of circumference
A	area
a	distance between midpoints of two adjacent coil ends
a	area
a_c	actual area of the stator conductor
a_{ch}	actual area of the rotor conductor
a_{st}	area of a strand of the conductor

B, b

B	flux density
B or B_g	flux density in the gap
B_c	flux density in the core
B_c	flux density in the stator core
B_i	flux density in the air gap of the interpole
B_{pc}	flux density at the center section of the pole
B_q	maximum flux density in the air gap
B_{rc}	flux density in the rotor core
B_{rs}	flux density at the slotted section of the pole
$B_{t\ 1/3}$	flux density in the stator tooth at 1/3 the distance from the minimum section
B_t	actual flux density in the tooth

B_t'	fictitious flux density in the tooth
b	width
b_e	equivalent pole arc
b_i	width of interpole
b_o	slot width at the air gap
b_o	width of the slot opening in the stator slot
b_p	width of pole shoe
b_p	width of the center section of the pole
b_r	width of the rotor slot
b_{rh}	height of the ventilating holes in the rotor iron
b_{ro}	width of the slot opening in the rotor slot
b_s	slot width
b_s	width of the stator slot
b_t	width of the stator tooth at the stator bore
b_{tm}	width of the stator tooth at a distance half way down the slot
b_{tr}	width of the rotor tooth at the outside diameter of the rotor
b_1	width of the stator slot at the bottom part of the tapered section
b_2	width of the stator slot at the top of the top conductor
$b_{t\,1/3}$	width of stator slot 1/3 distance up from the inside stator bore

C, c

C	capacitance
C_1	ratio of the maximum fundamental of the field form to the actual maximum of the field form

C_M	demagnetizing factor
C_p	ratio of the average value of the field form to the maximum value of the field form
C_q	cross magnetizing factor
C_W	winding constant
C_X	slot reactance reduction factor
c	number of parallel groups
c	specific heat
c	number of parallel paths in the winding

D, d

D	outside diameter of the stator punching
d	inside diameter of the stator punching
d_b	diameter of the bender pin
d_r	outside diameter of the rotor
d_s	inside diameter of the rotor punching

E, e

E	line voltage
E_f	field voltage
$E_{F(top)}$	eddy current factor top
$E_{F(bot)}$	eddy current factor bottom
E_{ph}	phase voltage
e	induced emf, instantaneous value
e_s	emf of self-induction

F, f

F	force
F_C	ampere turns per pole for the stator core
F_{CR}	ampere turns per pole for the rotor core
F_{DM}	demagnetizing ampere turns per pole
F_f	resultant fundamental component of the field MMF
F_{FL}	field ampere turns per pole required to generate voltage at rated load
F_g	air gap ampere turns per pole
F_{NL}	field ampere turns per pole required to generate rated voltage at no load
F_{OL}	field ampere turns per pole required to generate rated voltage at overload
F_R	rotor iron ampere turns per pole
F_S	stator iron ampere turns per pole
F_{SC}	ampere turns per pole required to circulate rated current on steady state short circuit operation
F_T	ampere turns per pole for the stator teeth
F_{TR}	ampere turns per pole for the rotor teeth
f	force on a single conductor
f	frequency in cycles per second

G, g

g	single air gap
g_e	effective air gap

H, h

H	field intensity
HP	output in horsepower
h	height
h	heat transfer coefficient
h_c	core height
h_c	depth of the stator core
h_l	height of the slot occupied by the conductors
h_o	depth of the stator slot opening
h_p	length of magnetic patch in a pole
h_r	depth of the rotor slot
h_{rc}	depth of the rotor core
h_{ri}	depth of the rotor slot from the top edge of the top conductor to the bottom edge of the bottom conductor
h_{r2}	depth of the rotor slot from the bore to the top edge of the top conductor
h_s	depth of the slot
h_s	depth of the stator slot
h_{st}	uninsulated height of the strand
h'_{st}	depthwise distance between the centerlines of adjacent strands
h_t	length of magnetic patch in a tooth
h_t	depth of the tapered part of the stator slot
h_{te}	end length extension of stator coil for unit slot throw
h_w	depth of the straight part of the stator slot from the bottom of the tapered section to the top of the top conductor

I, i

I	current (for a-c effective value)
I_c	amperes per conductor
I_f	field current
I_{f2}	field current in auxiliary coil
I_n	rated current
I_{ph}	phase current
i	current, instantaneous value

K, k

K_d	distribution factor of the stator winding
K_{df}	distribution factor of the field winding
K_E	end turn leakage reactance factor
K_i	stacking factor of the iron
K_p	pitch factor of the stator winding
K_{pf}	pitch factor of the field winding
K_Q	watts per pound loss
K_r	Carter's coefficient for the rotor slots
K_s	Carter's coefficient for the stator slots
K_{sk}	skew factor
K_t	constant used in the determination of the 1/2 mean turn of random wound coils
K_X	factor to account for difference in phase of current in coil sides in same slot
k	constant

k	stacking factor
k_s	ratio of total length of armature L to the length effective for slot leakage
k_t	ratio of slot width to tooth width
k_v	ratio of total length L to equivalent armature length
k_{xco}	reduction factor for slot leakage permeance (for part of slot occupied by the conductors)
k_{xt}	reduction factor for slot leakage permeance (for part above the conductors)

L, l

L	coefficient of self-inductance
L	total length of stator stack
L_E	total length of the end extension of one turn
L_e	coefficient of self-inductance for the end winding leakage flux
L_F	self inductance of the field winding
L_f	self-inductance of the field winding
L_s	coefficient of self-inductance for the slot leakage flux
L_{sb}	coefficient of self-inductance of the bottom coil side for the slot leakage flux
L_{st}	coefficient of self-inductance of the top coil side for the slot leakage flux
L_{tt}	coefficient of self-inductance for the tooth top leakage flux
l	overall length of the stator iron
l	length

l	length of armature core without radial ventilating ducts
l_c	length of magnetic path in a core
l_e	equivalent length of armature core
l_e	length of the end winding for half a coil
l_{e2}	straight part of the coil extension beyond the core
l_r	overall length of the rotor iron
l_{rs}	solid length of the rotor iron
l_s	solid length of the stator iron
l_s	effective length of the armature for slot leakage flux
l_t	average length of the stator conductor. The 1/2 mean turn
l_t	mean length of a turn
l_{tr}	mean length of the rotor turn
l_y	length of magnetic path in a yoke

M, m

M	coefficient of mutual inductance
M	magnetomotive force (mmf)
M_c	mmf for the core
M_d	total mmf of armature reaction
M_d'	total mmf of armature reaction measured in shunt field amperes
M_f	field mmf
M_g	mmf for the air gap
M_t	mmf for the teeth

$M_{tb} = M_{bt}$	coefficient of mutual inductance between the top and bottom coil side for the slot leakage
M_y	mmf for the yoke
m	number of phases
m_1	number of phases in primary
m_2	number of phases in secondary

N, n

N	number of turns, total for single phase windings, per phase for polyphase windings
N_e	number of turns per winding element
N_f	number of field turns per pole
N_f	number of field turns per pole
N_{st}	number of strands per conductor in depth
N_x	number of turns linked with a flux ϕ_x
n	rpm
n_c	number of conductors per coil
n_e	total number of effective series conductors in the stator
n_n	normal or rated speed
n_o	no-load speed
n_r	number of rotor conductors per slot
n_{rc}	number of slots in the pole center section
n_s	number of conductors per slot
n_s	number of stator conductors per slot
n_v	number of radial vents

P, p

P	power
P_{Fe}	iron losses
P_F	friction losses
P_W	windage losses
p	number of poles

Q, q

Q	total number of stator slots
Q_r	number of rotor slots wound
Q_r'	number of slot pitches on the rotor surface (solid pole center) or total number of rotor slots punched (slotted pole centers)
q	charge on a capacitor
q	slots per phase per pole

R, r

R	resistance
R	radius
R_c	resistance of choke coil
R_f	resistance of shunt field rheostat
R_f	resistance of the field winding
R_{ph}	resistance of the stator winding per phase
RPM	rotor revolutions per minute
r	radius of the stator bore

r	resistance
r_a	resistance of armature winding
r_c	corner radius of the wire
r_e	effective stator resistance per phase

S, s

S	cooling surface
s	current density
SCR	short circuit ratio

T, t

T	torque
T	thermal time constant
T	period of a wave
T_a	armature time constant
T_c	period of commutation
T_d'	transient time constant
T_{do}'	open circuit time constant
t	time in seconds
t	lamination thickness

U, u

u	number of conductors side by side in the slot

V, v

V	terminal voltage (for a-c effective value)
V_r	peripheral velocity of the rotor
v	terminal voltage instantaneous value
v_c	surface velocity of the commutator

W, w

W	weight
W_c	watts loss in the stator core
W_{DNL}	watts loss in the damper winding at no load
W_{DFL}	watts loss in the damper winding at full load
W_{DOL}	watts loss in the damper winding at overload
W_{PNL}	watts loss in the pole face at no load
W_{PFL}	watts loss in the pole face at rated load
W_{POL}	watts loss in the pole face at overload
W_{TNL}	watts loss in the stator teeth at no load
W_{TFL}	watts loss in the stator teeth at rated load
W_{TOL}	watts loss in the stator teeth at overload

X, x

X	reactance factor
X	reactance
X_{ad}	the fictitious reactance of armature reaction
X_{ag}	quadrature axis armature reaction

X_c	capacitive reactance
X_d	synchronous reactance
X_d'	saturated transient reactance
X_d''	subtransient reactance
X_{Db}	leakage reactance of the damper winding and eddy current circuits
X_{du}'	unsaturated transient reactance
X_F	leakage reactance of the field winding
X_{FS}	ratio of the rotor slot leakage flux to the useful flux
X_p	Potier reactance
X_s	inductive reactance
X	leakage reactance of the stator winding

Y, y

y	number of slots spanned by the coil

Z, z

Z	total number of conductors on an armature

<u>Lambda</u>

λ	permeance per unit length
λ_a	specific permeance of the air gap
λ_b	belt leakage permeance

$\lambda_{bt} = \lambda_{tb}$ permeance per unit length for mutual induction between bottom and top coil side in the slot

λ_{Dd} specific permeance of the damper winding and eddy current circuits

λ_E specific permeance of the stator end ~~winding~~

λ_F leakage permeance of the rotor

λ_{FE} specific permeance of the rotor end winding

λ_h heat conductivity

λ_i specific permeance of the embedded portion of the stator winding

λ_{rs} specific permeance of the embedded portion of the rotor winding

λ_s permeance per unit length for the slot leakage flux

λ_{sb} permeance per unit length of the bottom coil side for slot leakage flux

λ_{st} permeance per unit length of the top coil side for the slot leakage flux

λ_{tt} permeance per unit length for the tooth top leakage flux

Mu

μ relative permeability

Rho

ρ resistivity

Alpha

α (α)	ratio of the number of slots to the number of slot pitches (solid pole centers) or the ratio of the number of slots wound to the number of slots punched (slotted pole centers)
	pole embrace per unit
α m	electrical angle between two vectors in a fractional slot winding
α s	electrical angle between adjacent stator slots

Beta

β

Delta

Δ	delta connection
Δ	thickness of lamination (L & W)

Epsilon

ϵ	voltage regulation
ϵ	voltage drop

Zeta

Z

Eta

η	efficiency

Theta

θ

Tau

τ pitch

τ pole pitch

τ_p pole pitch

τ_{pr} rotor pole pitch at rotor O.D.

τ_{rs} rotor slot pitch at the rotor diameter

τ_s slot pitch

τ_s stator slot pitch at the inside stator bore

τ_{sg} slot pitch at the gap

τ_{sk} skew in inches of the iron for a length equal to the core length

$\tau_{s\,1/3}$ stator slot pitch at 1/3 the distance up the tooth from the inside stator bore

τ_v width of one stack of lamination plus width of one ventilating duct

Phi

ϕ flux

ϕ_P flux in the pole iron

ϕ_T theoretical total flux in the air gap

Omega

ω electrical angular velocity

ACKNOWLEDGMENTS

The design manuals and derivations upon which this study is based were written by James N. Hibbard. Indeed, completion of the study within one year would not be possible without these manuals to use as a starting point.

The design procedure is that initiated by Lee Kilgore of Westinghouse Electric. The same procedure is used by many if not most of the electrical generator designers in the aircraft electrical industry and is, therefore, familiar to most of them.

The calculations in this first report borrow from the work of E.C. Barnes, E.I. Pollard, David Ginsberg, Herbert Roter, Kennard and Spooner and others. Where possible, references have been given on the curve sheets that were derived or borrowed from the reference.

DISTRIBUTION LIST

DISTRIBUTION LIST OF REPORTS FOR NASA CONTRACT NO. NAS3-2783

National Aeronautics & Space Administration Marshall Space Flight Center Huntsville, Alabama		
Attention:	James C. Taylor (M-ASTR-R)	(1)
	Richard Boehme (M-ASTR-EC)	(1)
National Aeronautics & Space Administration Goddard Space Flight Center Greenbelt, Maryland		
Attention:	F.C. Yagerhofer	(1)
	H. Carleton	(1)
National Aeronautics & Space Administration Manned Spacecraft Center Houston, Texas 77001		
Attention:	A.B. Eickmeier (SEDD)	(1)
	Jerome H. Grayson (Site 8)	(1)
National Aeronautics & Space Administration Lewis Research Center 21000 Brookpark Road Cleveland, Ohio 44135		
Attention:	N.T. Musial, Patent Counsel	(1)
	George Mandel, Library	(3)
	R.L. Cummings, Auxiliary Power Generation Office	(1)
	Charles Corcoran, Electrical Systems Section	(1)
	A.W. Nice, Space Electric Power Office	(1)
	E.A. Koutnik, Space Electric Power Office	(1)
	H.A. Shumaker, Auxiliary Power Generation Office	(3)
National Aeronautics & Space Administration 4th and Maryland Avenue, S.W. Washington, D.C. 20025		
Attention:	James R. Miles, Sr. (SL)	(1)
	P.T. Maxwell (RPP)	(1)
	A.M. Greg Andrus (FC)	(1)

National Aeronautics & Space Administration
Scientific and Technical Information Facility
Box 5700
Bethesda 14, Maryland (6) plus two reproducible copies

Jet Propulsion Laboratory
4800 Oak Grove Drive
Pasadena, California
Attention: G.E. Sweetnam (1)

Diamond Ordnance Fuze Laboratories
Connecticut Ave. & Van Ness Street, N.W.
Washington, D.C.
Attention: R.B. Goodrich (Branch 940) (1)

U.S. Army Research & Development Laboratory
Energy Conversion Branch
Fort Monmouth, New Jersey
Attention: H.J. Byrnes (SIGRA/SL-PSP) (1)

Engineers Research & Development Laboratory
Electrical Power Branch
Fort Belvoir, Virginia
Attention: Ralph E. Hopkins (1)

Reliance Electric & Engs. Company
24701 Euclid Avenue
Cleveland, Ohio 44117 (1)

Sundstrand Aviation-Denver
2480 West 70th Avenue
Denver, Colorado 80221
Attention: Robert Boyer (1)

Thompson Ramo Wooldridge, Inc.
7209 Platt Avenue
Cleveland, Ohio 44104
Attention: Mr. Wellington (1)

Westinghouse Electric Corporation
Aerospace Electrical Div.
Lima, Ohio (1)

G. M. Defense Research Lab.
General Motors Corporation
Santa Barbara, California (1)

Aerojet-General Corporation
Azusa, California (1)

Allis-Chalmers
Norwood Works
Milwaukee, Wisconsin (1)

Armour Research Foundation
10 West 35th Street
Chicago, Illinois 60616 (1)

A.O. Smith Corporation
Milwaukee, Wisconsin (1)

Astra, Incorporated
Box 226
Raleigh, North Carolina (1)

General Dynamics Corporation
1601 Brookpark Road
Cleveland, Ohio
Attention: George Vila (1)

Materials Research Corporation
Orangeburg, New York 10962
Attention: Vernon E. Adler (1)

Aeronautical Systems Division
Wright Patterson Air Force Base
Dayton, Ohio
Attention: ASRMFP-3 (1)

University of Pennsylvania
Power Information Center
Moore School Building
200 South 33rd Street
Philadelphia, Pennsylvania 19104 (1)

Duke University
College of Engineering
Department of Electrical Engineering
Durham, North Carolina
Attention: T.G. Wilson (1)

Naval Research Laboratory
Washington, D.C. 20025
Attention: B.J. Wilson (Code 5230) (1)

Bureau of Naval Weapons
Department of the Navy
Washington, D.C. 20025
Attention: W.T. Beatson (Code RAEE-52) (1)
Milton Knight (Code RAEE-511) (1)

Battelle Memorial Institute 505 King Avenue Columbus, Ohio 43201	(1)
Dynatech Corporation 17 Tudor Street Cambridge, Massachusetts 02139	(1)
AiResearch Division The Garrett Corporation Los Angeles, California 90045	(1)
Motor and Generator Dept. General Electric Company 3001 East Lake Road Erie, Pennsylvania	(1)
Mechanical Technology, Inc. 968 Albany-Shaker Road Latham, New York Attention: Dr. Beno Sternlicht	(1)